Synthesis and Characterization of Poly(vinylphosphonic acid) for Proton Exchange Membranes in Fuel Cells

Dissertation
zur Erlangung des Grades

Doktor der Naturwissenschaften

am Fachbereich Chemie,
Pharmazie und Geowissenschaften
der Johannes Gutenberg-Universität Mainz

vorgelegt von

Bahar Bingöl
geboren in Istanbul (Türkei)

Mainz, 2007

Zusammenfassung

Vinylphosphonsäure (VPA) wurde bei 80 °C durch freie radikalische Polymerisation polymerisiert. Es wurden Polymere (PVPA) mit verschiedenen Kettenlängen erhalten. Das höchste Molekulargewicht, M_w, das erreicht wurde, war 6.2×10^4 g/mol, das mittels statischer Lichtstreuung bestimmt wurde. Hochauflösende NMR-Spektroskopie wurde verwendet, um Informationen über die Mikrostruktur der Polymerketten zu erhalten. Die Analyse der verschiedenen Tetraden ergab, daß die hochmolekularen Polymere eine ataktische Struktur aufweisen. ^{13}C-NMR Untersuchungen zeigten die Gegenwart von Kopf-Kopf und Schwanz-Schwanz Verknüpfungen. Der Anteil dieser Verknüpfungen wurde mit 23.5 % durch eine detallierte Analyse der ^{1}H-NMR Spektren bestimmt.

Die Analyse der Polymeren ergab ferner, daß es sich um eine Zyklopolymerisation des Vinylphosphonsäureanhydrids als Zwischenprodukt handelt. Mittels Titrimetrie wurde bestimmt, daß sich hochmolekulare PVPA wie eine monoprotische Säure verhält.

Protonenleiter mit Phosphonsäuregruppen sind vielversprechend, weil sie eine hohe Konzentration an Ladungsträgern besitzen, thermische Stabilität aufweisen und oxidationsstabil sind. Mischungen und Copolymeren von PVPA sind in der Literatur bekannt, jedoch wurde PVPA bisher nicht ausreichend charakterisiert. Deswegen haben wir das protonenleitende Verhalten einer gut charakterisierten PVPA-Probe erforscht. Grundsätzlich ist PVPA leitend, wobei allerdings der Wassergehalt der Probe eine wesentliche Rolle spielt. Die Phosphonsäuregruppe neigt bei höheren Temperatur zur Kondensation. Es enstehen Phosphonsäureanhydride. Die Bildung dieser Gruppen wurde mittels Festkörper-NMR detektiert. Die Bildung der Anhydride beeinflußt die Protonenleitfähigkeit der PVPA erheblich, da nicht nur Ladungsträger verloren gehen, sondern wahrscheinlich auch deren Mobilität reduziert wird.

Abstract

Vinylphosphonic acid (VPA) was polymerized at 80 ºC by free radical polymerization to give polymers (PVPA) of different molecular weight depending on the initiator concentration. The highest molecular weight, $M_{w,}$ achieved was 6.2 x 10^4 g/mol as determined by static light scattering. High resolution nuclear magnetic resonance (NMR) spectroscopy was used to gain microstructure information about the polymer chain. Information based on tetrad probabilities was utilized to deduce an almost atactic configuration. In addition, ^{13}C-NMR gave evidence for the presence of head-head and tail-tail links. Refined analysis of the ^{1}H NMR spectra allowed for the quantitative determination of the fraction of these links (23.5 percent of all links). Experimental evidence suggested that the polymerization proceeded via cyclopolymerization of the vinylphosphonic acid anhydride as an intermediate. Titration curves indicated that high molecular weight poly(vinylphosphonic acid) PVPA behaved as a monoprotic acid.

Proton conductors with phosphonic acid moieties as protogenic groups are promising due to their high charge carrier concentration, thermal stability, and oxidation resistivity. Blends and copolymers of PVPA have already been reported, but PVPA has not been characterized sufficiently with respect to its polymer properties. Therefore, we also studied the proton conductivity behaviour of a well-characterized PVPA. PVPA is a conductor; however, the conductivity depends strongly on the water content of the material. The phosphonic acid functionality in the resulting polymer, PVPA, undergoes condensation leading to the formation of phosphonic anhydride groups at elevated temperature. Anhydride formation was found to be temperature dependent by solid state NMR. Anhydride formation affects the proton conductivity to a large extent because not only the number of charge carriers but also the mobility of the charge carriers seems to change.

Table of contents

CHAPTER 1

INTRODUCTION

1.1 Introduction

Fuel cells have attracted the interest of many researchers coming from different fields ranging from engineering to chemistry for several reasons. A major reason is that fuel cells are promising in the sense that they may be an alternative for producing clean energy from renewable sources for both stationary and mobile applications.[1]

Fuel cells are beneficial because they can convert fuel into the electricity efficiently. They are about twice as efficient as internal combustion engines. Fuel cells are simple; they do not have any moving parts (except fuel pumps etc) and lead in theory to highly reliable, and long-lasting systems. They are silent which may be important for portable power applications and local power generation in combined heat and power schemes.

The most significant barrier, which prevented the commercialization of fuel cells, is their high cost. In order to be accepted in the future, especially for automative applications, they have to compete with internal combustion engines in price, which will require major breakthroughs in new technologies.

1.2 How do fuel cells function?

A polymer electrolyte membrane fuel cell (PEMFC) is an electrochemical cell which continuously can convert the chemical energy of a fuel and oxidant to electrical

energy.[2] The cross-section of a single polymer electrolyte fuel cell is shown schematically in Figure 1.1.

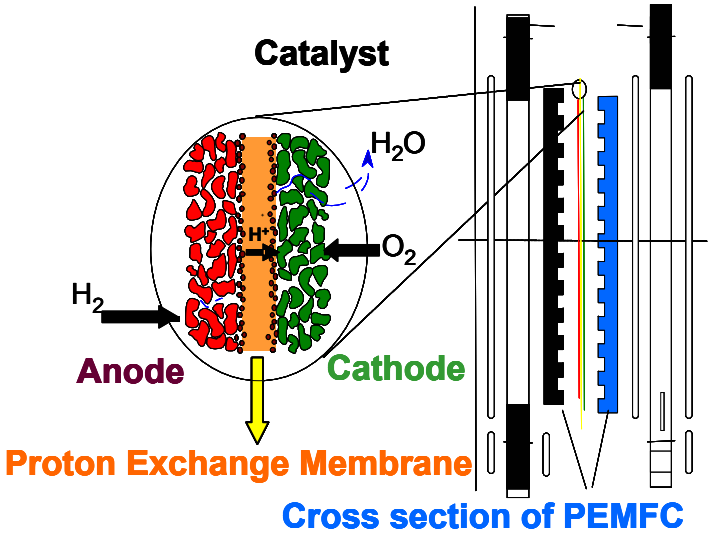

Figure 1.1: Cross section of a PEMFC.

The electrochemical heart of the PEMFC is the membrane electrode assembly (MEA). The MEA consists of a proton exchange membrane, electrodes, catalyst layers, and gas diffusion layers. Hydrogen gas is the preferred fuel in PEMFCs on account of its high reactivity for the electrochemical anode reaction and because its oxidation produces water, which is environmentally friendly. Hydrogen ionizes into protons and electrons at the anode. The protons are conducted through the proton exchange membrane to the cathode. On the other hand, electrons travel along an external electrical circuit to the cathode, where they react with oxygen to form water. Although a good electrical contact must be made between two electrodes, the gases have to remain separated. The proton exchange membrane provides ionic communication between anode and cathode. Moreover, it serves as a separator between the two reactant gases. The site at which the

fuel interacts with the electrolyte and the electrode is sometimes called the three phase contact. Maximum possible contact between electrolyte, electrode, and gases is necessary. This influences the rate of the electrochemical reaction. The PEM electrodes are of gas diffusion type and generally designed such that they provide maximum surface area per unit material volume available for the reactions. In order that the electrochemical reactions can take place at useful efficiency, they must be catalyzed.[2] The catalyst layer is located adjacent to the electrolyte within both anode and cathode of a PEMFC. The best catalyst for both anode and cathode is platinum.

The resulting voltage from one single fuel cell depends largely on the type of the fuel, and is quite small. (For example, the voltage resulting is 0.7 V if hydrogen and oxygen are used as fuel and oxidant Scheme 1.1

Scheme 1.1: Overall fuel cell reaction with hydrogen as fuel and oxygen as reactant).

The voltage gained from a single fuel cell can be increased by connecting the fuel cells in series. Such a collection of fuel cells in series is called a stack. There are different ways of producing a stack. The simplest way is by connecting the edge of each anode to the cathode of the next cell (Figure 1.2a). A better method of cell interconnection is to use a bipolar plate. This makes connections all over the surface of one anode and the cathode of the next cell (Figure 1.2b). Bipolar plates also serve as a means of feeding oxygen to the cathode and fuel gas to the anode.[3]

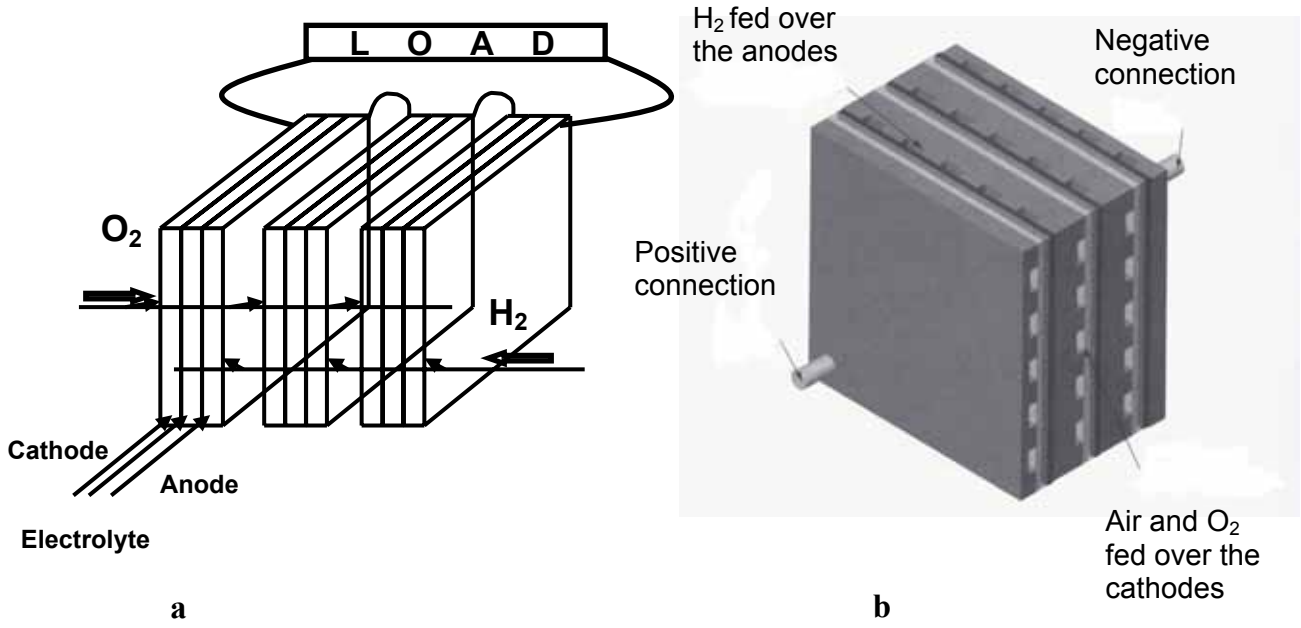

Figure 1.2: A three-cell stack a) by simple edge connection b) by bipolar plates connection.

Proton-conducting membranes form the core of the PEMFCs. There are some requirements that these materials must fulfill in order to be used in fuel cell applications. The most important ones are high proton conductivity (> 0.001 S/cm at 100 °C), electrochemical, chemical, thermal stability, low levels of swelling, and low gas permeability.[4]

1.3 Development of Polymer Electrolyte Fuel Cell Membranes

The first practical proton exchange membrane fuel cell was developed by General Electric in the United States in the 1960s to be used in manned space vehicles. The membrane was a polystyrene sulfonate ion exchange membrane, which however suffered

from insufficient electrochemical stability under fuel cell operation conditions. It had a lifetime of only about 500 h.[5]

Perfluorinated membranes such as Nafion® and Dow® (Scheme 1.2) were discovered by the companies DuPont and Dow Chemical, respectively.These materials were generated by copolymerization of a perfluorinated vinyl ether comonomer with tetraflouroethylene. Both Nafion® and Dow® are perflourosulfonated ionomer membranes that consists of a tetraflouroethylene backbone with hydrophilic sulfonic acid side chains. The relative amount of acidic groups in these ionomers are typically expressed in equivalent weights (EW), which is the average polymer mass (in g) per mole of $-SO_3H$ groups. The membranes from Du Pont and Dow Chemical differ not only in their EW, but also in the side chain structure. Dow® membranes are a short side chain perflourinated ionomer whereas Nafion® membranes are long side chain perflourinated ionomer. The x,y, and z values of the Nafion membrane can be varied to produce materials at different equivalent weights and pendant chain lengths.

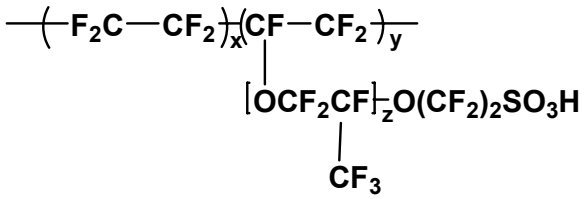

x = 6-10
y =z = 1

a

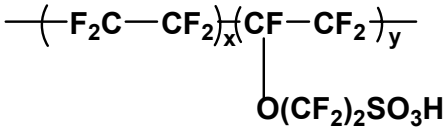

x = 3-10
y = 1

b

Scheme 1.2: Chemical structure of a) Nafion® b) Dow.

Nafion combines the extreme hydrophobicity of the polymer backbone with the extreme hydrophilicity of the sulfonic acid function, which leads to a hydrophilic/hydrophobic nano-separation[6] (Figure 1.3) when the material comes in contact with water. The hydrophilic domains spontanouesly take up water and swell to form nanochannels. These nanochannels are formed by the aggregation of sulfonic acid functional groups. They are responsible for the transport of water and protons. In the nanochannels, charge carriers are formed by dissociation of the acidic functional groups in the presence of water, and proton conduction takes place through the hydrophilic

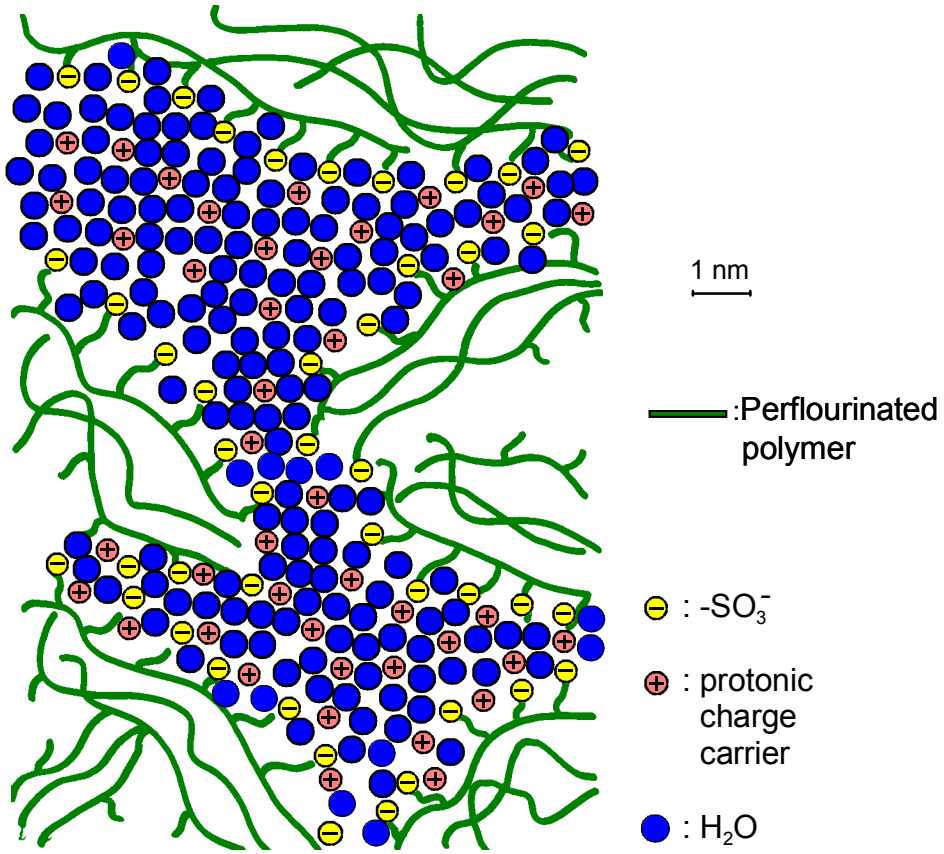

Figure 1.3: Microstructure of Nafion[7].

channels. On the other hand, hydrophobic domains provide the polymer with morphological stability and prevents its dissolution in water.[7]

The major disadvantage of the Nafion membrane is its extremely high cost, which makes its applictaions in cost critical situations such as fuel cells for electrical vehicles unlikely. Additionally, the operation temperature cannot be increased above the boiling point of water (100 °C at $p=10^5$), since the high proton conductivity of hydrated polymers relies on the presence of water in the hydrophilic domains.[8]

Limited operation temperature leads to a the low CO tolerance of the electrocatalyst.[9] As already mentioned, PEMFC use hydrogen as the fuel and air as the oxidant. Operating the fuel cell with pure hydrogen gives the best performance but pure hydrogen can be expensive and difficult to store. Alternatives to pure hydrogen include natural gas, propane, or alcohols. When hydrogen is produced by reforming of hydrocarbons such as natural gas, propane, or alcohols, some contaminants such as carbon monoxide species can persists in the fuel feed since carbon monoxide is formed during the production of hydrogen from the alcohols as well as from the hydrocarbons. The general reaction for steam reforming of a hydrocarbon to hydrogen is as follows:[1]

$C_nH_m + n\,H_20 \longrightarrow n\,CO + (n + 1/2\,m)\,H_2$	(1.1)

In other words, reformed hydrogen-rich gas contains carbon monoxide. It is well-known that the platinum is the best electrocatalyst for hydrogen oxidation. Hydrogen oxidation involves the adsorption of the gas onto the catalyst surface followed by the dissociation of the molecule and electrochemical reaction to form two protons as follows:[1]

$$2\,Pt_{(s)} + H_2 \longrightarrow Pt\text{-}H_{ads} + Pt\text{-}H_{ads}$$

$$Pt\text{-}H_{ads} \longrightarrow H^+ + e^- + Pt_{(s)}$$

Scheme 1.3: Oxidation of hydrogen catalysed by platinum.

where $Pt_{(s)}$ is a free surface site and $Pt\text{-}H_{ads}$ is adsorbed hydrogen atom on the Pt active site. Some problems may arise in a fuel cell when impure hydrogen is used. PEMFC performance degrades when carbon monoxide is present in the fuel gas; this is referred as to as CO poisoning. In other words, the presence of a even small amount of CO results in poisoning of the hydrogen oxidation reaction occurring at the anode of the fuel cell, and consequently a lower cell potential and energy conversion.

The further reactions of CO can be the water shift reaction ((1.2)) or methanation to methane to CO_2 ((1.3)).[1]

$CO + H_2O \rightleftharpoons CO_2 + H_2$	(1.2)
$CO + 3\,H_2 \rightleftharpoons CH_4 + H_2O$	(1.3)

It is found that the CO poisoning effect arises because CO adsorbs prefentially on platinum catalyst surface.[10] The contaminants remaining in the fuel (CO) poisons the catalyst by blocking the active sites for the chemisorption of hydrogen since CO is more strongly adsorbed to platinum than hydrogen as indicated by a greater potential required for the oxidation of CO than hydrogen. Consequently, sites are not available for hydrogen adsorption and subsequent oxidation. When hydrogen and CO are present, the rate of electrooxidation of hydrogen is so rapid that the surface potential is governed by

hydrogen electrooxidation reaction. Because this potential is less than that needed to oxidize CO, the CO remains at the surface, and hydrogen oxidation reaction is hampered. [1, 10] The presence of CO poisons the catalyst in most fuel cells that operate below 250 °C.[1]

As mentioned before high proton conductivity relies on the presence of water when Nafion is considered; a dry membrane possesses a lower or even vanishing conductivity. Water management of the membrane is one of the major issues in PEM technology. Although water is a product of the reactions at the cathode, it is not easy to keep the water in the membrane. Factors influencing the water content in the membrane are water drag through the cell and back diffusion of water from the cathode to anode if the cathode side holds more water. During the fuel cell operation, protons that are moving from the anode to the cathode pull molecules with them. This process is called electro-osmotic drag. As a consequence of electro-osmotic drag, the anode side of the electrolyte can become dried out.[3]

In short, there are several drawbacks to the practical use of Nafion that include cost, maximum operation temperature, problems associated with the transport of water and recycling of the perfluorinated materials.[3]

In search of alternative materials, blends of polymers with oxoacids have been explored.[11] The property of phosphoric acid to interact via hydrogen bonds facilitates the preparation of blends of phosphoric acid with a large variety of polymers such as poly(ethyeneoxide) (PEO),[12, 13] polyvinylalcohol, PEO-PMMA,[14] poly(benzimidazole) (PBI),[15] and poly(diallydimethylammonium)dihydrogen phosphate ($PAMA^+H_2PO_4^-$). The

blends of phosphoric acid with poly(benzimidazole) has been successfully tested in fuel cells which were operated up to 200 °C.[16]

Another approach toward high-temperature proton-conducting membranes is the substitution of water by N-heterocycles such as imidazole, pyrazole, and benzimidazole, which also leads to proton conductivities comparable to hydrated polymers in the temperature range between 150 and 250 °C.[17] However, the proton conduction in these polymers does not require a water phase. Nitrogen-containing aromatic heterocycles exhibit moderate conductivities in their pure liquid state due to the some degree of self-dissociation.[18] The self-dissociation reaction of imidazole is shown as an example in Equation (1.4).

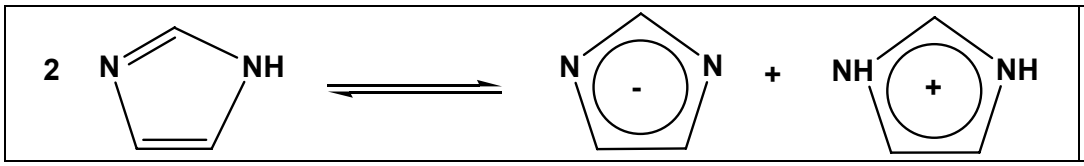

(1.4)

Employing of N-heterocyles as proton solvents in fuel cell membranes requires their immobilization to eliminate the risk of leakage during fuel cell operation. Immobilization of the hetereocycles also prevents any long range diffusion of the charge carrying species by so called "vehicle diffusion". N-Heterocycles can be immobilized to a polymer backbone by using flexible spacers to maintain the high local mobility. Schuster and his coworkers reported the preparation and transport properties of model systems consisting of short-etyhleneoxide chains terminated by imidazole as the proton solvent. In this system, excess protons are transported via structure diffusion, which involves proton transfer between heterocycles with structural reorganization by a hydrogen-bond

breaking and forming process.[19] The proton conductivity of this system is an intrinsic property of the polymer, which depends on the glass transition temperatures, the free volume, and volume fraction of imidazole. The proton conductivity of such a system can further be increased by doping with a small amount of acids, which are extrinsic charge carriers. Other than this system, water-free proton conducting solid electrolytes based on organic/inorganic hybrid namely siloxane oligomer functionalized with imidazole-terminated side chains[20] were reported. Oligomers and polymers with comb like architecture with a siloxane backbone were prepared to have systems with segmental flexibility (to allow high local mobility) and sufficiently high imidazole concentration (to provide a high amount of charge carries).[21]

The choice of the proper protogenic group plays an important role in the proton conductivity of polymer electrolyte separator materials. The protogenic group in perfluorosulfonic acid membranes is the sulfonic acid group. Heterocyles have also been used as protogenic groups as mentioned above. The ideal protogenic group should exihibit proton donor and acceptor properties. In other words, it should be amphoteric, and show a high degree of self-dissociation. It also should have a high dielectric constant to enhance the charge separation. It should tend to form intermolecular hydrogen bonds like the N-heterocycles. It should be stable under fuel cell operation conditions. Sulfonic acid, phosphonic acid, and imidazole functionalized model compounds with an identical alkyl chain were compared in terms of their proton conductivity, proton diffusion coefficient, thermo-oxidative stability, electrochemical stability, and their hydration behavior to identify the most suitable proton solvent for PEM fuel cell membranes for intermediate temperature at low humidity operation.[22] The sulfonic acid functionalized

model compound showed low conductivity in its dry state, which was expected from a highly proton donating (acidic), but poor proton accepting (basic) property of the $–SO_3H$ function. The degree of self dissociation in pure H_2SO_4 is only about 0.1 %, which leads to low concentrations of $-SO_3H_2^+$ and $–SO_3^-$ in a water-free hydrogen bonded network. Imidazole based system showed the largest electrochemical stability window, but its conductivity and thermo-oxidative stability were low. Moreover, it has very high oxidation overpotential for oxygen reduction on platinum. The reaction rates for hydrogen oxidation and oxygen reduction on Pt surfaces are significantly higher for phosphonic acid based systems than for imidazole based systems. Phosphonic acid based systems offer the possibility to obtain high proton conductivities over a wide temperature range between room temperature to 200 °C which may facilitate the start-up properties of fuel cells. Proton conductivity may depend on water up-take at low temperatures. After the drying of the material at higher temperatures, the proton conduction mechanism may be dominated by structure diffusion within a hydrogen bonded network formed by phosphonic acid functionality alone. Phosphonic acid based systems proved to have a high number of charge carrier as expected from its pronounced amphoteric character. Dissociation constants of proton solvents may be used to compare the number of charge carriers.The pK_a value of pure phosphonic acid is much higher than that of pure imidazole (Table 1.1). In short, phosphonic acid based compound showed the most advantageous behavior under low humidity conditions, and at intermediate temperatures.

Table 1.1: pK_a values of proton solvents.

Proton solvent	pK_a
Imidazole	6.99[23]
Phosphonic acid	1.3 Step(1), 6.7 Step (2)[23]

The proton conductivity behavior of some chemical structures with different protogenic groups and architecture is compared in Figure 1.4. The proton conductivity of imidazole decreases remarkably upon its immobilization in both polymeric and oligomeric systems. Propylene diphosphonic acid and pure imidazole have similar proton conductivities, whereas heptylphosphonic acid exhibits higher proton conductivity.

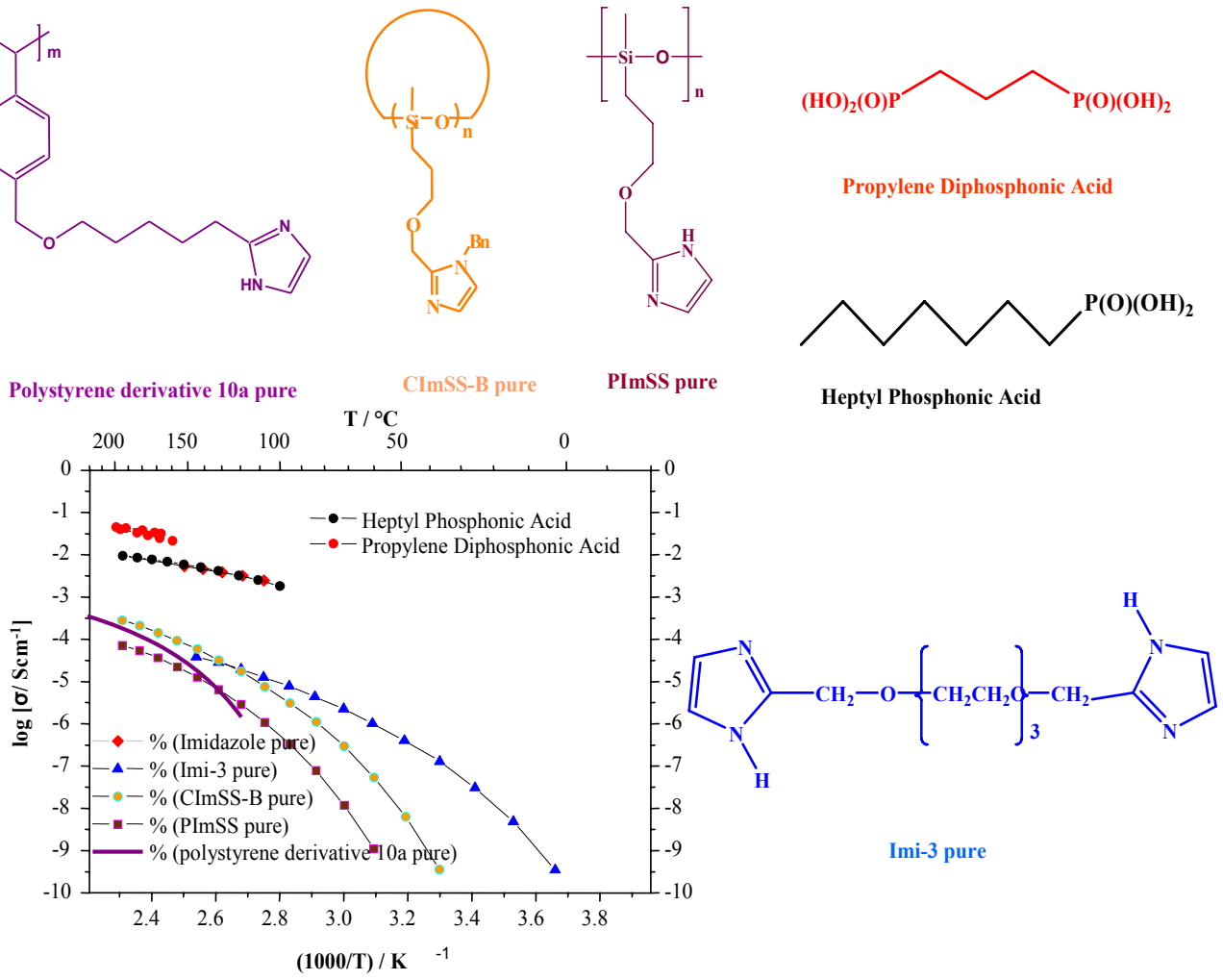

Figure 1.4: Comparison of proton conductivity of different chemical structures.

There are many reports about phosphonic acid containing chemical structures such as poly(arylene ether)s,[24] copolymers of α, β, β- trifluorostyrene with p-dimethylphosphonate-α,β, β-trifluorostyrene,[25] poly(arylphoshazenes),[26] vinylphosphonic acid incorporated into Nafion,[27] and phosphonated perfluorocarbon polymers.[28] These structures with phosphonic acid function were already studied as an alternative to the sulfonic acid group in PEM fuel cell membranes operating in high humidity

environments because of their higher thermal stability and oxidation resistance. However, in these systems, proton transport is based on the presence of water.

For the first time, the phosphonic acid function was immobilized via flexible spacers bound to cyclic siloxanes by Steininger and her coworkers,[29] where phosphonic acid groups are present at high concentration and act as intrinsically proton conductivities. Moreover, poly(vinylphosphonic acid)-heterocycle composite materials were investigated in terms of their proton conduction properties under the operating conditions of fuel cells and it was suggested that the proton conduction mechanism does not rely on vehicle molecules such as water.[30]

The aim of this work is to investigate the details of homopolymerization of vinylphosphonic acid (VPA) and the properties of poly(vinylphosphonic acid) (PVPA) as a potential candidate to be a component of PEMs in a low humidity environment at operating temperatures higher than 100 °C. The details of the microstructure are important for its thermal stability, and for the condensation of phosphonic acid groups, which are important parameters in determining the proton conductivity of PVPA. PVPA samples with different microstructure may have different types of rings resulting from the condenstation of phosphonic acid functionality. This may have an influence on both thermal stability and proton conductivity of PVPA.

CHAPTER 2

EXPERIMENTAL

2.1 Materials

All chemicals were used as received unless noted otherwise. VPA (Aldrich, 97 % purity, stabilized with 30-50 ppm hydroquinone) was washed with diethyl ether before polymerization to remove the stabilizer. Dimethyl vinylphosphonate (DMVP) (Aldrich, 85%), and diethyl vinylphosphonate (DEVP) (Aldrich, 97%) were distilled under reduced pressure. 2,2'-Azobis(isobutyroic acid amidine)dihydrochloride (AIBA) (Aldrich, 97 %), and 2,2′-Azobis(2-methylpropionitrile) (Fluka, 98 %) were used as initiators. Ethylxanthogenacetic acid (Aldrich) was the chain transfer agent in reversible addition fragmentation polymerization.

2.2 Characterization

2.2.1 Nuclear Magnetic Resonance

2.2.1.1 Nuclear Magnetic Resonance in Solution

^{1}H-, ^{31}P-, and ^{13}C-NMR spectra were recorded in solution with Bruker spectrometers operating at 500 MHz, 202.46 MHz, and 176.03 MHz, respectively. They were collected using D_2O as solvent if not otherwise stated. The concentration of the samples will be indicated where necessary. 85 % phosphoric acid, and 3-(Trimethylsilyl)propionic-2,2,3,3-d_4 acid sodium salt were used to calibrate the ^{31}P- and

^{13}C-NMR spectra, respectively. The chemical shift of the methine protons of PVPA and PDMVP are given by the center of the resonance whereas the chemical shift region is indicated for the different tetrad sequences of methylene protons of PVPA in their ^{1}H-NMR spectra. The assignments of the resonances of tetrad sequences are discussed in Chapter 5.

^{1}H- and ^{31}P-NMR spectra of PDEVP and PDISP were collected in chloroform. Triphenylphosphine were used as reference in $CDCl_3$ for the ^{31}P-NMR spectra.

2.2.1.2 Magic Angle Solid State Nuclear Magnetic Resonance (MAS-NMR)

The solid state nuclear magnetic resonance experiments were performed in cooperation with Dr. Young Joo Lee from the Max Planck Institute for Polymer Research, Mainz. All solid state NMR spectra were collected by Dr. Y. J. Lee.

^{1}H-MAS NMR experiments were performed either on a Brucker Avance 700 or on an ASX500 spectrometer, equipped with a 2.5 mm fast MAS probe. All ^{1}H-MAS NMR spectra were acquired at spinning frequencies of 30 kHz.

^{31}P-MAS NMR experiments were carried out at an operating frequency of 202.45 MHz on a Brucker ASX500 spectrometer, equipped with a 2.5 mm fast MAS probe. The spinning frequencies were either 10 kHz or 30 kHz. Two dimensional double quantum (2D DQ) ^{31}P-MAS spectra were recorded with rotor-synchronized back-to-back (BABA) pulse sequence at spinning frequency of 30 kHz.

^{13}C-CP MAS NMR spectra were acquired at an operating frequency of 176.06 MHz on a Brucker Avance 700 spectrometer. Unless stated otherwise, all spectra were collected at room temperature, which leads to a sample temperature up to 50-60 ˚C due to the frictional heat at high spinning frequency.

2.2.2 Molecular Weight Determination

2.2.2.1 Molecular Weight Determination by Light Scattering

Light scattering was performed with a commercial set-up ALV-5000 equipped with a helium-neon laser operating at 633 nm and 20 mW. Polymer solutions of different concentration were first dialyzed against the standard 5 g/L NaH_2PO_4 aqueous solution which was used as the solvent in all cases. The equilibrated solutions were filtered using mixed cellulose membrane filters (Millipore HA) of 0.45 μm pore size. The concentrations of the equilibrated solutions were determined by ^{1}H-NMR after construction a calibration curve, for which ^{1}H-NMR spectra of a series polymer solutions of known concentration were recorded in the presence of 3-(Trimethylsilyl)propionic-2,2,3,3-d_4 acid sodium salt. The calibration curve was realized by comparing the intensities of the resonances due to the polymer backbone with that of the reference salt. Construction of calibration curves were repeated for each PVPA sample of different molecular weight. All measurements were performed at 25 ˚C using cylindrical sample cells. The refractive index increment (dn/dc) was determined in 5 g/L NaH_2PO_4 by a scanning Michelson interferometer operating at the same wavelength as the laser. Dynamic light scattering experiments were carried out with PVPA solutions (1g/L in 0.1 M $NaNO_3$) of different molecular weight to measure the hydrodynamic radius of different molecular weight polymers. The dynamic light scattering experiments of poly(vinylphosphonates) (PDEVP, PDISP) were performed in ethanol and the concentration of the polymer solutions was 10 g /L.

2.2.2.2 Molecular Weight Determination by Size Exclusion Chromatography

The gel permeation chromatography instrument was equipped with three PVXL-TSK columns of 6000, 5000, 3000 Å pore size. A sodium nitrate solution in water (0.1 M) was used as eluent. The measurements were performed at 40 ˚C on aqueous polymeric solutions (1g/L in 0.1 M $NaNO_3$). All samples were solved by 0.1M $NaNO_3$ and were filtered through mixed cellulose membrane filters (Millipore HA) of 0.45 μm pore size.

2.2.3 Infrared Spectroscopy

FT-IR spectra were obtained on a Nicolet 730 FTIR Spectrometer. All samples were measured in the pellet form with KBr.

2.2.4 Potentiometric Titration

Titrations of both VPA and PVPA were conducted with a Metrohm Titranda 836 at 25 °C. Solutions of VPA and PVPA (1mg/1mL) were prepared in water and titrated with a 0.1 N standard solution of NaOH. Titration of PVPA was repeated in the presence of a low molecular weight salt. 50 mg PVPA was dissolved in 50 mL of 0.85 M NaCl solution.

2.2.5 Dielectric Spectroscopy

The conductivity of PVPA was measured with an SI 1260 impedance/gain-phase analyzer (Schlumberger) dielectric spectroscopy in the frequency range from 10^{-1} to 10^{-6} Hz in an open system under dry conditions. Pellets were prepared and placed on a gold electrode. The thickness and the diameter of the pellets are shown in Table 2.1.

The conductivity behavior of various molecular weights PVPA samples were investigated in the range of 20 °C and 210 °C. Three different temperature programs were applied. In the first temperature program, conductivity was measured as a function of temperature between 20 °C and 210 °C in four steps. After every step the sample was kept at the final temperature for an hour. In the first step, the conductivity data were collected from 20 °C to 100 °C. The sample was cooled down to 20 °C. In the second

Table 2.1: Dimensions of the PVPA pellets.

Sample name	Diameter (mm)	Thickness (mm)	Temperature program
PVPA (1)	10	0.85	1
PVPA (1)	10	0.52	3
PVPA (1) 2 days annealed	10	0.33	2
PVPA (2)	10	0.59	1
PVPA (3)	10	0.46	1
PVPA (4)	10	0.62	1

step, the conductivity was measured between 20 °C and 140 °C. In the third step, conductivity was measured between 20 °C and 180 °C. The final measurement was carried out from 20 °C to 210 °C. This temperature program was applied to record the conductivity of dried PVPA samples. The second temperature program involves measurement of the conductivity in the range of 20 °C to 150 °C, which was used to study the conductivity behavior of the annealed samples. The samples were annealed at 150 °C for different time lengths (such as 1 day or 2 days) prior to the conductivity

measurements. In the third temperature program, the conductivity of PVPA samples were first recorded at 20 °C, after which the temperature was increased to 100 °C, where the samples were kept for several hours, and the conductivity data were acquired. This temperature program was used to investigate the conductivity of dried PVPA samples as a function of time at a constant temperature (100 °C). All samples were heated from one temperature to the next one (where the data were collected) in a very short time, after which 10 minutes were allowed to the sample to achieve a constant temperature prior to the data collection. The data collection was started when the fluctuation of the sample temperature was not higher than 0.25 ˚C per minute.

Though the investigation of the conductivity by means of dielectric spectroscopy gives no proof of about the nature of the conductivity, from the comparison with PFG-NMR-data, it can be concluded that all conductivity is based on the proton conductivity.

2.2.6 Elemental Analysis

Elemental analysis was done by a commercial Polymer Standard Service.

2.3 Free Radical Polymerization of Vinylphosphonic Acid

VPA (1.0 g, 9.3 mmoles), AIBA (2.5 mg, 9.2×10^{-3} mmoles) and distilled water (0.5 mL) were put in a Schlenk flask, which was evacuated and backfilled with argon prior to the polymerization. The reaction mixture was heated to 80 °C for three hours. The product was dissolved in water and dialyzed with a Spectra/Por® regenerated cellulose dialysis membrane of 1000 g/mol of cut off. The resulting polymer was freeze dried and was dried to constant weight at 50 °C, 10^{-3} mbar. The mol percent of initiator to the monomer is 0.1 in the polymerization described above. Polymerization was also

carried out with 1.0 and 10 mol percent of initiator following the same procedure. The water content of the reaction with the highest concentration of initiator was increased to solubilize the initiator in the medium. The product of this reaction (PVPA (3)) was dialyzed with lower pore size membrane (500 g/mol of cut-off) since a lower molecular weight polymer was expected. The reaction conditions are given in Table 2.2.

Table 2.2: Polymerization conditions for VPA.

Sample	mol % (initiator/monomer)	Water content (%)
PVPA (1)	0.1	33.3
PVPA (2)	1.0	32.8
PVPA (3)	10	44.4

The yield of the polymerization reactions was determined by gravimetry after purification by dialysis followed by drying to constant weight at 50 °C. The fraction of monomer converted to the polymer was found by ^{1}H-NMR comparing the intensities of the resonances of the polymer backbone with that of monomer left over in the medium before purification. All spectra regarding the calculation of conversions are given in Appendix I.

PVPA (1)

^{1}H-NMR (D_2O): δ=2.50 (CH-P), 2-1.2 (CH_2)

^{31}P-NMR (D_2O): δ= 29.80 (P-OH), 21.50 (P-O-P)

Yield: 70 %

$(C_2H_5PO_3)_n$: Calcd. C 22.24, P 28.67, H 4.66; Found C 20.94, P 26.03, H 5.16.

M_w= 62 000 g/mol by static light scattering in 5 g/L aqueous NaH_2PO_4

IR (KBr): 1173 (P=O), 1453 (CH_2), 1033, 933 (P-O)

PVPA (2)

^{1}H-NMR (D_2O): δ=2.45 (CH-P), 2.30-1.10 (CH_2)

^{31}P-NMR (D_2O): δ= 31.2 (P-OH), 22.5 (P-O-P)

Conversion: 96 % Yield: 63 %

M_w= 44 700 g/mol by static light scattering in 5 g/L aqueous NaH_2PO_4

PVPA (3)

^{1}H-NMR (D_2O): δ= 2.40 (CH-P), 2.35-1.20 (CH_2)

^{31}P-NMR (D_2O): δ= 30.38 (P-OH), 22.25 (P-O-P)

Conversion: 98 % Yield: 23 %

IR (KBr):1141 (P=O), 1452 (CH_2), 1003, 991 (P-O)

2.4 Synthesis of Poly(vinylphosphonic acid) from Dimethyl Vinylphosphonates

2.4.1 Free Radical Polymerization of Dimethyl Vinylphosphonate

DMVP (3 mL, 25.3 mmoles), AIBA (6.8 mg, $2.5x10^{-3}$ mmoles) and distilled water (1.5 mL) were reacted to poly(dimethyl vinylphosphonate) (PDMVP) in a Schlenk flask, which was evacuated and backfilled with argon prior to the polymerization. The synthesis and purification procedures were the same as described for VPA.

PDMVP

^{1}H-NMR (D_2O): δ= 3.8 (P-O-CH_3), 3-1.1 (CH_2-CH-P)

^{31}P-NMR (D_2O): δ= 36.52 (P-O-CH_3)

Conversion: 42% Yield: 23%

IR (KBr): 1035 (P=O), 1190 (P-O-CH_3), 2965, 2853 (CH_2), 1365, 1459 (CH in methyl)

2.4.2 Hydrolysis of Poly(dimethylvinylphosphonate)

Poly(dimethylvinylphosphonate) was dissolved in water and reacted with excess HBr at 110 °C for 8 h to give PVPA (4). After dialysis with a membrane of 500 g/mol cut-off, the product was freeze dried and was dried to constant weight at 50°C under vacuum at 10^{-3} mbar. Complete hydrolysis was achieved.

PVPA (4)

^{1}H-NMR (D_2O): δ= 2.28 (CH-P), 2.4-1.2 (CH_2)

^{31}P-NMR (D_2O): δ= 31.26 ((P-OH), 23 (P-O-P)

IR (KBr): 1116 (P=O), 1004, 929 (P-O), 1452 (CH_2)

2.5 Free Radical Polymerization of Diethyl and Diisopropyl Vinylphosphonate

Diethyl vinylphosphonate (DMVP) (5.6 mL, 36 mmoles) and diisopropyl vinylphsophonate (DISP) (7 mL, 36 mmoles) were reacted with 2,2′-Azobis(2-methylpropionitrile (AIBN) (6.0 mg, $3.7x10^{-3}$ mmoles) in bulk, respectively. (DISP was synthesized according to the procedure by Pike and his coworkers[31]) The polymerization was carried out in a Schlenk flask, which was evacuated and backfilled with argon prior to the polymerization. The reaction mixture was heated to 80 °C for three hours. Both, poly(diethyl vinylphosphonate) (PDEVP), and poly(diisopropyl vinylphosphonate) (PDISP) were purified by precipitation in petroleum ether, in which both monomers were soluble.

PDEVP

^{1}H-NMR ($CHCl_3$): δ= 1.27 (CH_3), 4.07 (O-CH_2), 3.03-0.94 (CH_2-CH-P)

^{31}P-NMR ($CHCl_3$): δ= 35.88-22.23 (P-O-C_2H_5)

Conversion: 24%, Yield: 12 %

IR (KBr): 1229 (P=O), 1022, (P-O-C), 776.1 (P-O-CH_2CH_3), 2983, 1364,1163 (CH_3), 1392, 2907 (O-CH_2)

PDISP

^{1}H-NMR ($CHCl_3$): δ= 1.26 (CH_3), 4.64 (O-CH), 3.02-0.58 (CH_2-CH-P)

^{31}P-NMR ($CHCl_3$): δ= 33.51-20.83 (P-O-$CH(CH_3)_2$

Conversion: 80%,Yield : 62.3 %

IR (KBr): 1252 (P=O), 1369, 1381 (P-O-$CH(CH_3)_2$), 2978, (CH_3), 1463 (O-CH), 1100-1200 (C-C-C, C-C-O)[32]

2.6 Reversible Addition Fragmentation Chain Transfer (RAFT) Polymerization of Vinylphosphonic Acid

VPA (2.8 g), AIBA (0.0016 mg), ethylxanthogenacetic acid (0.0047 mg), and distilled water (1 mL) were put in a Schlenk flask, which was evacuated and backfilled with argon prior to the polymerization. The polymerization was carried out both at 60 ˚C and 80˚C for several hours.

CHAPTER 3

SYNTHESIS OF POLY(VINYLPHOSPHONIC ACID)

3.1 Introduction

Although poly(vinylphosphonic acid) may be considered as the simplest case of a polymeric diprotic acid and may be compared in its usefulness and scope of potential applications with poly(acrylic acid) (PAA) and poly(vinylsulfonic acid) (PVSA), little is known about the details of its synthesis. Recent interest in PVPA relates to its possible application in fuel cells as the key constituent of the polymer electrolyte membrane (PEM).[22] Other applications concern with the protection of metal surfaces in a form of primer[33] or as a reactive component in dental cements.[34-36]

Copolymers of vinylphosphonic acid with acrylonitrile,[37] N-isopropylacrylamide,[38] styrene,[39] vinylpyrrolidone,[40] acrylic- and methacrylic acid[41] have been reported, and their application for pervaporation membranes,[37] hydrogels for drug delivery[38] as component in biomimetric mineralization,[42] and of PEM fuel cells[30, 40] has been suggested.

Levine reported the free radical polymerization of VPA.[41] However, no information about details of the synthesis, purification, and characterization were given. PVPA has already been prepared to be utilized in dental cements starting with vinyl phosphonyl dichloride. Vinyl phosphonyl chloride was polymerized in an inert solvent (1,1,1-trichloroethane) with AIBN. Poly(vinyl phosphonyl chloride) was hydrolyzed by pouring it slowly into water to give PVPA (Scheme 3.1).

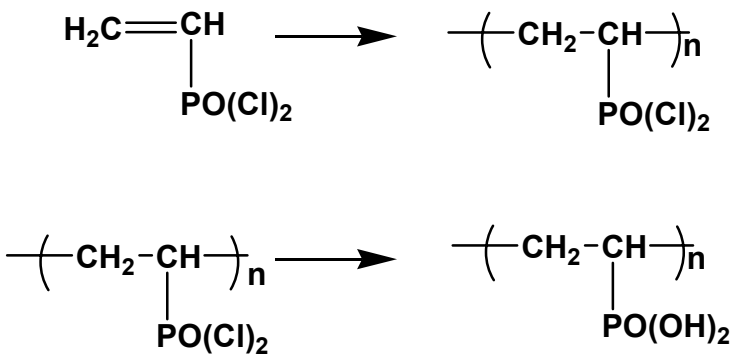

Scheme 3.1: Synthetic route to PVPA.

Homopolymerization of vinylphosphonates has been described briefly in the literature**.** Free radical polymerization of diethyl vinyl phosphonate,[43] diisopropyl vinylphosphonate,[31, 44] and dimethyl vinylphosphonate[42] have been reported. Vinylphosphonates have low tendency to polymerize,[44] which was attributed to the chain transfer to the alkoxy groups linked to the phosphorous atom of the monomer and polymer.[31] Lack of detailed investigations of the polymerization behavior of vinylphosphonates leaves an open question about the reasons behind their low polymerizability.

This chapter describes the synthesis of PVPA obtained by two paths which helps to elucidate the mechanism of free radical polymerization of vinylphosphonic acid. PVPA may be synthesized either by free radical polymerization of vinylphosphonic acid or by first polymerizing vinylphoshonic acid methyl ester followed by saponification of the polymer to obtain PVPA after complete hydrolysis.[36]

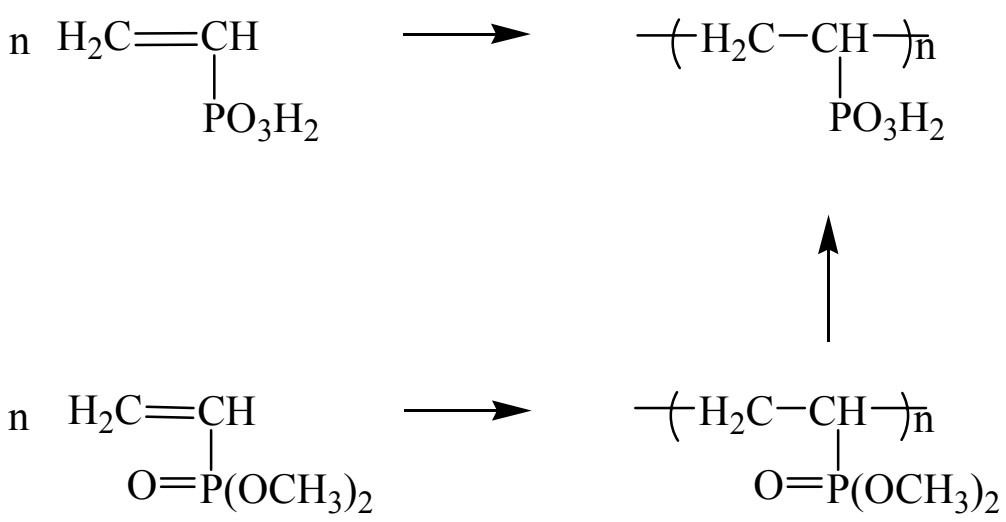

Scheme 3.2: Two synthetic pathways to PVPA.

Additionally, the polymerization of vinylphosphonic acid was studied in the presence of reversible addition fragmentation (RAFT) chain transfer agents to achieve chain length control in collaboration with Hugh Chaffey-Millar and Dr. Christopfer Barner-Kowollik from Centre for Advanced Macromolecular Design (CAMD), School of Chemical Sciences and Engineering, University of NSW, Australia. The results of the RAFT process will be discussed, because they are of importance to support the suggested polymerization mechanism of vinylphosphonic acid. Additionally, a comparison of the possible polymerization techniques to prepare PAA), PVSA, and PVSA is given at the end of this chapter.

3.2 Polymerization of VPA

The free radical polymerization of VPA was carried out in bulk with a small amount of water to solubilize the initiator (AIBA). AIBA is an azo-type initiatior, and the decomposition of AIBA generates radicals in pairs (Scheme 3.3). Polymerization at reasonable rate did only occur at a temperature of 80 ˚C or higher.

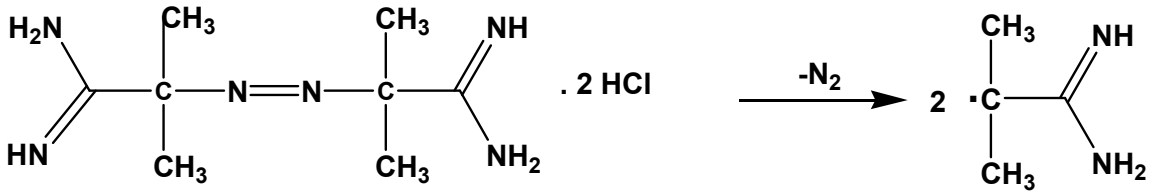

Scheme 3.3: Decomposition of 2,2'-Azobis(isobutyroic acid amidine)dihydrochloride

A yield of 70% of colorless polymer (PVPA (1)) solid was reproducibly obtained when the polymerization was carried out at 80˚ C for 3 hours with 0.1 mol percent of AIBA. This material had a molecular weight M_w of 6.2 x 10^4 g/mol as determined by static light scattering of its solution in 5 g/L aqueous NaH_2PO_4. The weight averaged molecular weight (M_w) was extracted from static light scattering data by double extrapolation to PVPA concentration c=0 and the scattering vector q=0 (Figure 3.1). The addition of low molecular weight salt was necessary to suppress polyelectrolyte effects.

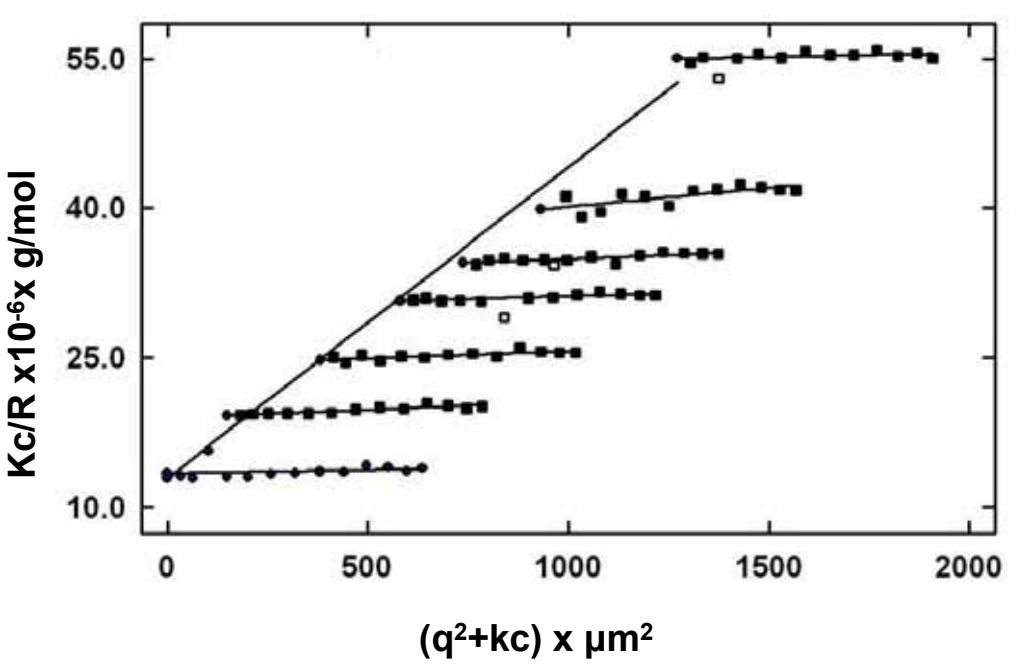

Figure 3.1: Zimm Plot of PVPA (1) in 5 g/L NaH_2PO_4.

The fraction of initiator was changed from 0.1 mol percent to 10 mol percent to vary the molecular weight of the polymer.[45] The conversion and yield were 95 % and 63 % respectively for the polymerization reaction containing 1.0 mol percent initiator. The molecular weight M_w of these samples (PVPA (2)) was 44700 g/mol as determined by static light scattering in the same way as PVPA (1).

PVPA (3) was prepared by polymerizing VPA in the presence of 10 mol percent of AIBA. The fraction of water in this reaction was increased compared to the other reactions with less initiator to achieve complete dissolution of AIBA. The conversion and yield of this reaction was 98% and 23%, respectively. The molecular weight of this polymer was too small to be measured by static light scattering. Dynamic light scattering and size exclusion chromatography was used to gain information about the size of the chains. This made it possible to compare the length of chains of PVPA (3) with those of

higher molecular weight PVPA samples (PVPA (1), and PVPA (2)). Size exclusion chromatography revealed the elution volumes and by dynamic light scattering the hydrodynamic radii R_h were obtained for different molecular weight PVPA samples. Size Exclusion Chromatography techniques separate the molecules according to their size in solution. As a sample passes through the column, molecules which are too big to penetrate the pores of the stationary phase are excluded. These molecules are eluted first from the column. Smaller molecules which can permeate through the pores of the column are eluted later. In other words, elution volume is determined primarily by the hydrodynamic radius. The elugrams of all different chain length PVPA samples are shown in Figure 3.2.

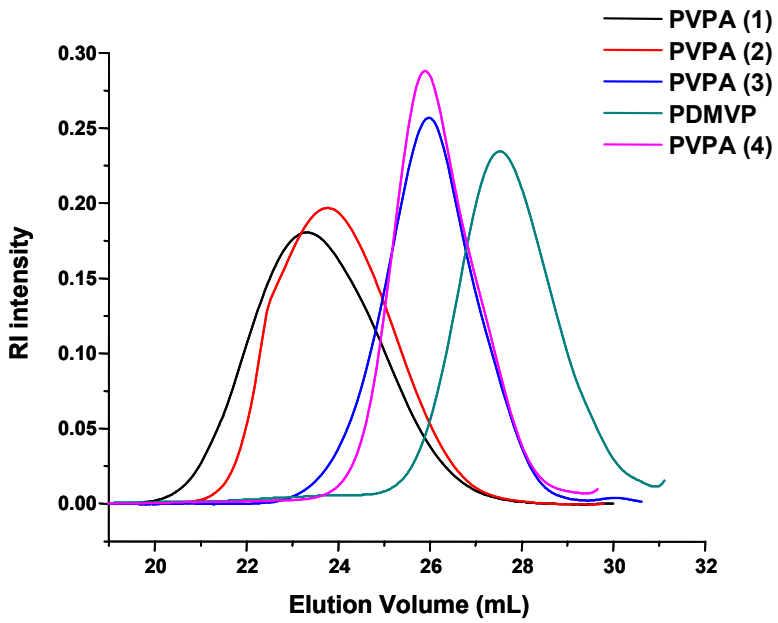

Figure 3.2: Size exclusion chromatography elugrams of different molecular weight PVPA samples.

The molecular weight can be related to the hydrodynamic volume, and hydrodynamic radius as in Equation (3.1). Hydrodynamic radii of different molecular weight samples were determined by dynamic light scattering of their aqueous solution in $NaNO_3$ at pH= 2.5. The hydrodynamic radius of PVPA (3) was measured as 2.27 nm, whereas the PVPA (1), and PVPA (2) have a hydrodynamic radius of 6.02 nm, and 5.24 nm, respectively (Table 3.3)**.** The comparison of the hydrodynamic radii and elution volumes of PVPA revealed that PVPA (3) has a lower molecular weight than the other PVPA samples produced directly by the polymerization of VPA. At this point of study, we cannot use size exclusion chromatography elugrams to obtain the molecular weight and molecular weight distribution of PVPA samples since we do not have any calibrants. To extract information regarding molecular weight and polydispersity of a polymer from size exclusion chromatography elugrams, the size exclusion chromatography system should be calibrated by running a series of narrow molecular mass distribution calibrants. Although elution volumes and hydrodynamic radii of PVPA samples did not allow us to determine the absolute M_w of PVPA, they can be used to compare the chain length of the PVPA (3) with those of known molecular weight, namely PVPA (1) and PVPA (2).

Table 3.1: Comparison of hydrodynamic radii and maxima of elution volumes of various molecular weight PVPA's (X: too small to be measured by static light scattering).

Sample	**Maxima of elution volume (mL)**	**Hydrodynamic radius (nm)**	**M_w (g/mol)**
PVPA (1)	23.39	6.02	62000
PVPA (2)	23.75	5.24	44700
PVPA (3)	26.02	2.27	X
PDMVP	27.55	1.78	X
PVPA (4)	25.85	1.78	X

The absolute M_w of PVPA (3) could be calculated by the help of present data if the intrinsic viscosities or Mark-Houwink constants of the polymers were known. Having the hydrodynamic radii of PVPA samples in hand, calculation of their hydrodynamic volumes is possible by Equation (3.1) assuming that the shape of these PVPA macromolecules in solution can be approximated as spherical. Hydrodynamic volume can also be expressed in terms of molecular weight and intrinsic viscosity [η] as in Equation (3.1), from which the calculation of M_w is possible.

$V_h = 4/3\ \pi\ R_h^3$	(3.1)
$V_h = \log [\eta]\ M_w$	(3.2)

Another possible way of calculating the M_w with the present data would be possible by viscosity measurements applying the Mark-Houwink Equation (3.3) if the constants K and a were known for PVPA.

$[\eta] = K M^a$	(3.3)

The yields for the reactions giving rise to high- (PVPA (1)) and intermediate (PVPA (2)) molecular weight polymers are similar. Lowest yield was observed for the polymerization with the highest amount of initiator. Nearly same amount of monomer was converted to polymers during the polymerization reactions with 1.0 mol percent and 10 mol percent. In other words, although the conversion for these two polymerization reactions was similar, they differed in their yield. This indicates that the extent of the shorter chains formed during the polymerization in the presence of 10 mol percent initiator was higher, some of which later diffused out of the dialysis membrane during the purification step.

3.3 Polymerization of Dimethyl Vinylphosphonate and Its Hydrolysis to Poly(vinylphosphonic acid)

Another route for the preparation of PVPA utilized the polymerization dimethyl ester of vinylphosphonic acid followed by hydrolysis of the resulting polymer. The polymerization of DMVP was carried out under the same conditions as described for the free acid (VPA). The conversion was determined by ^{1}H-NMR as 31.3% (Appendix I) by comparing the intensities of the methyl group signal with that of the double bonds. The yield was 23% after freeze drying. This material was saponified with an excess of HBr at 110 °C to give a sample of PVPA (4) (Scheme 3.2).

The molecular weight of PVPA (4) prepared by the hydrolysis of PDMVP was much lower as compared to the samples prepared directly from VPA under the same

conditions. This was concluded from the elution volume obtained by Size Exclusion Chromatography and the hydrodynamic radius measured by dynamic light scattering. The hydrodynamic radius of PVPA (4) was found as 1.78 nm. The molecular weight of this sample was too low to be measured by static light scattering.

3.4 Free Radical Polymerization of Vinylphosphonates

The polymerization of diethyl and diisopropyl vinyl phosphonate cannot be carried out in aqueous medium because of their insolubility in water. Therefore, they were polymerized in bulk using AIBN as initiator at 80 ˚C. The mol percent of the initiator was 0.1 in both cases. The half-life time of AIBN ranges from 50 min to 76 min depending on the solvent used at 80 °C.[46] (Although the polymerization of DEVP and DISP were not performed in any solvents listed in Table 3.2, the values may be informative about the approximate length of time needed for initiator decomposition in our system)

Table 3.2: Half life of AIBN in different solvents at 80 °C.

Solvent	**Half-life (min)**
acetic acid	76
dioxane/water	71
nitrobenzene	50
toluene	74.5

The conversion was determined by ^{1}H NMR comparing the intensity ratios of methylene (-OCH_2) and methine(OCH) protons of PDEVP and PDISP with that of double bonds left in the reaction medium after polymerization. Conversion was found as 23% and 80% for PDEVP, and PDISP, respectively (Appendix I). The reaction mixtures after the

polymerization were poured to cold petroleum ether to precipitate the polymer, and to remove the rest of initiator, monomer, and oligomers. The yield after the purification step was 12% and 63% for PDEVP, and PDISP, respectively. There is a remarkable difference in the conversion of DEVP and DISP. It is not very clear whether this difference is accidental. The conversions of the homopolymerizations of these two monomers were not reported as different in the literature. However, there are limited number of work regarding these monomers. Further work is necessary to find out the reasons behind the higher conversion observed during the polymerization of DISP. The higher conversion of DISP than DEVP and DMVP makes DISP monomer a good candicate as a precursor for the synthesis of PVPA. To obtain PVPA from DISP, one should first polymerize DISP and then hydrolyse PDISP. The hydrolysis of PDISP (Scheme 3.4) is expected to proceed under milder conditions (e.g. lower temperature) than that of PDEVP and PDMVP.

Scheme 3.4: Hydrolysis of PDISP.

Free radical polymerization of DEVP and DISP lead to low molecular weight polymers indicated by their small hydrodynamic radii, which were measured by dynamic light scattering in ethanol. The dynamic light scattering data of poly(vinylphosphonates) should be treated carefully since the experimental error is high since short chains are

considered. However, they clearly present that the homopolymerization of vinyl phosphonates does not give high molecular weight polymers as in the case of VPA.

Table 3.3: Hydrodynamic radii of poly(vinylphosphonates) in ethanol.

Polymer	mol % (initiator/monomer)	Yield (%)	Radius (nm)
PDMVP	0.1	23	1.74
PDEVP	0.1	12	3.44
PDISP	0.1	63	1.65

3.5 Polymerization Mechanism of Vinylphopshonic Acid

3.5.1 Suggestion of a Polymerization Mechanism based on the Differences in Microstructures of PVPA obtained by different pathways

Comparison of PVPA prepared by the two paths provided insight into the mechanism of free radical polymerization of vinylphosphonic acid. The mechanism of VPA was understood by looking into the microstructure of both PVPA (1) and PVPA (4). The detailed analysis of the microstructures of differently prepared PVPA will be given in Chapter 5. Only points relevant to deduce information about the mechanism of the polymerization of VPA are discussed in this chapter.

The microstructure of both polymers was elucidated inspecting their ^{1}H-and ^{13}C-NMR spectra. Although both PVPA samples have very similar ^{1}H NMR spectra, their ^{13}C NMR spectra differ considerably. The ^{1}H-NMR spectrum of PVPA synthesized from DMVP is consistent with a chain structure composed of head-to-tail linked monomers of a nearly atactic configuration. Both VPA, and DMVP have an asymmetric substitution pattern and the two ends of the double bond are distinct. For mono-substituted monomers, it is usual to call the less substituted end ‘the tail ‘and the more substituted

end ‘the head’. This terminology describes two modes of addition (Scheme 3.5), namely tail and head addition, during which three types of linkages can form (head-to-tail, head-to-head, and tail-to-tail.)

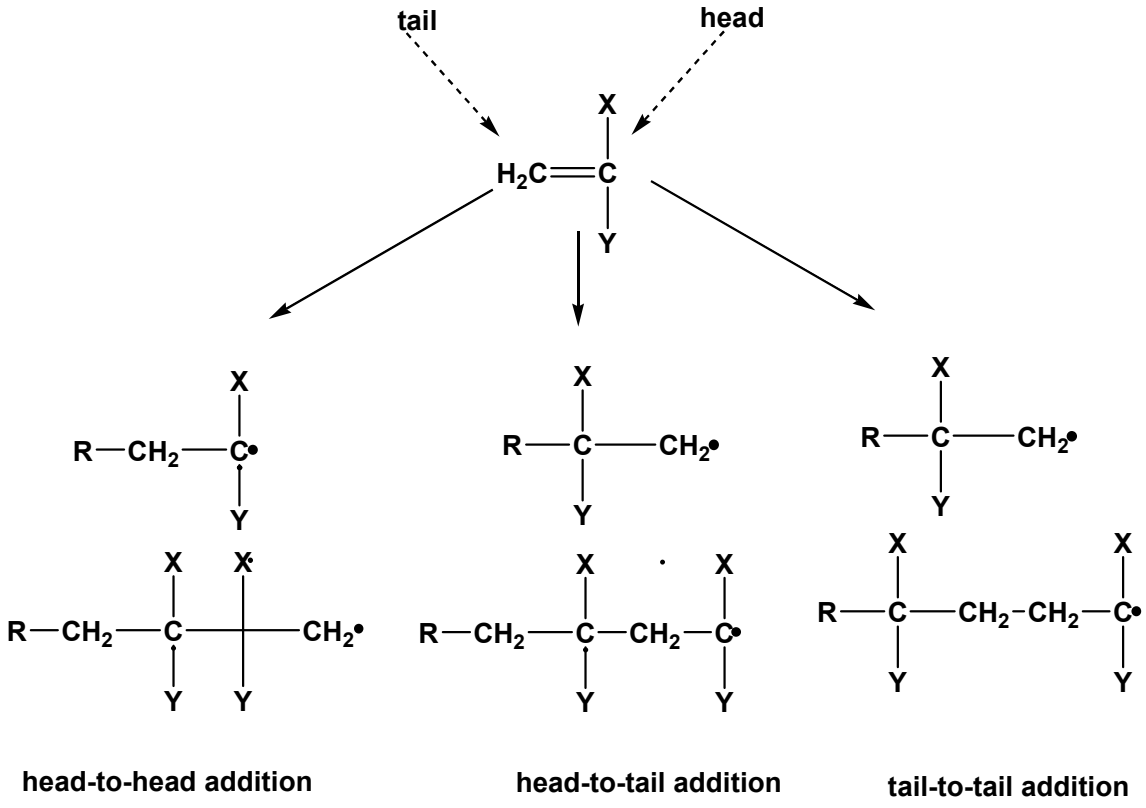

Scheme 3.5: Types of possible additions during the propagation step.

The marked difference in the ^{13}C-NMR spectra of PVPA (1) and PVPA (4) implied that the radical polymerization of VPA follows a different mechanism than the polymerization of its dimethyl ester which gives the expected approximately atactic polymer. Although the pattern of the signals in ^{1}H-NMR of PVPA (1) and PVPA (4) looked similar, at first glance, the ratio of the signal intensities was substantially different beyond experimental error.

The observed structure can be rationalized assuming that VPA was not the true monomer, but rather its anhydride undergoes polymerization (Scheme 3.6). Formation of anhydrides of phosphonic acids is well known. They readily form in water at polymerization temperatures.[43] Once the anhydride is formed in equilibrium with the free acid, it may undergo free radical polymerization following the two pathways b and c shown in Scheme 3.6. Intramolecular propagation to form a six-membered ring reproduces the pattern of a head-to-tail addition with concomitant formation of a methine (secondary) radical, while the propagation to form a five-membered ring produces the pattern of a head-to-head linkage with concomitant formation of a methylenic (primary) radical. Attack of this radical to a further vinyl group in the β position would produce the observed tail-to-tail links. Once the polymer is formed and investigated in dilute aqueous solution at or near room temperature the anhydride structures will disappear[47] or become scrambled so that only the main chain sequence pattern gives evidence of the reaction paths. These results suggested that the polymerization proceeded via cyclopolymerization* of the vinylphosphonic acid anhydride as an intermediate. Cyclopolymerization mechanism leads to the formation of five- and six-membered rings during the polymerization. The fraction of five- and six-membered rings cannot be quantified separately yet in our case.

* Cyclopolymerization was studied by G. Butler and his coworkers in details. They established that diallyl quaternary ammonium salts undergo radical polymerization to give linear saturated polymers, whereas monoally ammonium compounds failed to polymerize. Diallyldimethylammonium salts is as an example for a monomer, the polymerization of which procedes via cyclopoymerization.

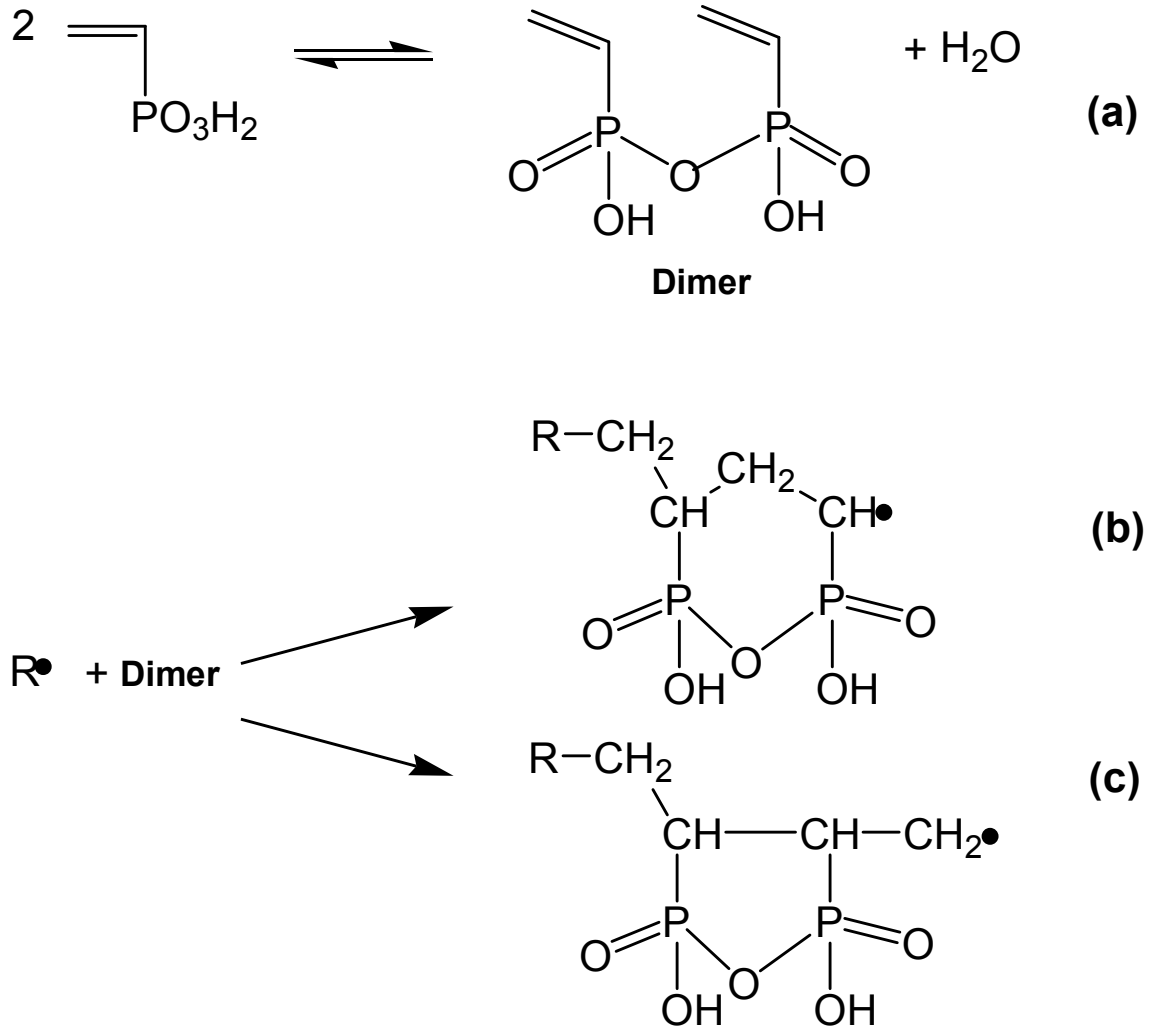

Scheme 3.6: Suggested mechanism of cyclopolymerization involving vinylphosphonic acid anhydride.

The relative properties for reaction according pathway b and c will be evaluated from the NMR spectra.

3.5.2 Reversible Addition-Fragmentation Chain Transfer (RAFT) Polymerization

Methods for controlling the molecular weight and architecture in free radical polymerization lead to the combination of the versatility of a radical process with the

ability to generate complex macromolecular architectures such as comb, star, and block copolymers for use in different fields such as bioengineering and nanotechnology.[48, 49] There exists a variety of living radical polymerization processes including atom transfer radical polymerization (ATRP), nitroxide-mediated polymerization (NMP), and reversible addition-fragmentation chain transfer (RAFT) polymerization.

Although the chemistry of these different methods varies considerably, a common feature of them is their need to protect the majority of the growing polymer chains from bimolecular termination reactions that normally occur in conventional free-radical polymerization. Controlled radical polymerization processes rely upon protecting the propagating species from bimolecular termination through its reversible trapping as dormant species. The success of controlled radical polymerizations depends greatly upon choosing control agents and reaction conditions such that there exists an optimal balance between the rates of several competing reactions.[50]

Living radical polymerization mechanism is distinguished from the conventional radical polymerization (Scheme 3.9a) by the existence of a reversible activation process. The dormant chain P-X is supposed to be activated to the polymer radical P$^{\bullet}$ by thermal or photochemical stimuli. In the presence of monomer M, P$^{\bullet}$ will undergo propagation until it is deactivated back to P-X. If a living chain experiences the activation-deactivation cycles frequently enough over a period of polymerization time, all living chains will have a nearly equal chance to grow, yielding a low- polydispersity product.[51]

RAFT polymerization has received increasing attention since it is able to control the polymerization of a variety of monomers without using a metal catalyst.[52] The RAFT process consists of the simple introduction of a small amount of chain transfer agent

(RAFT agents) in a conventional free-radical system (monomer+initiator). In the RAFT process, control is achieved using chain transfer agents possessing thiocarbonylthio groups with substituents R and Z. These chain transfer agents are known as RAFT agents (Scheme 3.7).[53]

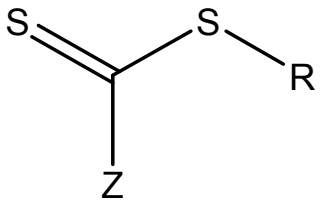

Scheme 3.7: General chemical structure of thioesters.

The Z group strongly influences the stability of thiocarbonyl-thio radical intermediate. Strong stabilizing groups will favor the formation of the intermediate, RAFT adduct radical. Conversely, other groups can act to strengthen or weaken the S=C bond, examples being, respectively, alkoxy groups or fluorine. The R group is required to be a good leaving group in comparison with the growing polymeric chain and a good re-initiating species towards the monomer used. It also contributes toward the stabilization of the radical intermediate although to a lower extent than the Z group.[54]

The mechanism of RAFT polymerization is believed to involve a series of chain transfer reactions (Scheme 3.8b). The propagating radical adds to the thiocarbonyl sulfur center of the dithioester to produce an intermediate carbon-centered radical. This carbon-centered radical can then undergo β scission, either to reform the propagating radical or to liberate a new carbon centered radical (leaving group) (V). Step V shows the fragmentation of the intermediate occurring reversibly either toward the initial growing

chain or to the free re-initiating group (R) and a macro chain-transfer agent. The R group reinitiates the polymerization by reacting with monomers and starts a new polymer chain (VI). The R group of the RAFT agent is chosen so that it undergoes β-scission from the RAFT-adduct radical in preference to the propagating species, but also so that it is capable of reinitiating polymerization. As a result, the initial RAFT agent is rapidly converted into polymeric RAFT agent, and $R^{\bullet}$ is converted into more propagating species. The core step of RAFT polymerization is the equilibrium between propagating radicals Pm, Pn, and dormant polymeric RAFT agents (VII). A fast equilibrium is necessary for all the polymeric radicals to propagate with the same probability and achieve low polydispersity polymers.[52] Step II and III describe the unavoidable reactions of termination present in all free radical polymerization systems, by either combination (III) or disproportionation (II). However, as the termination products are small in number relative to living chains, the final product consist of a large majority of polymeric chains showing the re-initiating group (R) at one end, and the thiocarbonyl-thio group at the other.

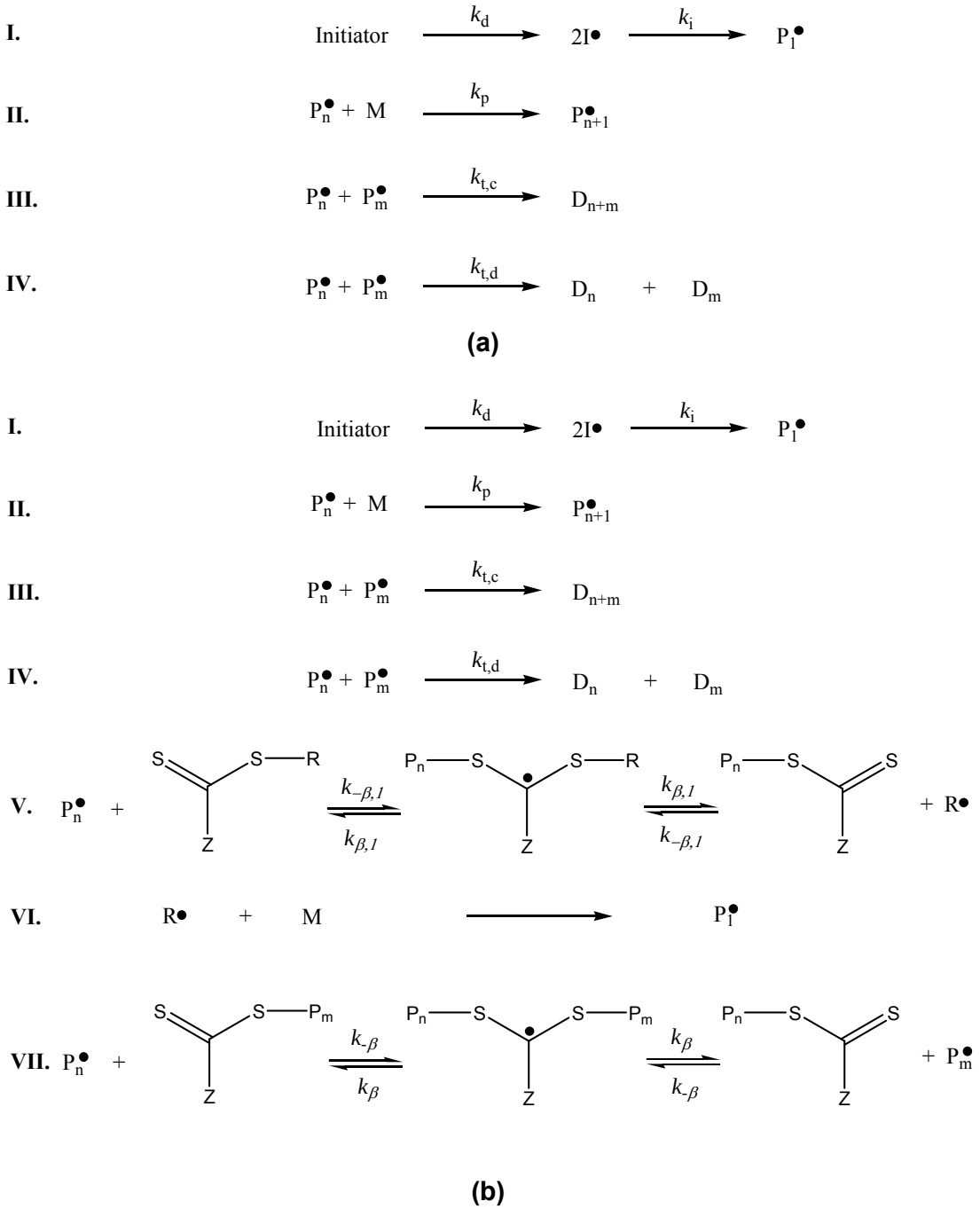

Scheme 3.8: a) Basic mechanism of free radical polymerization[54] b) General reversible addition fragmentation chain transfer polymerization mechanism[54].

3.5.2.1 Reversible Addition-Fragmentation Chain Transfer (RAFT) Polymerization of Vinylphosphonic Acid and Its Dimethyl Ester

The polymerization of VPA acid and its dimethyl ester was investigated in the presence of ethylxanthogenacetic acid (Scheme 3.9), which was used as the RAFT agent. The Z group in this structure is O-Et. RAFT agents with an alkoxy group can also be referred as xanthates.

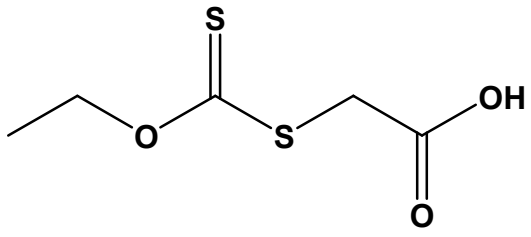

Scheme 3.9: Chemical structure of ethylxanthogenacetic acid.

The experiments were carried out at a slightly lower temperature (60-70 °C) than the conventional free radical polymerization (80 °C) of these two monomers. (The free radical polymerization of VPA was tested at 60 and 70 °C prior to the introduction of RAFT agent to the medium, and it was found to be successful at these temperatures.) The reason why it was necessary to lower the temperature was to prevent the possible hydrolysis of the RAFT agent in water. Xanthates may undergo hydrolysis in acidic medium at high temperatures. This is a general problem in aqueous RAFT polymerization.[55] The possible hydrolysis reaction of ethylxanthogenacetic acid is shown in Scheme 3.10.

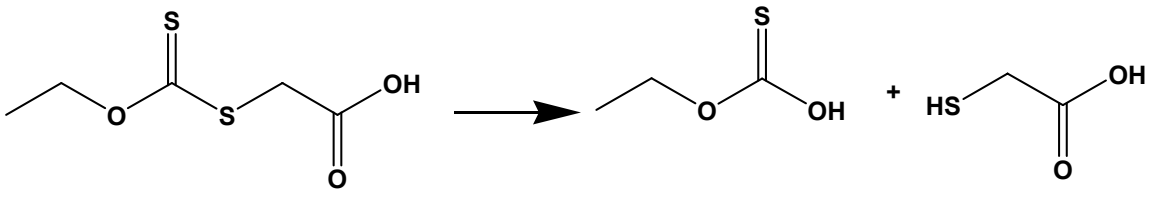

Scheme 3.10: Possible hydrolysis reaction of ethylxanthogenacetic acid in acidic medium at higher temperatures.

Introduction of RAFT agent in the polymerization mixture of VPA resulted in the complete inhibition of the polymerization. This is believed to be caused by the thermodynamic unfavourability of fragmentation of the primary propagating radical from the RAFT adduct radical intermediate (Scheme 3.11 a) (It is possible that both primary and secondary propagating radicals are formed during the polymerization). If the primary propagating radical does not fragment from the RAFT adduct radical intermediate, after some time both ends of the RAFT agent will be occupied by this primary radical, and therefore, RAFT agent cannot function any more and polymerization is inhibited. This observation is also consistent with the proposed cyclopolymerization of VPA.

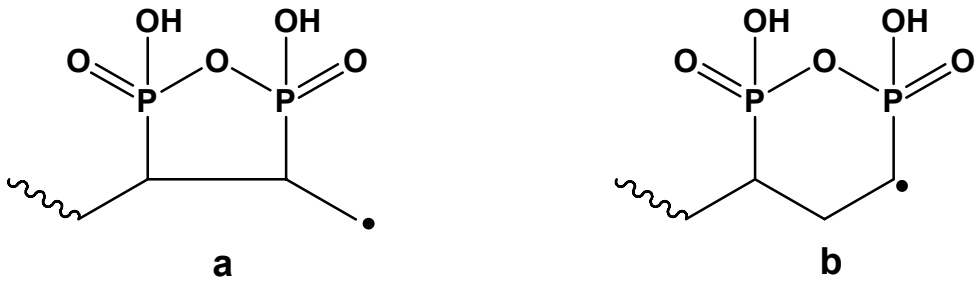

Scheme 3.11: a) 5-membered b) 6-membered head-to-head propagating species.

Introduction of the RAFT agent to the polymerization mixture of DMVP did not inhibit its polymerization, and PDMVP was obtained successfully. Increase of average molecular weight with conversion of monomer into the polymer would have revealed whether the process is living. At this stage of the study, it is not very clear whether control over molecular weight of PDMVP could be achieved successfully by using this RAFT agent since the evolution of molecular weight could not be followed yet with increasing conversion successfully. However, there are indications for the growth of molecular weight with increasing conversion such as increasing viscosity of the PDMVP samples.

3.5.3 Summary of Free Radical Polymerization and Its Mechanism of VPA

PVPA was synthesized by free radical polymerization by two different pathways. The first way considers the direct polymerization of VPA, and the second route utilized DMVP ester as monomer followed by the complete saponification of PDMVP to obtain PVPA. These two different pathways gave rise to polymers with different microstructure. Comparing the microstructure of the PVPA samples synthesized by different routes, it was suggested that the polymerization of VPA proceeds over cyclopolymerization of vinylphosphonic acid anhydride as an intermediate. The inhibition of RAFT polymerization of VPA is in accordance with the suggested polymerization mechanism. It is evident that this reaction mechanism which is proposed here for the first time has a strong impact on the explanation of the temperature and solvent dependence of the rate of polymerization as well as copolymerization behavior of VPA.

3.6 Polymerization of Acrylic Acid

Acrylic acid (AA) is one of the monomers that can only polymerize via free radical mechanism. It can be polymerized by conventional free radical polymerization with different initiation methods such as photoinitiation, [56, 57] redox initiation,[58] thermal initiation. Atactic PAA was prepared using conventional free radical initiators, whereas photochemical polymerization of AA in ethanol solution at – 78 ˚C with sensitizing by benzoins gave the syndiotactic form.

The sodium or ammonium salts of AA can be polymerized easily in water in the presence of potassium persulfate at 30 °C.

Acrylic esters can be converted to their polymers in the presence of peroxide catalyst at moderate temperatures. Additionally, alkyl acrylates can be polymerized to high conversions in emulsion by activation with persulfate in the absence of air at 50 °C. Long-chain alkyl ammonium salts or a long-chain alkyl sodium sulfate are suitable emulsifiers.[59]

Polymers based on AA and its esters can also be synthesized by living ionic polymerization in addition to the conventional free-radical polymerization. The advantage of the living polymerization to the conventional radical polymerization is the control of some key elements of macromolecular structures such as molecular weight, polydispersity, chain architecture, and end functionality.

Monodisperse PAA was initially prepared by anionic polymerization of tert-buyl acrylate followed by its hydrolysis, which leads to an isotactic crystalline polymer. Since the advent of controlled radical polymerization, it is also possible to prepare PAA starting from the monomer AA. Early works on controlled radical polymerization of AA showed

that this monomer is reluctant in both atom transfer radical polymerization ATRP), and nitroxide mediated polymerization (NMP).[60] With ATRP, some incompatibility with the transition metal complex catalyst was suspected.[61] With NMP, the acidic group was proposed to be involved in side reactions with nitroxide. No mechanism was suggested for these side reactions. Besides, unwanted chemical reactions, extremely high propagation rate constant in free radical polymerization and rapid gelation[62] are other difficulties that may be encountered and may ruin the control of the polymerization. Inspite of these challenges, synthesis of well defined homopolymers of AA was reported in a small umber of publications when controlled radical polymerization was used.[60] Polymerization of AA was found to be controlled with reversible addition fragmentation transfer (RAFT). The first example homopolmerization of AA was performed in dimethylformamide solution at 60 °C.[63] Later Ladaviere was able to polymerize AA in protic media[64] (alcohol and water solution) by RAFT.

3.7 Polymerization of Vinyl Sulfonic Acid

Vinylsulfonic acid (VSA) can be polymerized by free radical polymerization. Alderman and Hanford reported that VSA was polymerized in bulk very slowly to give a soft, rubbery, dark-colored, water-soluble polymer upon initiation either by irradiation with UV[65] or using hydrogen peroxide.[66] Jones and Barner claimed that VSA polymerized readily if it was distilled in the absence of oxygen.[67] Breslow and Hulse prepared PVSA and found out that the polymerization proceeds readily in the presence of UV light, hydrogen peroxide or potasium persulfate,[68] whereas Overberger, Baldvin and Gregore reported that VSA did not polymerize under the conditions used with radical and

cationic catalysis[69] without giving any experimental details. Both the rate of polymerization and molecular weight of the polymer were found to be affected by the monomer concentration. The increase in the rate of the polymerization of VSA with increased concentration was explained on the basis of electrostatic effects. In dilute solution, vinylsulfonate ions (Scheme 3.12) repel each other making the polymerization difficult. However, in more concentrated solutions negative charges are partially neutralized by ion-pair formation and the approach of two vinylsulfonate ions becomes easier.[68]

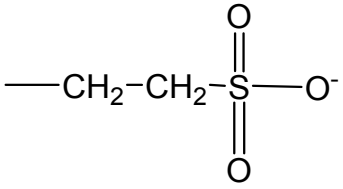

Scheme 3.12: Chemical structure of anion of VSA

Sodium vinylsulfonate has been reported to polymerize readily in aqueous solution.[70]

The initiation of sodium vinylsulfonate can be achived by irradiation with UV- or γ rays , or using peroxides and potassium persulfate.[71] Other than sodium salt of VSA, its barium, calcium, and ammonium salt were shown to polymerize. The polymers prepared by the salts of VSA can be converted to polysulfonic acids by ion exchangers.

The polymerization of free acid proceeds slower than its corresponding sodium salt and leads to lower yields. VSA polymerizes as anion and it has been suggested that there is increased resonance stabilization in the anion.[69]

The ethyl ester of VSA can also be polymerized by UV light as descried for its free acid. However, the polymerization of the esters of VSA was very slowly.[66]

Table 3.4: A summary of the possible polymerization techniques for VPA, VSA, and AA monomers (√: possible, X: not possible, and empty space: no literature present or not discussed here.

Monomer	**UV initiation**	**Redox initiation**	**Thermal initiation**	**Other Polymerization Techniques**
VPA	**X**	**X**	√ [41, 72]	
VPA salt			**X**	
VPA esters	√	**X**	√	Anionic polymerization (X)
VSA	√ [65, 68]	√ [68]		
VSA salt	√ [71]	√ [71]		
VSA ester	√[66]			
AA	√ [56]	√ [58, 73]	√	Controlled radical polymerization√
AA salt		√		
AA esters			√	Anionic polymerization[74] (√),in emulsion [59](√), controlled radical polymerization[51] (√)

3.8 Comparison of Possible Polymerization Techniques for VPA, VSA and AA

VPA, VSA and AA are the simplest cases of monomeric acids. They are analogs of each other; they differ only in the type and valency of their center atom to which ionizable units are bonded. Among these three vinyl acids, AA is the most extensively studied monomer. There are only a few reports about the VPA and VSA.

It is known that polymerization of AA is only possible *via* free-radical mechanism.VPA and VSA can also be prepared by the same mechanism, which is the only one up to now reported in the literature. Free radicals can be generated by thermal or photochemical homolytic cleavage of covalent bonds, or by redox processes. Photoinitiation and redox process can be employed to initiate the polymerization of both AA and VSA at room temperature. The advantage of photo and redox initiation is that the polymerization can be carried out at low temperatures (e.g. room temperature). However, higher temperatures are required to create free radicals by thermal initiators.

The temperature of the polymerization is an important parameter influencing the side reactions as well as the termination step. To minimize the unwanted side reaction, it was tried to carry out the polymerization of vinylphosphonic acid at lower temperatures than 80 °C using photo and redox initiators.[*]

Photopolymerization is defined as the reaction of monomers (or macromonomers) to produce polymeric structures by light-induced initiation (excitation of the photoinitiator), and subsequent polymerization. Photopolymerization requires three essential elements: electromagnetic radiation (hv), chromophore containing

[*] The synthetic procedure of the experiments regarding photopolymerization and redox polymerization are given in Appendix III.

photoinitiators (PI), and monomers with unsaturated moieties such as a vinyl group. Ultraviolet (UV: 190 ~ 400 nm) or visible light (Vis: 400 ~ 800 nm) can be used for photopolymerization depending on the photoinitiator used. Photoinitiation involves photon absorption, PI molecular excitation, and finally reactive fragment formation after PI decomposition. The absorption of UV or Vis radiation can be considered to be a two-step process, the first of which involves the electronic excitation. The lifetime of the excited species (PI^*) is brief (10^{-8} to 10^{-9}), and its existence is being terminated by relaxation processes.[75] The most common type of relaxation involves conversion of the excitation energy to heat. Relaxation may occur by decomposition of PI^* to form new species such as radicals [$I^{\cdot}$] or ions [I^+ / I^-]. These fragments serve as direct initiators for radical polymerization or anionic/cationic polymerization (Scheme 3.13).

$PI + h\nu \rightarrow PI^* \rightarrow PI$ (decay)	(a)
$PI + h\nu \rightarrow PI^* \rightarrow [I^{\bullet}]$ or $[I^+ / I^-]$	(b)

Scheme 3.13: Excitation of photoinitiators.

The photopolymerization of VPA was carried out with 2,2-dimethoxy-2-phenylacetophenone as an initiator in methanol. 2,2-dimethoxy-2-phenylacetophenone belongs to the Irgacure family, and has its maximum absorption at 365 nm. It is one of the most frequently used photoinitiators.

Irradiation of 2,2-dimethoxy-2-phenylacetophenone results in the formation of free radicals, which later initiate the polymerization (Scheme 3.14).

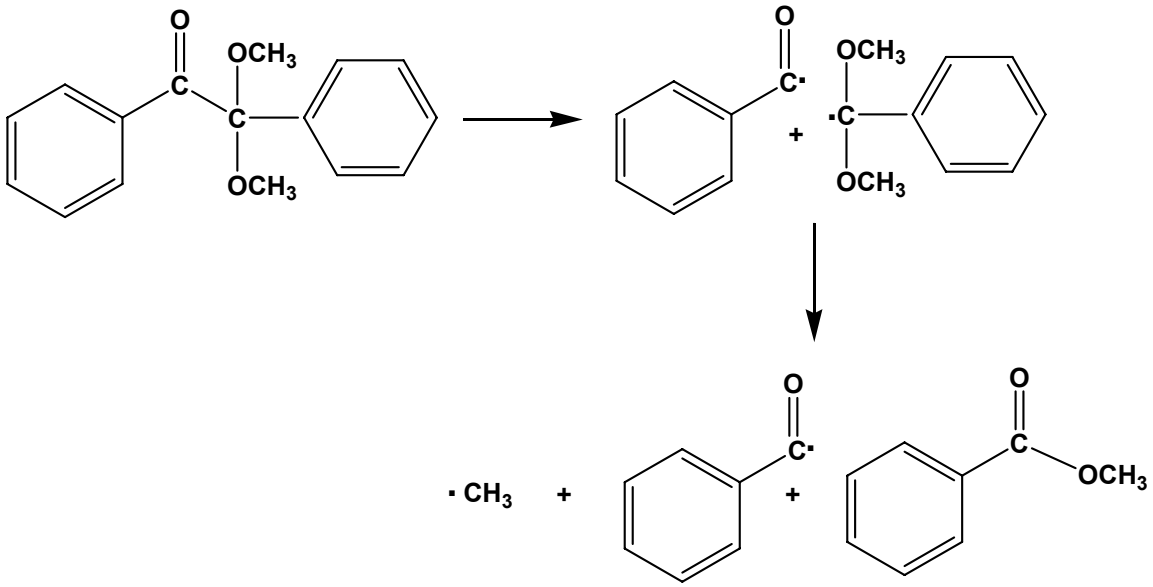

Scheme 3.14: Reactive radical generation by 2,2-dimethoxy-2-phenylacetophenone photo-decomposition[76] .

Redox initiation systems are in common use when the initiation is required at low temperatures. The bond dissociation energy required to cleave the covalent bonds of thermal initiators are in the range of 125-160 kJ/mol. However, the activation energy required is lower (40-80 kJ/mol) in the initiation step of the redox polymerization. This allows the redox polymerization to be carried out under milder conditions than radical polymerization by thermal initiation, which is expected to lower the possibility of side reactions leading to high molecular weight polymers.[77] Redox initiation involves electron transfer from ions or atoms containing unpaired electrons followed by the bond dissociation in the acceptor molecule.

It was tried to initiate the free radical polymerization of VPA by redox pairs because of the advantages of the redox processes. Well-known redox pair for vinyl polymerization (such as ammonium persulfate with N,N,N'N'-tetramethylethylene-

diamine) (TEMED) was used to polymerize vinylphosphonic acid in aqoues medium (Scheme 3.15).

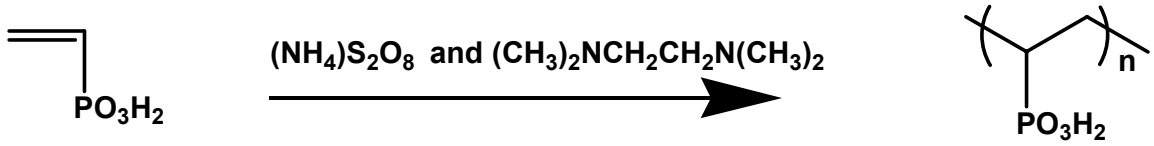

Scheme 3.15: Redox polymerization of vinylphosphonic acid.

Persulfate is one of the commonly used oxidants for the redox polymerization of vinyl monomers. It was used together with TEMED as a reducing agent. Initiation of polymerization can result both from hydroxyl and sulfate radical depending on the reaction conditions, radicals and monomer reactivities.

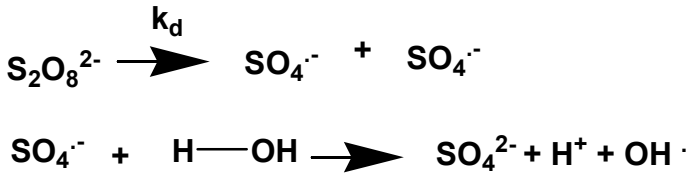

Scheme 3.16: Initiation by ammonium persulfate.

Neither redox nor photopolymerization lead to the polymerization of VPA. In short, it is not possible to carry out the polymerization of VPA at lower temperatures unlike AA and VSA. The reason for this is found in the temperature dependence of the

formation of the anhydride which is not present at T ≤ 80 ˚C in sufficient amount to undergo cyclopolymerization.

The esters of AA, VSA and VPA (DEVP and DISP) can be polymerized by free radical polymerization both with thermal and photoinitiators.

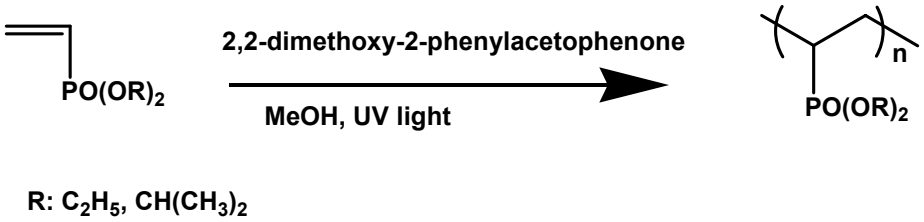

Scheme 3.17: Photopolymerization of vinylphosphonic acid esters.

The photopolymerizaton of DEVP and DISP was carried out with 2,2-dimethoxy-2-phenylacetophenone in methanol (Scheme 3.17). The products were washed with petroleum ether, where the photoiniator is soluble. Only oligomers (5-6 mers) were obtained in both cases as determined by ^{1}H-NMR by comparing the resonances of the benzene ring in the initator with that methine and methylene protons bonded to the P=O in DISP and DEVP, respectively.

Salts of both, AA and VSA are known to polymerize. However, the sodium salt of VPA does not undergo polymerization.*

The esters of AA (such as tertiary butyl acrylate) was polymerized by anionic mechanism to give monodisperse polymers.[78-81] The anionic polymerization of DEVP was carried out with secondary butyllithium as the initiator both in the presence and

* The experiments regarding the polymerization of the salts of vinylphopshonic acid are described in Appendix III.

absence of LiCl in THF (Scheme 3.18). The polymerization was quenched with methanol. LiCl is an inorganic salt that can form complexes with the active species that could prevent the course of anionic polymerization. Adding LiCl to the reaction medium was shown to be an efficient pathway to avoid the secondary reactions in the case of anionic polymerization of alkyl methacrylates and tert-butyl acrylates. LiCl was added to the polymerization medium for the same reason in case of diethylvinyl phosphonate. However, no polymerization was observed.

The experiments were repeated with a sterically hindered initiator (diphenylbutyllitium), which is known to limit the nucleophilic attack on the carbonyl group in polymerization of methyl methacrylate. However, none of these reactions led to the formation of polymer. There is no report about the anionic polymerization of vinylsulfonates.

In conclusion, VPA can not be polymerized at lower temperatures (at room temperature or 40 ˚C) and the sodium salt of this monomer failed to polymerize. This is additional experimental evidence suggesting that the polymerization of VPA does not follow the same mechanism as AA and VSA. As already mentioned, the polymerization of VPA proceeds *via* anhydride formation, which does not form at lower temperatures. This is believed to be the reason why redox and photopolymerization experiments with VPA failed. These observations are consistent with the proposed polymerization mechanism for VPA. Among these three monomers, AA is the only one up to now, the polymerization of which can be carried out in a controlled manner.

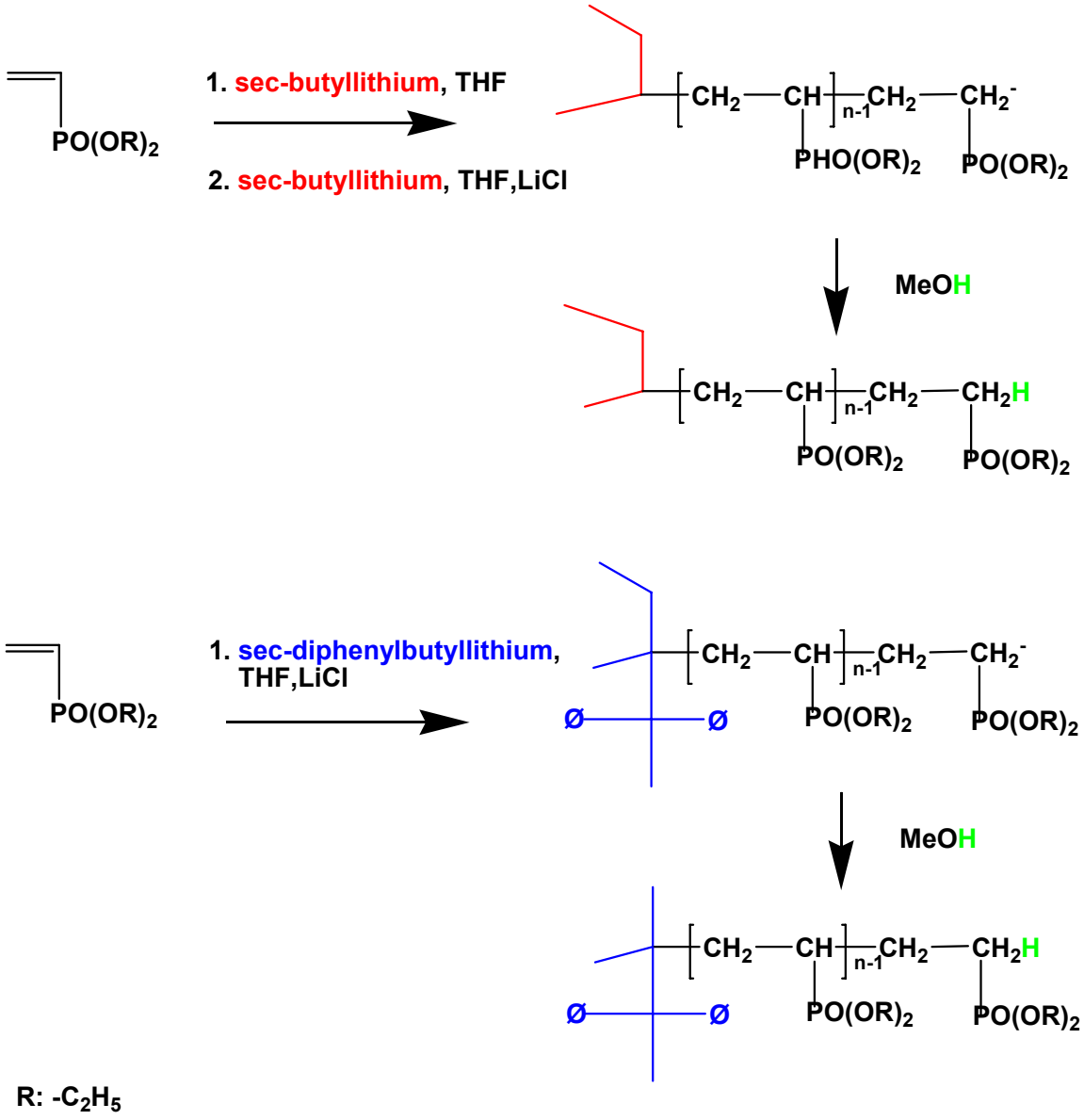

Scheme 3.18: Hypothetic path for anionic polymerization of DEVP.

CHAPTER 4

ACIDITY

4.1 Introduction

Polyelectrolytes are defined as macromolecules with ionizable groups in each repeating unit. There are polyacids, polybases, and polyampholytes depending upon whether the ionizable centers are cationic, anionic or whether a mixture of acidic and basic groups occurs in the chain.

The polyelectrolytes can be distinguished by their behavior against pH variations. Charged polymers are usually termed as strong polyelectrolyte when the charge amount and its distribution along the polyelectrolyte are not sensitive to large pH variations and depend only on the initial chemistry. The iogenic centers are completely dissociated into ions. The number of elementary charges of a fully charged polyelectrolyte should be of the same order as the number of monomeric units (degree of polymerization).[82] They remain fully charged over a wide pH range. Poly(diallyldimethylammoniumchloride),[83] and PVSA[84] may serve as examples for strong polyelectrolytes. On the other hand, when the amount of charged sites varies as a function of pH, and therefore distribution of ionization sites varies along the chain, the polymer is defined as a weak polyelectrolyte such as PAA or poly(methacrylic acid). In other words, an equilibrium between dissociated and nondissociated ionogenic* centers exists.

---

* able to create ions

Polyelectrolytes exhibit properties related to their macromolecular as well as their electrolyte nature. They behave like other macromolecules in their uncharged state. However, perturbations appear upon charging. Their remarkable properties are due to the interference between both types of properties. They have been the research interest of many scientists due to their wide applications. Natural polyelectrolytes (mainly polysaccharides) have been utilized for a long time as thickeners or gelling agents in foods, pharmaceuticals, and cosmetics. Synthetic polyelectrolytes have been applied as dispersants in latex particles. Polyelectrolytes are widely employed as water conditioners and flocculating agents for the treatment of waste water.[82]

Weak polyacids and polybases are characterized by dissociation-association equilibria in solution. The acid-base equilibria of weak polyelectrolytes in solutions have been investigated for many decades.[85]

A carboxylic acid in aqueous solution dissociates as

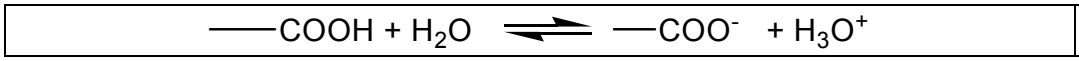

(4.1)

Its dissociation constant, K_a, is expressed by

$$K_a = \frac{(-\mathrm{COO}^-)(\mathrm{H_3O}^+)}{(-\mathrm{COOH})} \tag{4.2}$$

where parentheses denote the activity of each species. Often, however, the conventional dissociation constant, K_0, defined by

$$K_0 = \frac{[-\mathrm{COO}^-][\mathrm{H_3O}^+]}{[-\mathrm{COOH}]} \tag{4.3}$$

is used instead of K_a since the activities of $-COO^-$ and –COOH are unknown, but only their analytical concentrations [in brackets] are known. Therefore, K_0 is not always a true constant, while K_a must be.

The relation between pH and degree of ionization (α) for a carboxylic acid can be stated by Henderson-Haselbach equation (Eq . (4.4)).

$pH= pK_0-\log [(1-\alpha)/\alpha)]$	(4.4)

where the degree of ionization α is defined by

$\alpha = [-COO^-] / [-COOH] + [-COO^-]$	(4.5)

However, in the dissociation of polyelectrolytes an additional amount of work ΔG_{el} is required to remove the proton against the strong electrostatic forces of the charges already present in the molecule. This requires the modification of the Henderson-Haselbach equation (4.4) by,

$pH= pK_0-\log [(1-\alpha)/\alpha)]+0.434\Delta G_{el}/RT$	(4.6)

where pK_0 characterizes a monocarboxylic analogue of the polymer and ΔG_{el} is expressed in terms of electrostatic potential (ψ)

$\Delta G_{el}=e\ \psi$	(4.7)

The dissociation behavior of weak polyelectrolytes in solution is commonly described by an apparent dissociation constant (pK_{app}), which reflects the overall acid dissociation equilibrium of the polyelectrolyte. Due to the electrostatic interactions of the individual charged functional groups along the polyelectrolyte chain, the apparent dissociation constant is strongly influenced by the degree of dissociation and electrostatic screening by added salt.[86] This an important difference between polyelectrolytes and low molecular weight electrolytes, where distinct deprotonation equilibrium constants, due to distinct ionization processes, can be observed. However, for polyacids only average equilibrium constants depending on the ionization degree can be extracted. It is well-known that the apparent acidity of a weak polyacid decreases with progressive ionization of the polymer.[87] It was pointed out by Overbeek that this effect should be associated with the increasing difficulty to remove protons from polyions with increasing charge. A plot of pK_{app} versus α typically shows a monotonic increase in pK_{app} with α in the absence of any conformational change in the polymer. The slope and curvature of such plots are influenced by the concentration of added salt. A high salt concentration suppresses the rise of pK_{app}. The dependence of pK_{app} on the ionization degree is true for linear weak polyacids as well as star-shaped polymers.[88]

The first step in the characterization of a polymeric acid or base is to record its titration curve. PVPA has been studied in this direction in the past by Levin et al.[41] both in the presence and absence of salts. However, it remains unclear how this authors obtained their sample and how the purification was achieved. The titration curve of a high molecular weight sample of PVPA with known microstructure is presented in this

chapter. Additionally, the titration behavior of PVPA is compared with its sulfonic and carboxylic acid analogs at the end of this chapter.

4.2 Titration of Poly(vinylphosphonic acid)

VPA and PVPA is a diprotic and polyprotic acid respectively, where the ionizable groups are attached to a carbon atom, which is a part of a polymer backbone in the case of PVPA. Such monomeric or polymeric acids (bases) are rare. Derivatives of arsonic acid (e.g. ethylene arsonic acid, 2-propenyl arsonic acid, butenyl arsonic acid) and boronic acid (e.g. 2-thienylboronic acid, 1-propene-1-boronic acid) posess two acidic protons at the same center atom. Poly(vinylthiophene boronic acid), and poly(phenylacetylene)s bearing phosphonic acid functional groups are the only examples of polyelectrolytes, where two protons are attached to the same center (Scheme 4.1). However, there is not much known about the titration behavior of such polyelectrolytes. Among these polyelectrolytes, only the titration behavior of poly(acetylene)-based polymers were investigated.[89] Poly(4-phosphonophenyl)-acetylene is a strong polyelectrolyte with a two-step dissociation process. The first step ends at pH= 6 and the second one starts at around pH= 7.5

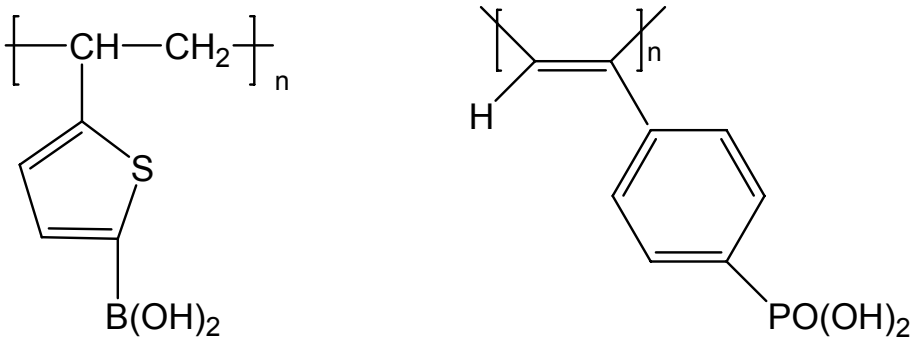

poly(vinylthiophene boronic acid) **poly((4-phosphonophenyl)-acetylene)**

Scheme 4.1: Polyelectrolytes with two acidic protons at the same center.

The titration of VPA, PVPA (1) and PVPA (1) containing low molecular weight salt was carried out with 0.1 N NaOH solution. The development of the pH with the nominal degree of neutralization α is displayed in for a) a salt-free solution of PVPA as purified carefully by dialysis followed by freeze drying, b) a solution of PVPA containing NaCl in a nearly 50 fold excess with regard to the $–PO_3H_2$ groups present in the polymer, where α is the nominal degree of neutralization in terms of equivalents of base added per phosphonic acid group.[72]

For comparison the titration curve of VPA is shown as well. The VPA displayed the expected behavior of a diprotic acid with a pK_{a1} (step1) of 2.74 and pK_{a2} (step 2) of 7.34 and well defined endpoints. The degree of neutralization α is defined as 0.5 for the first step to be completed and as 1.0 for the second step. The slope of the titration curve at the first and second midpoint was found as 100 mV and 168 mV, respectively. For a ideal titration (e.g. titration of a strong acid with a strong base), the slope at the midpoint is around 60 mV. The difference between the slopes of titration curves of VPA and strong acid indicates the deviation from the ideality.

Crofts and Kosolapoff have investigated the dissociation constants of alkylphosphonic acids.[90] The dissociation constants of VPA can be compared with those of alkylphosphonic acid with the same number of carbon atoms, namely ethylphosphonic acid. The first and second dissociation constants of ethylphosphonic acid were found as 2.43 and 8.05, respectively indicating that the first proton of ethylphosphonic acid is easier to dissociate than that of VPA.

Contrary to the monomer, the polymer obtained by its free radical polymerization in its purified form shows an almost linear increase of pH with α up to the nominal degree of neutralization of 0.5, followed by an asymptotic approach of pH to its limiting value at $\alpha = 1.0$. A clear endpoint cannot be identified. Addition of excess NaCl during titration results in a significant change of the titration curve. Again, a clear endpoint cannot be discerned, but the absolute value of pH at any given α is considerably smaller (up to $\alpha \leq 0.8$) as compared to the salt-free polymer indicating a substantial buffer effect. Our titration curve in the presence of excess NaCl resembles the one found in the literature,[41] which had been described as "pure". Figure 4.1 compares our results with those by Levin. We conclude that the experiment described by Levine[41] et al. were probably carried out for a sample which still contained much neutral salt.

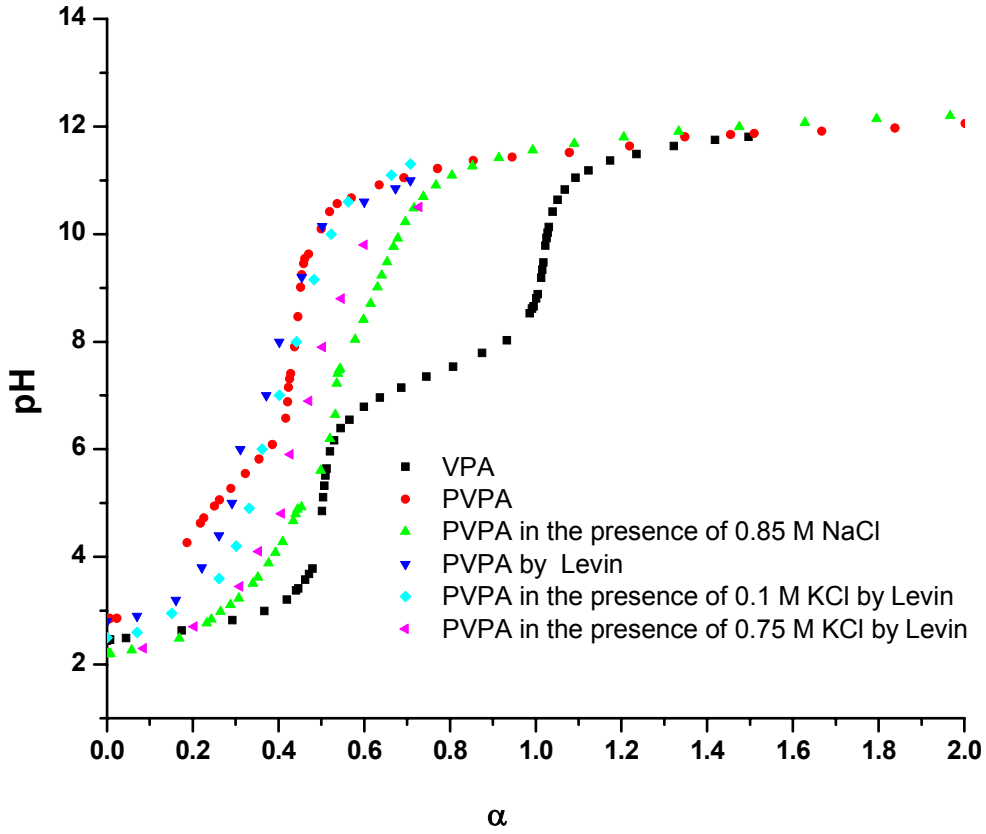

Figure 4.1: Titration curves of VPA, salt-free PVPA, and PVPA in the presence of excess (0.85 M) NaCl, "pure" PVPA by Levin, PVPA in the presence of 0.1 M and 0.75 M KCl by Levin; α is the nominal degree of neutralization in terms of equivalents of base added per phosphonic acid group

The dependence of the apparent dissociation constant of weak polyacids on the salt concentration in aqueous solution and on the nominal degree of neutralization has been discussed in literature.[86] It is worth pointing out that even in the presence of neutral salt, it seems to be impossible to dissociate the second proton from the already

deprotonated phosphonic acid groups in the polymer for electrostatic reasons and consequently PVPA behaves more like a monoprotic acid. Shortly, PVPA exhibits the characteristic features of polyelectrolytes in solution, which can be deduced from evaluation of its titration behavior.

4.3 Titration of Poly (acrylic acid)

The potentiometric titration of PAA has been studied over a range of salt and polymer concentrations from both, experimental and theoretical points of view since it is the simplest common synthetic polycarboxylic acid.[74, 86, 87, 91-93] The study of the solution behavior of PAA in its partially or fully ionized form has a profound importance from the theoretical viewpoint since it is widely used as a model of 'normal' behavior to be expected from the polyelectrolytes in general.

The titration curve of PAA and PAA in the presence of a neutral salt is presented in Figure 4.2. For comparison, titration curve of AA is also shown. AA is a monoprotic acid with pK_a of 4. 76 and has a well defined endpoint.[72] The titration curves of PAA differ considerably from the monomeric acid. It is apparent that the electrostatic interactions play an important role in the solution behavior of PAA. Titration curve of PAA demonstrates that the acidity of the polymeric acid decreases continuously upon neutralization.

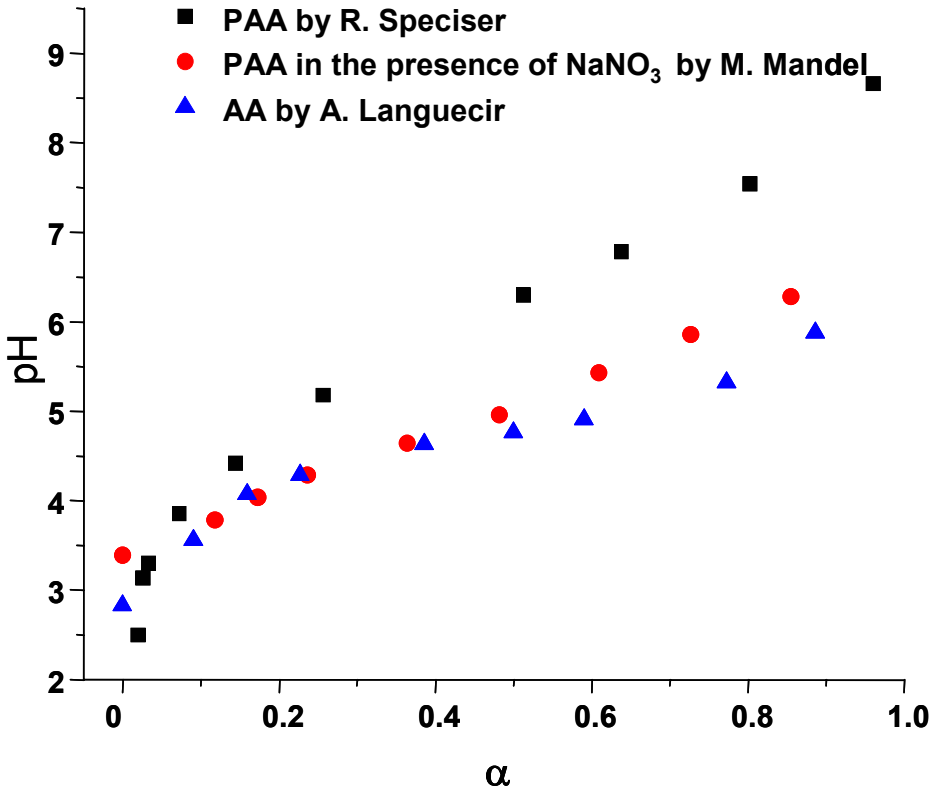

Figure 4.2: Potentiometric titrations of AA, [94] PAA,[95] and PAA in the presence of 0.2 M $NaNO_3$[82].

Early work on the potentiometric titration of polylelectrolytes revealed that the titration curve of polyelectrolytes are independent of their molecular weight.[96] However, very recent potentiometric titration experiments with different molecular weight samples of PAA displayed the chain length effects on the titration curves of PAA. The titration behavior of PAA with molecular weight M_w equal to 1800, 5000, and 50 000 Da are investigated. [94] The titration curves of different molecular weight PAA were compared in terms of their pH at half neutralization ($\alpha = 0.5$). The lowest molecular weight PAA had a pH value of 5.98, whereas when the degree of polymerization was increased from 25 to

700, the pH value went up to 6.62 at α= 0.5. The PAA sample with 70 repeating units had a pH of 6.36 at α equal to 0.5. However, it is difficult to understand why there should be such a strong dependence on the molecular weight.

The titration curve of PAA ($5.5x10^{-3}$ M) in the presence of a low molar mass electrolyte (0.2 M $NaNO_3$) is shown in Figure 4.2.[82] The titration of PAA in the presence of sodium nitrate shows the absence of a buffer region and a monotonous increase of the pH with increasing degree of dissociation. In other words, the logarithm of the apparent dissociation constant, pK_{app} increases steadily with ionization degree. This continuous increase in pK_{app} explains the absence of a buffering effect. Additional work is required to transfer the proton from the newly formed polyion to the bulk against the attraction of the negatively charged polyion. As the concentration of low molecular weight salt was increased, the increase in pK_{app} was suppressed implying the possibility of a higher number of protons to be dissociated as expected due to the electrostatic screening.[87]

4.4 Titration of Poly (vinylsulfonic acid)

PVSA is the simplest strong polyacid. It is a polymer with interesting features from the scientific viewpoint. For instance, it can be regarded as a model compound for naturally occurring sulfuric acid esters of polysaccharides as well as a model for ion exchangers.[70]

Potentiometric measurements proved that PVSA displays a titration behavior which is entirely analogous to strong acids such as hydrochloric acid apart from the low activity coefficients of the protons due to the electrostatic potential of the macromolecule.[65] Figure 4.3 presents the titration behavior of PVSA both in the presence

and absence of salt, as well as titration behavior of hydrochloric acid and ethanesulfonic acid for comparison. Hydrochloric acid and ethanesulfonic acid are strong acids and their titration curves display the expected increase in pH with increasing degree of neutralization.The titration curves of PVSA in the presence and absence of NaCl are parallel to each other. Addition of NaCl (0.1 M) screens the large electrostatic potential off leading to a decrease in pH value. All points determined in the polyelectrolyte titration in the presence of low molecular weight salts lie on the HCl titration curve. In other words, the titration curve of PVSA in the presence of salts resembles to the titration curve of low molecular weight acids. [97] A straight line with slope of 1 was obtained upon plotting pH versus the logarithm of $(1-\alpha)/\alpha$ for ethanesulfonic acid and PVSA. This indicates that the dissociation constant of PVPA stays constant along the whole concentration regime as in the case of ethanesulfonic acid. These results are strange and contradictory to the contribution of ΔG_{el} to the titration behavior. As already indicated in section 4.1, additional amount of work (ΔG_{el}) is necessary to remove proton against the strong electrostatic forces of the charges already present in the molecule. Therefore, the titration curves of PVPA in the presence of a neutral salt cannot overlap with that of HCl. The results present in the literature regarding the titration behavior of PVSA indicates that PVSA samples used for titrations contain some low molecular weight species as impurities. The low molecular species may be the rests of monomer or salts, which could not be removed entirely during the purification step. Eisenberg and his coworkers purified the PVSA by dialysis after polymerization of VSA. Kern et. al. polymerized sodium salt of VSA and converted the polymer to its free acid form by addition of HCl, the precipitate, NaCl, was removed from the medium by dialysis. However, complete

removal of salts from polyelectrolytes is very difficult. Shortly, bearing the purification steps used to obtain PVSA and the contribution of of ΔG_{el} to the titration behavior, the titration curves of PVSA were obtained with polymers of low purity.

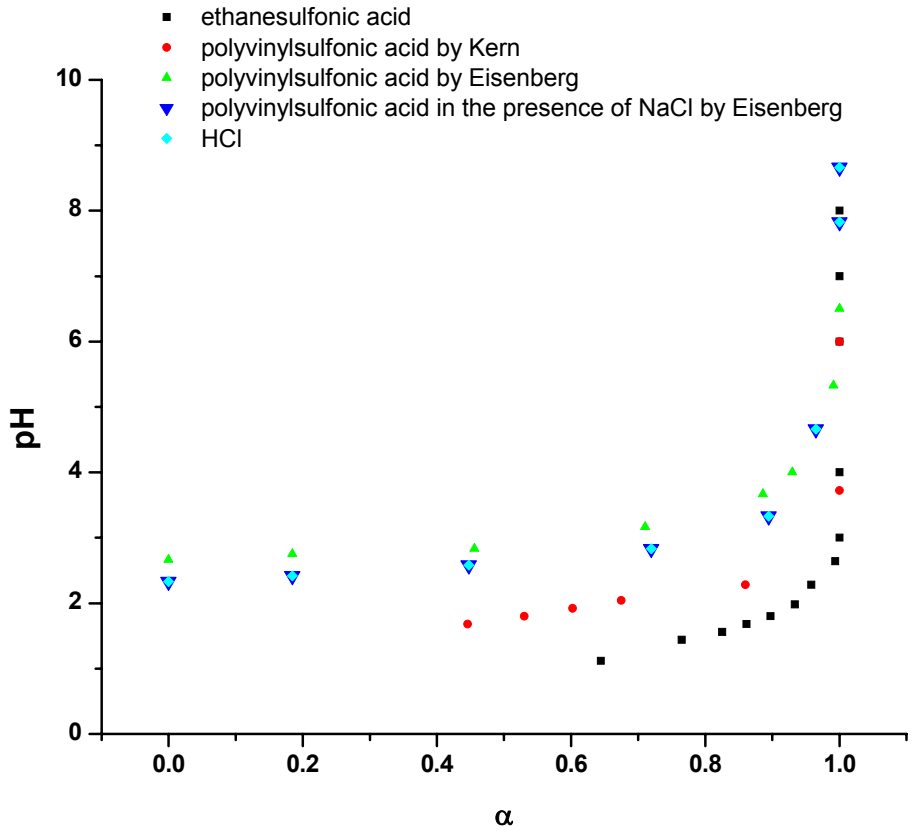

Figure 4.3: Potentiometric titrations of ethanesulfonic acid, and PVSA by different authors, and PVSA in the presence of NaCl[65, 97], and HCl; α is the nominal degree of neutralization in terms of equivalents of base added per sulfonic acid group.

4.5 Comparison of titration behavior of PVPA, PVSA, and AA

PVPA, PAA, and PVSA are the simplest cases of polyacids. They are analogs of each other (Scheme 4.2). They all exhibit the characteristic features of polyelectrolytes in their aqueous solutions. PVPA and PAA are weak polyelectrolytes, whereas PVSA is a strong polyacid. Therefore, the complications such as partial ionization that is encountered with PAA, and PVPA do not arise in the case of PVSA.[70, 97]

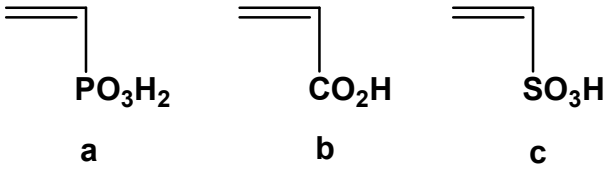

Scheme 4.2: Chemical structures of a) VPA b) AA c) VSA

One can compare the acidity of VPA with that of AA by the help of their dissociation constants. VPA (pK_{a1}=2.74) is a stronger acid than AA (pK_a=4.76). Their polymeric forms are similar in that their acidity decreases continuously upon increasing degree of neutralization, which can be followed by a monotonous increase of pH. There is a remarkable difference between their monomeric and polymeric forms in their pH value at half-neutralization (α= 0.5). The difference in pH between VPA and its homopolymer is 4.49 at α= 0.5, whereas this difference in the case of PAA ranges from 1.22 to 1.86 depending on the molecular weight of the polymer. This difference was suppressed by the addition of excess low molecular weight salt to the medium to 0.13 in the case of PVPA and the absolute value of pH at any given α is considerably smaller (up to α≤ 0.8) as compared to the salt-free polymer indicating a substantial buffer effect.

PAA displayed a similar behavior upon addition of neutral salt, the difference in the pH between AA and PAA was decreased to 0.44 at α= 0.5. However, the addition of neutral salts did not lead to the observation of well-defined end-points neither in PVPA nor in PAA.

PVSA is a much stronger acid compared to both PVPA, and PAA. The dissociation behavior of PVSA cannot be compared with those of PVPA, and PAA. Upon titration, there are two possibilities about the placement of dissociated protons. It is possible that these protons are still in the attraction sphere of the polyanion or they can diffuse to the solution. This is valid for PVPA, PAA, and PVPA. It is difficult to exclude one of the possibilities. There might be some of protons in the attraction sphere of the polyion, and the rest in the solution. In case of PVSA, more protons should be localized in the dilute solution than in the vicinity of the polyion. However, it is known that the number of sodium ions of the sodium of polyacrylate is very low in the solution.[70] Therefore, it can also be expected that the number of protons will be much higher in the close vicinity than in the solution for PAA, and PVPA in contrast to PVSA. Additionally, the titration curves of PVSA are contradictory to the contribution of ΔG_{el} to the titration behavior.

As a conclusion, the titration behavior of high molecular weight PVPA with known microstructure was investigated by potentiometric titration. These results were compared with the titration behavior of PAA, and PVSA, which were already documented.

CHAPTER 5

MICROSTRUCTURE

5.1 Introduction

Free radical polymerization is an important method for preparing polymers. The propagation step of radical polymerization comprises a sequence of radical additions to the carbon-carbon double bond. During the growth of a typical vinyl polymer, an asymmetric center is created every time a monomer molecule adds to the propagating chain end. This introduces the possibility of stereoisomerism, since the new asymmetric center has either the same configuration as the asymmetric center that is its immediate predecessor or the appropriate counter configuration. Carrying out the synthesis under such conditions that both types of additions are possible will lead to the production of a polymer with a large number of stereoisomeric forms.

Most monomers give rise to a chiral center (Scheme 5.1) due to their asymmetric substitution pattern and their polymers will have tacticity. In vinyl monomers the substituted carbon is termed as the α carbon and is pseudosymetric since if the chain ends are disregarded, these carbons do not have four different substituents to be classified as an asymmetric.[54] (Two valances of a backbone carbon atom are bound to sections of the polymer which may differ in the length, but are identical in the neighborhood of the carbon atom under consideration).

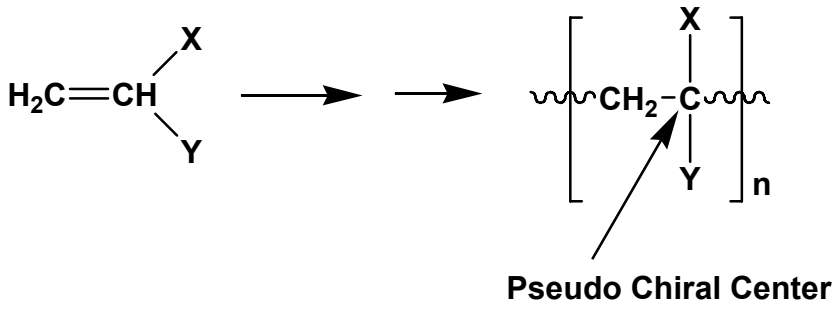

Scheme 5.1: A representation of a homopolymer chain with a pseudo chiral center.

If all monomer units are added in the same direction during the polymerization, a regioregular structure will be formed. However, it is possible that some of the monomers are added to the polymer chain in the inverted direction which will result in a regioirregular structure. This is referred as regioisomerism. The predominant head-to-tail structure may be interrupted by head-to-head and tail-to-tail linkages (Scheme 5.2). In other words, addition to double bonds may not be completely regiospecific.

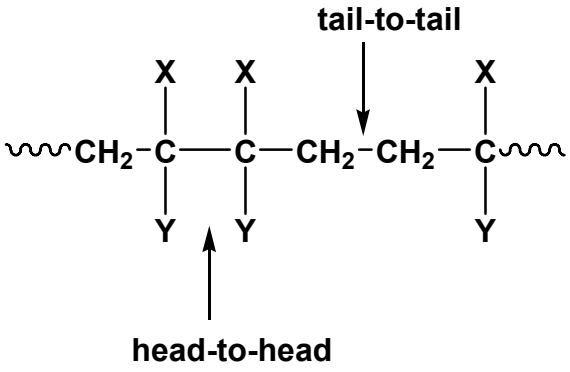

Scheme 5.2: Head-to-head and tail-to-tail linkages.

The words isotactic, syndiotactic, and atactic are used to describe the different sterosequences in vinyl polymers (Scheme 5.3). The polymer chains are called isotactic if the substituents X, and Y are on the same side of the zigzag backbone plane, i.e. they have identical configuration. Syndiotactic chains are formed if the substituents alternate from side to side, i.e. they have opposite configurations. Both isotactic and syndiotactic chains are stereoregular structures. The atactic structure is characterized by an irregular, random arrangement of neighboring substituent groups on either side of the backbone. These stereochemical isomers can be presented with either a three dimensional (Scheme 5.3a) or a two dimensional projection (Scheme 5.3b), called "Fischer Projection".[98]

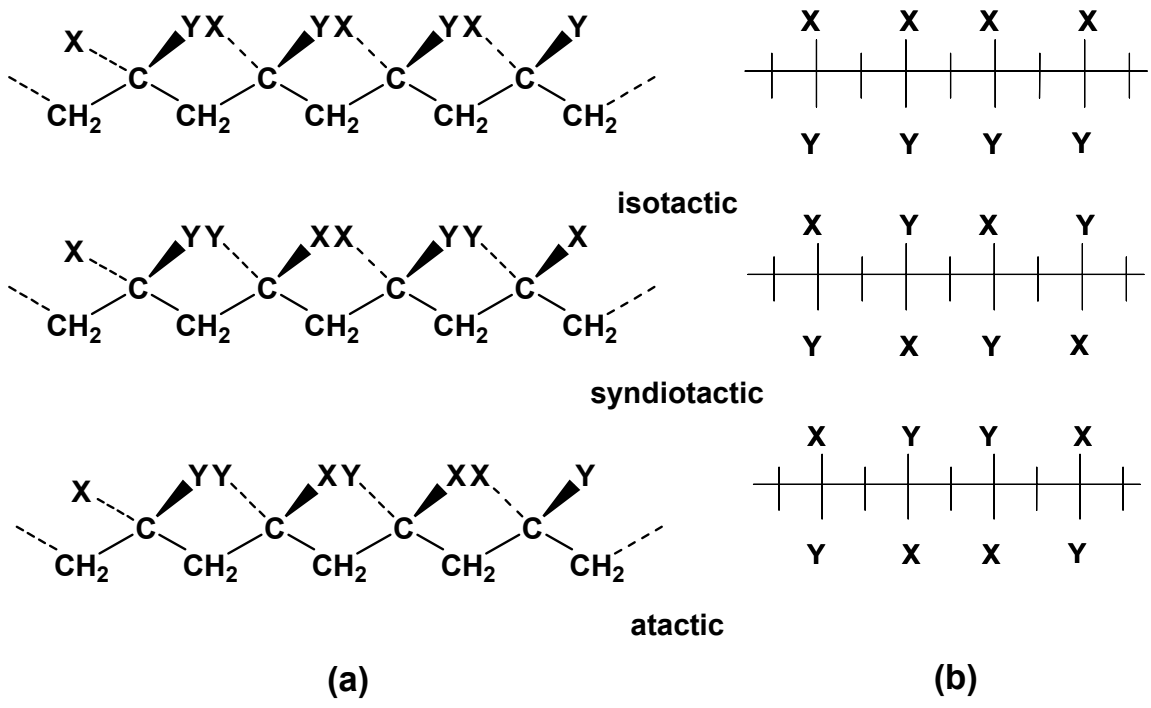

Scheme 5.3: Different possible stereochemical arrangements in a) three dimensional b) in two dimensional representation.

In treatment of polymer stereochemistry, one only deals with relative configurations. In other words, stereochemistry of polymers reveals information about whether an asymmetric carbon atom is surrounded by like or dislike further asymmetric centers. Therefore, the smallest structural unit which contains stereochemical information is the diad. The diads are of two types: meso (m) and racemic (r). A meso diad has two chiral centers of like configuration. On the other hand, two chiral centers have opposite configuration in a racemic diad (Scheme 5.4).[54] It is usual to discuss triads, tetrads, pentads, etc. in terms of the consitutents of diads.

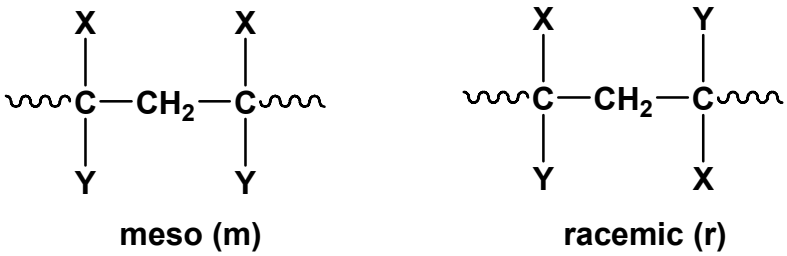

Scheme 5.4: Types of diads.

One of the earliest methods used for obtaining information about stereoregularity in polymers was to compare the solution NMR spectra of a polymer with those of a model compound and other polymers. For example, 2,4,6-trimethyl heptane was used as a model compound to study the stereochemical isomerism in polypropylene. The NMR-peak assignments can be established by comparing the spectra of the polymer to those from the isotactic, or syndiotactic polymers if they are available.

Statistical methods can be used to establish the chemical shift assignments of the polymers based on the relative intensities of peaks in case the statistics of the chain propagation are known or can be determined. Different statistics such as Bernouillian and

Markovian are avaible to describe the chain growth. The statistics of the propagation step can be described by Bernouillian statistics only if the chain end does not influence the stereochemistry of the addition of the monomer. When a monomer is added to the growing chain, the relative fraction of m and r diads are determined by the addition probabilities P_m, and P_r. In many cases, resolution of higher order n-ads is possible by NMR spectroscopy, and these peaks can be assigned applying the chain statistics. For Bernoullian type chain propagation the probabilities for the tetrad sequences are given by the following equations:[99]

$(mmm) = P_m^3$	(5.1)
$(mmr/rmm) = 2 P_m^2 (1- P_m)$	(5.2)
$(rmr) = P_m (1- P_m)^2$	(5.3)
$(mrm) = P_m^2(1- P_m)$	(5.4)
$(rrm/mrr) = 2 P_m(1- P_m)^2$	(5.5)
$(rrr) = (1-P_m)^3$	(5.6)

Note that the sequences mmr and rmm are not distinguishable for chains which do not have a directional sense, i.e. reading from either end gives the same configuration. This is true for most vinyl polymers.

If diad sequences are considered by the evaluation of possible different configurations of vinyl homopolymers, there are four possible diads, two of which can be distinguished because methine carbons are not true asymmetric centers. There are eight possible triads, only three are distinguishable. Similarly, only six out of possible sixteen

tetrads are unique. The number N (n) of distinguishable types of sequences containing n monomer units is given by [100]

$N(n) = 2^{n-2} + 2^{m-1}$	(5.7)

where m = n/2 for even n and m = (n-1)/2 for odd n.

The polymer chain statistics can provide information about the assignments.

The NMR spectrum is very sensitive to stereochemical isomerism in a variety of polymers. The resolution of the spectra depends on a number of factors such as the nuclei under observation. The proton spectra of polymers are frequently the easiest to acquire. However, they may not be as informative as the carbon spectra for stereochemical characterization. The reason for that is because protons have a small chemical shift range, and differences in chemical shifts between the stereosequences are often small. Other than stereochemistry, NMR can also provide information about the polymer molecular weights by qualitative detection of the chain ends.

Investigating the stereochemistry of polymers is very important since many properties of polymers have been shown to depend on the stereochemistry.[101] Significant stereocontrol of free radical polymerization of vinyl monomers has never been achieved. Mostly atactic polymers do result from free radical polymerization. However, the control of stereochemistry in free radical polymerization is a significant goal since it is a convenient method to produce polymers. The degree or level of stereocontrol in a polymerization reaction is determined by indicating the tacticity of the resulting polymers. Investigation of stereochemistry of polymers also gives insight to their polymerization mechanism. Therefore, we studied the stereochemistry of PVPA prepared

by the free radical polymerization. Chapter 5 gives a detailed analysis of the microstructures of PVPA synthesized by different pathways, which enabled us to suggest the polymerization mechanism of VPA. Additionally, the influence of temperature, pH, and molecular weight of PVPA are discussed on the basis of the NMR spectra.

5.2 Microstructure of Poly(vinylphosphonic acid)

Two synthetic pathways are described to synthesize PVPA by free radical polymerization (Chapter 3). One of these pathways starts with VPA as monomer. The other route concerns first the polymerization of the dimethyl ester of vinylphopshonic acid, which is later hydrolyzed to obtain PVPA (Scheme 3.1). The microstructures of these polymers were investigated by NMR spectroscopy and compared on the basis of their ^{1}H-, ^{13}C-, and ^{31}P-NMR spectra.

5.2.1 NMR Spectra of PVPA and Solvents

The microstructure of PVPA was investigated by NMR spectroscopy in solution, which requires the complete dissolution of the polymer in a deuterated solvent. The choice of solvent is important to be able to record high resolution NMR spectra of the polymers. Other than dissolution of the polymer in the suitable solvent, the NMR spectra have to be recorded in solutions of low viscosity to achieve the necessary small line width. The width of the resonance depends on the local structure and the molecular dynamics in the vicinity of the observed nucleus. A narrow line width is essential for identification and analysis of the configuration (tacticity) of the polymers.

We first studied the availability of the NMR solvents that can dissolve PVPA (1). PVPA is a polyacid and dissolves in deuterium oxide very well. However, the solvent

spectrum for PVPA is limited. Other than in water, it can be dissolved in d-methanol, d-concentrated sulfuric acid. However, only dilute solutions of PVPA can be prepared in the solvents other than water. Therefore, it was only possible to record ^{1}H-NMR spectra of PVPA with its dilute solutions in various solvents (Figure 5.1). The ^{1}H-NMR spectra of PVPA display broad resonances generally. There can be several reasons why the line width of the resonances is large. For example, d-sulfuric acid is a viscous solvent, and the viscosity of the solvent affects the rate of local motion. High resolution NMR spectra can only be obtained if the local motions of polymer chains are rapid such that local magnetic couplings are averaged out. Moreover, all the solvents mentioned above are capable of undergoing hydrogen bonding with PVPA, which may also decrease the relaxation rates of the polymer. The stiffness of the polymer backbone may also affect (decrease) the local motion of the polymer. In other words, non-zero dipole-dipole interaction due to the low mobility will increase the width of the signals. The best resolution of the ^{1}H-NMR spectra of PVPA was obtained in deuterium oxide. Five peaks can be resolved although they are broad and some of them overlap with each other. Therefore, deuterium oxide was chosen as the most suitable solvent for the investigation of the microstructure of PVPA. Additional advantage of deuterium oxide is that concentrated solutions of PVPA can be prepared in this NMR solvent. Note that the positions of the resonances due to the polymer backbone protons varies slightly in methanol-d_4, and deuterium oxide which may be due to the differences in the surrounding medium of the protons. Moreover, the strength of the hydrogen bonds may vary depending on the solvent which will lead to a shift in the positions of the resonances.

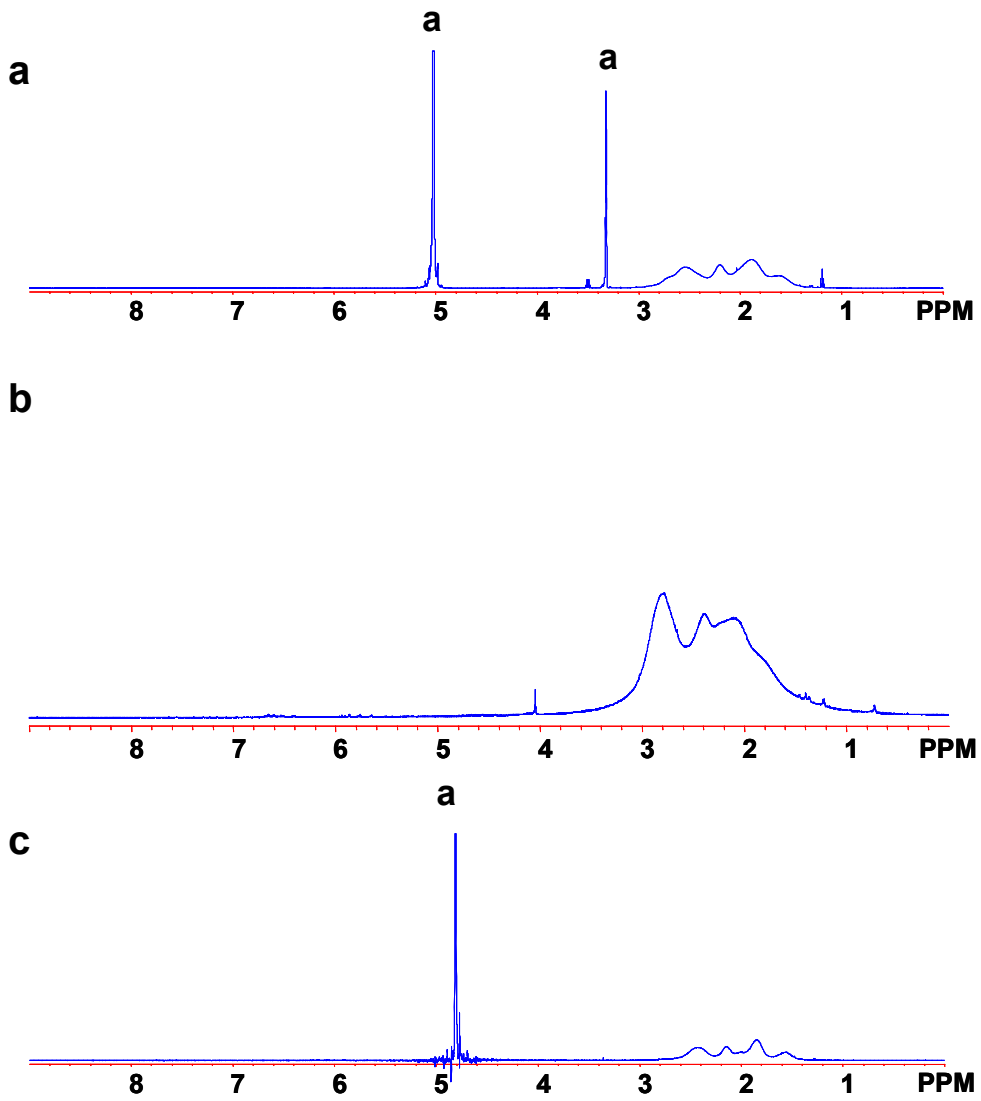

Figure 5.1: ^{1}H-NMR (500 MHz) spectra of PVPA in a) methanol-d_4 b) sulfuric acid-d_2 d) deuterium oxide (signals originating from the solvent medium is indicated by "a").

5.2.2 Microstructure of PVPA from the Direct Route

^{1}H-, ^{31}P-, and ^{13}C-NMR spectra of PVPA were studied in solution in detail to gain information about the microstructure of PVPA.

The ^{1}H-NMR spectrum of PVPA (1) has five resonances located at 2.28, 2.03, 1.18, 1.75, and 1.46 ppm. The signal at 2.28 ppm was assigned to the methine protons. This assignment was supported by the observation that the intensity of the signal at 2.28 ppm was just half of the sum of the intensities of all other peaks. The rest of the signals originated from the methylene protons. The intensities of the resonances belonging to the different methylene protons were obtained by deconvolution.

As described in Chapter 3, the polymerization of VPA proceeds via cyclopolymerization of its anhydride Scheme 3.6. Temperature plays an important role in the course of polymerization since it affects the equilibrium between VPA and its anhydride, and the formation of the VPA anhydride intermediate can be enhanced by increasing the temperature during the polymerization. After the polymerization, applying any heat treatment leads to the formation of phopshonic acid anhydride species by release of water, which results in the formation of rings. The formation of the anhydride species depends greatly on the temperature. This has been proved by Solid State NMR studies (Chapter 6). Therefore, it was of interest to investigate whether any of the above mentioned resonances in the ^{1}H-NMR spectrum of PVPA (1) has a temperature dependency. In other words, we investigated the change in the chemical shift and intensity of the resonances of PVPA (1) at different temperatures in solution. For that purpose, ^{1}H-NMR spectra of PVPA (1) were collected in deuterium oxide at 303, 323, and 353 K (Figure 5.2).

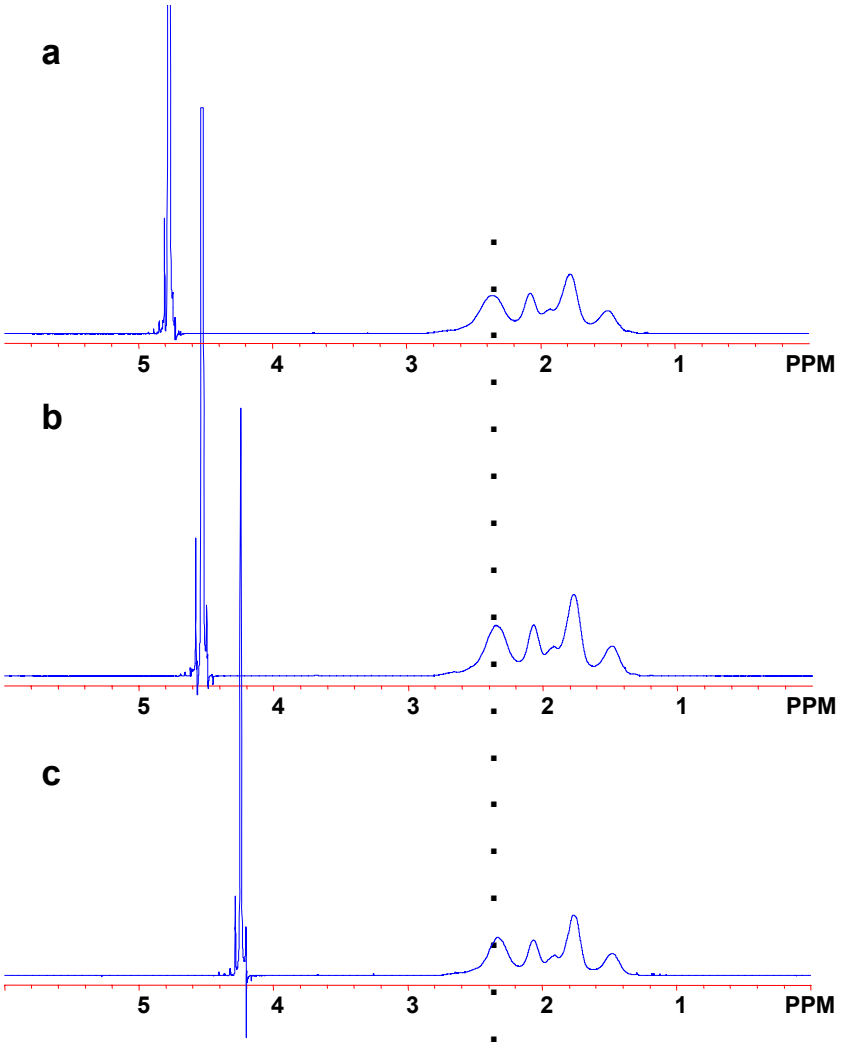

Figure 5.2: ^{1}H-NMR (500 MHz) spectra of PVPA (1) (50 mg/0.8 mol D_20) at a) 303 b) 323 c) 353 K (dots (…) on the spectra are placed in the center of the methine resonance at 303K).

All three spectra above were calibrated by the chemical shift of the DOH water peak, which changes depending on the temperature The change of the position of DOH resonance with the temperature has been attributed to the temperature dependence of the water hydrogen bonding.[102]

After calibrating the spectra taken at different temperatures with the corresponding chemical shift of HDO, very little change in the position of the resonances of PVPA (1) was observed at various temperatures. The change becomes more clear if the chemical shift of the methine resonances at various temperatures are given in Table 5.1. The center of the methine resonance shifts by 1.7% and 2.5% to higher field in the spectra recorded at 323K and 353 K, respectively when compared to the chemical shift of methine signal at 303K. The small changes seen may be due to the different dissociation degree of PVPA at various temperatures. However, the peak intensities did remain almost the same. In other words, none of these five resonances are temperature dependent, and it is not possible to observe the presence of the anhydride species by ^{1}H-NMR in solution.

Table 5.1: Chemical shift of the methine resonance at various temperatures.

Temperature (K)	**Chemical shift of methine resonance**
303	2.38
323	2.34
353	2.32

The chemical shifts in molecules like carboxylic or amino acids may have a strong dependence on pH.[103] Differences in pH may also affect the NMR spectra of PVPA since it is a polyacid. Therefore, PVPA solutions were investigated at various pH in terms of both proton and phosphorous nuclei.

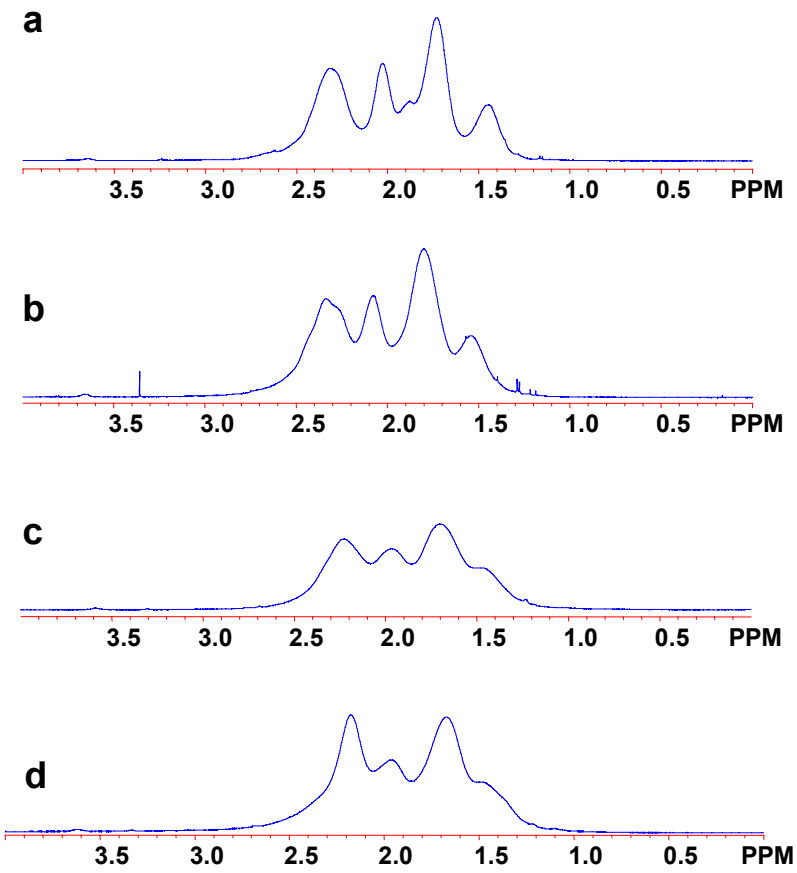

Figure 5.3: ^{1}H-NMR (500 MHz) spectra of PVPA (1) (50 mg/0.8 mL D_20) at pH= a) 1.1 b) 3.9 c) 7.3 d) 10 at 303 K.

Line broadening was observed with increasing pH when the ^{1}H-NMR spectra of PVPA at different pH were compared. As the line width of the resonances are increasing with increasing pH, it becomes more difficult to differentiate the five resonances which were observed in the ^{1}H-NMR spectrum of PVPA in its natural pH since the bandwidths of the resonances are increasing, and the signals start to overlap. For example, the shoulder at

the left side of the resonance at 1.80 ppm cannot be separated from the main resonance any more at pH= 3.9, 7.3 and 10. As pH increases, some of the phosphonic acid groups are deprotonated. In other words, some of the protons will be replaced by the sodium ion since the titrant was a NaOH solution. Therefore, the polymer chain will contain ONa groups in addition to OH groups at the phopshonic acid functionality. However, deprotonation did not give rise to additional peaks due to the replacement of the proton by sodium ion. Most probably, the spectrum containing the effect of neutralization is an average spectrum. The chemical shifts are only average values for protonated and deprotonated species due to a fast proton exchange between protonated and deprotonated species. Therefore, although no additional resonances were observed, slight shifts in the positions of the resonances are due to the differences in pH. At this stage of study, it would not be correct to correlate the peak position with the absolute values of pH since the solutions were prepared in D_20 for NMR measurements, and their pH were measured with a pH electrode calibrated with H_20-based buffers. A correction of 0.4 has to be added to pH meter readings to get pD values, which was not done during the calibration of pH electrode. The pH dependence of NMR spectra has already been reported in the literature for PAA.[104] It was shown that variations in pH cause a shift in the peak positions of the carbonyl carbon and the methine carbons of PAA. Deprotonation with increasing pH resulted in a down field shift of each resonance. Moreover, the resolution of the spectra was influenced by the variations in pH. There was no fine structure apparent in the spectra at low pH, whereas at high pH the peak resolution for the methine carbon was good, but poor for the methylene carbons.

The temperature dependence of PVPA solutions at different pH was investigated by increasing the temperature from 303 K to 353 K at constant pH. Increasing temperature lead to narrowing so that the resonances at high pH solutions have a better resolution, At 353 K it was possible to observe five resonances for the PVPA solution at pH= 10. The intensities of the resonances did not change with varying the temperature beyond the experimental errors that are due to the deconvolution of very closely located peaks.

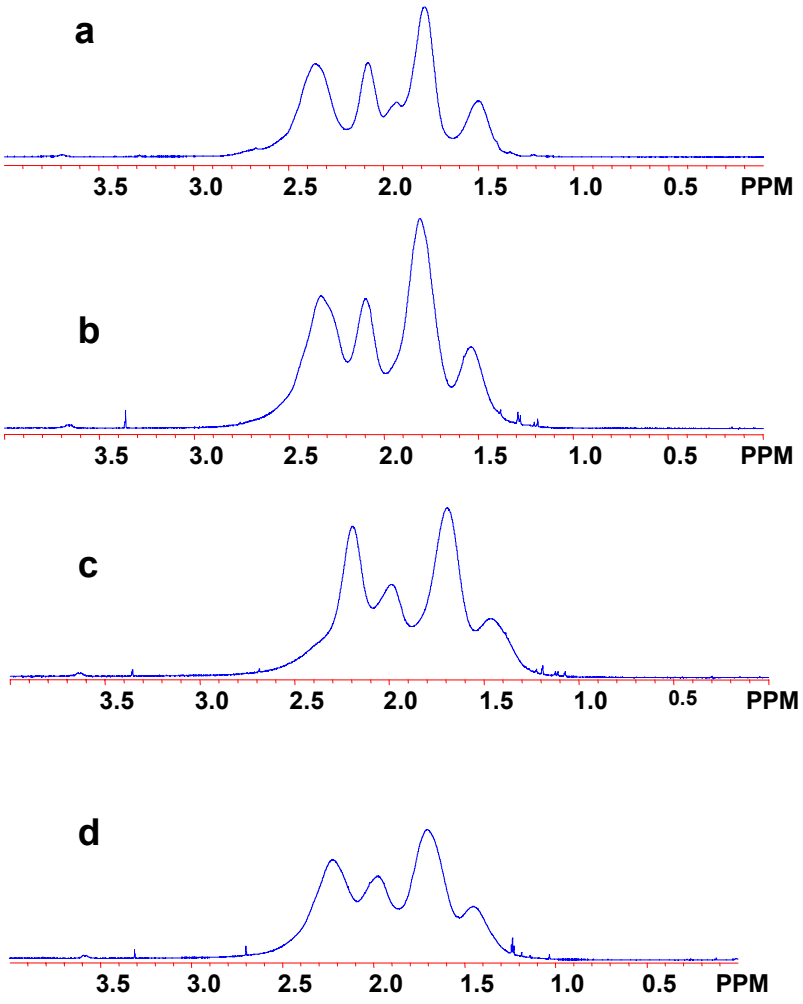

Figure 5.4: ^{1}H-NMR (500 MHz) spectra of PVPA (1) (50 mg/0.8 mL D_2O) at pH= a) 1.1 b) 3.9 c) 7.3 d) 10 at 323 K.

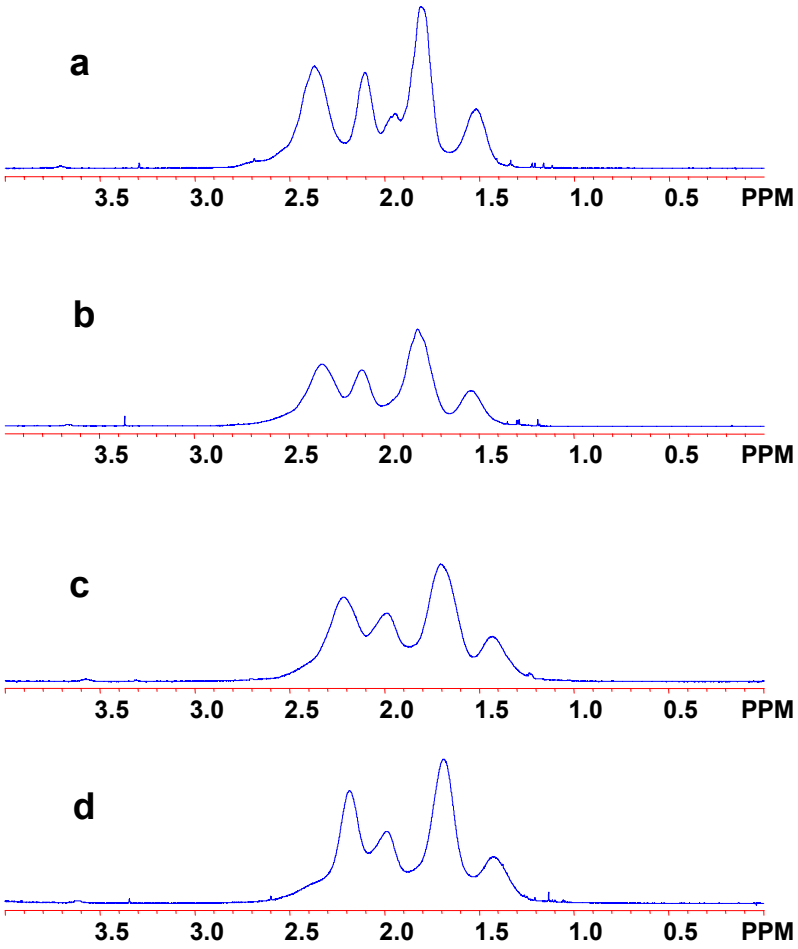

Figure 5.5: ^{1}H-NMR spectra of PVPA (1) (50 mg/0.8 mL D_2O) at pH= a) 1.1 b) 3.9 c) 7.3 d) 10 at 353 K.

PVPA possesses a heteroatom in its structure, namely phosphorous. Phosphorous has only one single isotope, ^{31}P, which is NMR active with a spin of ½. The sensitivity of ^{31}P is high, similar to ^{1}H. Therefore, the measurements do not require high sample concentrations. The chemical shift range of ^{31}P is much wider than that of ^{1}H or ^{13}C.

^{31}P-NMR spectra of PVPA solutions at different pH were collected. The ^{31}P-NMR spectrum of PVPA (1) contains a main resonance at 29.8 ppm and another less intense resonance at 21.5 ppm at its natural pH. The main resonance at 29.8 was assigned to the phosphorous atom at the phosphonic acid functionality, and the other peak was attributed to the phosphonic acid anhydride group, the assignment of which was based on the positions of the resonances of P=O and P-O-P group in the bulk solid state. The phosphonic acid anhydride species were found to resonate at 25 ppm in solid state. The phosphonic anhydride species can form both during synthesis or drying. Solid State NMR experiments gave the fraction of anhydride species as 14% after drying the polymer at 50˚ C to constant weight. However, the relative intensity of the resonance assigned to the anhydride species in solution is only 2.3% of the total integration, which is not matching to the results from the solid state NMR studies. It was already mentioned in Chapter 3 that quite rapid hydrolysis of the phosphonic acid anhydride takes place in water and free acid is formed. The same happens to some extent when PVPA is dissolved in deuterium oxide. The reason why the resonance due to the vinyl phosphonic acid anhydride still exists may be due the incomplete hydrolysis, and the intensity of this resonance should be related to the equilibrium concentration of phosphonic acid anhydride species under these temperature and solvent concentration. The quantification of the resonance of 21.5 ppm reveals the fraction of the anhydride species left as 2.3% after dissolving PVPA in deuterium oxide. The anhydride species could only be observed in the case of concentrated solutions of PVPA (50 mg/0.8 mL D20). The investigation of the temperature dependence of the phopshonic acid anhydride resonance did not show any change with increasing temperature. In other words, ^{31}P-NMR enables us to observe the

resonances belonging to the anhydride groups in solution, unlike ^{1}H-NMR*. However, the growth of the anhydrides can not be followed neither by ^{1}H- nor by ^{31}P-NMR in solution since the presence of water reverses the process.

Table 5.2: Comparison of ^{31}P-NMR data of different PVPA samples in solution and in the solid state

Polymer	δ (P=O)	δ (P-O-P)	% (P-O-P) by Solution NMR	% (P-O-P) by Solid State NMR
PVPA (1)	29.8	21.5	2.3	14
PVPA (4)	31.26	23.0	5.6	9

Increasing pH did affect the ^{31}P-NMR similar to the ^{1}H-NMR spectra of PVPA. Line broadening of the main resonance was observed with increasing degree of neutralization. However, resolution of the peaks was not affected in the same way as in the case of ^{1}H-NMR. Increasing bandwidth of the main resonance allowed the observation of some shoulders at both sides of the resonance. However, it was not possible to separate the shoulder from the main resonance neither at 303 K nor at 353 K.

The analysis of the ^{13}C-NMR spectrum of PVPA (1) provided important information about the mechanism of the polymerization of VPA and revealed the signature of cyclopolymerization when ^{13}C-NMR spectra of the PVPA samples prepared by different routes were compared. However, acquiring ^{13}C-NMR spectra of PVPA was much more difficult than recording its ^{1}H- and ^{31}P-NMR spectra.

* This is expected because phosphorous is much closer to the anhydride groups than the protons of the backbone. Therefore, it is able to sense the anhydride groups better than the protons at the backbone

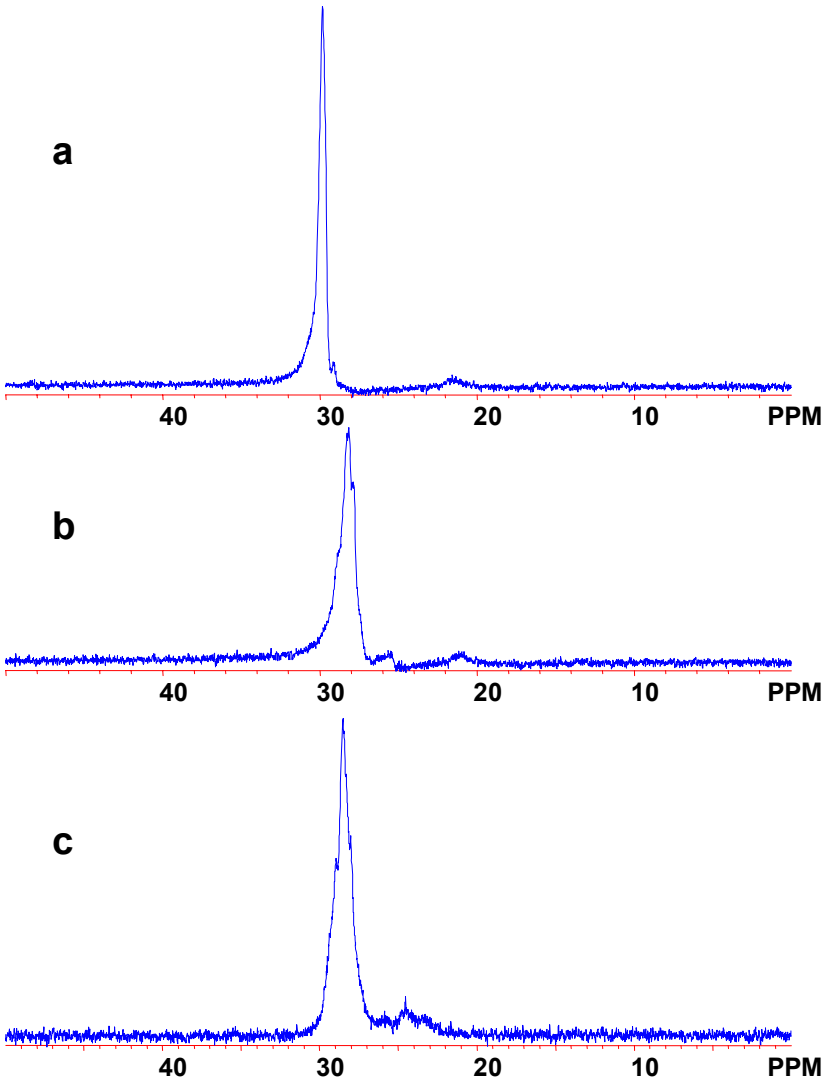

Figure 5.6: ^{31}P-NMR (176.03 MHz) spectra of PVPA (1)(50 mg/0.8 mL D_20) at pH= a) 1.1 b) 3.5 c) 8.9 at 303 K.

Long time experiments were essential to record ^{13}C-NMR spectra of PVPA. However, a higher resolution than in the ^{13}C-NMR spectrum shown below (Figure 5.7) was not achieved. However, the quality of this spectrum was good enough to deduce qualitative information. The reasons for encountering these difficulties include the low natural

abundance of ^{13}C nuclei (only 1.1% of the total carbon in a molecule consists of the spin of ½ carbon-13 isotope), and the rigidity of the carbon backbone of the polymer.

The ^{13}C-NMR spectrum of PVPA (1) exhibited two sets of signals. The first of the signals consists of a singlet at 35 ppm, which was assigned to the methylene carbon, and a doublet also centered at 35 ppm, which was assigned to the methine carbon. The doublet arises from the hyperfine splitting of the methine carbon signal as a consequence of the interaction with the phosphorous atom to which it was attached. In addition to these signals, one singlet at 38 ppm and a doublet centered at 37.5 ppm were observed, which is the second set of signals. The second set of signals was assigned to sequences arising from head-head and tail-tail links in the polymer as indicated in the Figure 5.7. The assignment of the second set of signals were done comparing the ^{13}C-NMR spectrum of PVPA obtained from the polymerization of VPA, which proceeds over the cyclopolymerization of the vinylphosphonic acid intermediate, with that of PVPA(4) obtained by the hydrolysis of PDMVP. The second set of the signals were absent in the ^{13}C-NMR spectrum of PVPA prepared by the hydrolysis of PDMVP, the polymerization of which does not follow the same mechanism as that of VPA.

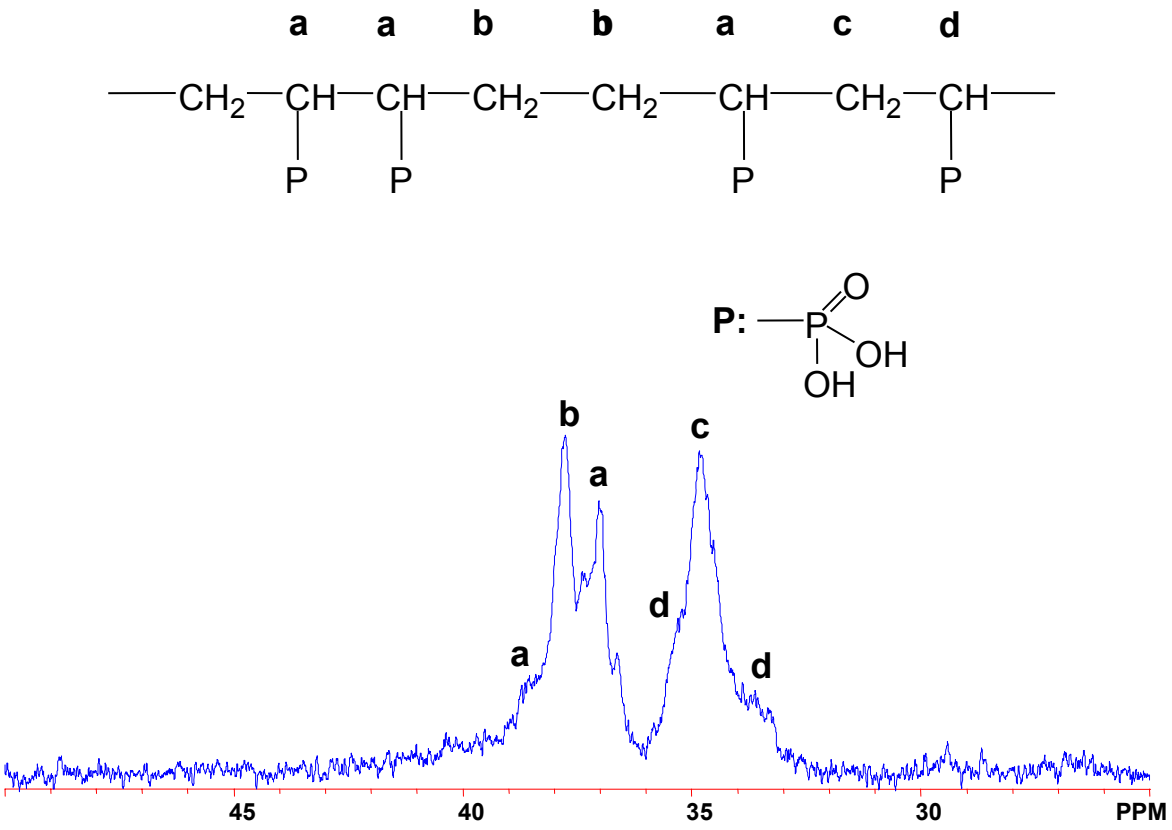

Figure 5.7: ^{13}C-NMR spectrum of PVPA (1).

The singlet labeled b was assigned to the two methylene carbons in between two methine carbons (tail-tail link) and the doublet originated from the two adjacent methine carbons (head-head link).

5.2.3 Microstructure of PVPA (4) Synthesized by the Hydrolysis of PDMVP

The microstructure of PVPA (4) prepared by the complete saponification of PDMVP was elucidated inspecting the ^{1}H, ^{31}P, and ^{13}C nuclei as a comparison to the microstructure of the PVPA obtained by the cyclopolymerization of VPA. All spectra were acquired with the PVPA (4) solutions in D_20 in their natural pH.

The ^{1}H-NMR spectrum of PVPA (4) has five resonances. Four of these resonances that are located at 1.18, 1.46, 1.75, and 2.03 were assigned to the methylene protons (Figure 5.9). The signal at 2.38 ppm belongs to the methine proton. This assignment was supported by the observation that the intensity of the signals due to the methylene protons is 2/3 of the sum of intensities of all peaks. The intensities of all peaks were obtained separately by deconvoluting the ^{1}H-NMR spectra.

As mentioned earlier, four different peaks were observed for the methylene protons. To analyze the stereochemistry of PVPA (4), one has to consider corresponding n-ads that give rise at least to four distinguishable signals. In this case, we have to consider tetrad sequences, which give rise to 6 distinguishable signals. The presence of only four resonances in the ^{1}H-NMR spectrum of PVPA (4) indicates that some of the signals overlap. The resonance at 1.18 ppm has the lowest intensity, the relative intensity of this resonance was found as 0.103 from the experimental spectrum of PVPA (4). This signal was assigned to the least probable tetrad sequence due to the lowest intensity. The least probable tetrad sequence is mmm, the formation of this tetrad sequence requires that all phosphonic acid functionalities are at the same side of the polymer backbone, i.e. they have the same configuration, the probability of which is the lowest due to the steric hindrance since the phosphonic acid group is bulky. After defining the probability of P_m,

it is possible now to calculate the probabilities of the remaining tetrad sequences. It was assumed that Bernouillian statistics was valid to describe the probabilities of the signals of the remaining 5 tetrads, and in consequence, the intensities of the remaining signals can be obtained.

Table 5.3: ^{1}H-NMR spectra with tetrad resolution in the region of methylene group resonance a) PVPA (4) from hydrolysis of PDMVP b) PVPA from polymerization of VPA

a)

Signal at	1.18	2.03	1.75	1.46
Assignment of stereosequence	mmm	rrr+rmr	mrm+rrm	mmr
Relative intensity found	0.103	0.284	0.378	0.235
Relative intensity calculated	0.103 [1)*]	0.282	0.381	0.234

b)

Signal at	1.95	2.05	1.80	1.55
Assignment of stereosequence	mmm	rrr+rmr	mrm+rrm	mmr
Relative intensity found	0.125	0.213	0.478	0.184
Relative intensity calculated [2)*]	0.103	0.278	0.378	0.241

* [1] Defined by the experimental intensity
* [2] After subtraction of contributions to signal intensities by protons labeled a and d.

The assignment of these intensities to the correct tetrad sequence was done after considering all possible combinations of assignments that will produce the experimental spectrum at the end. There are three possible combinations of the remaining tetrad sequences with their calculated probabilities (Table 5.4). The first probability was chosen because it produced the most consistent spectrum (giving rise to the minimum amount of error) with the experimentally observed one.The assignment of the resonances is shown in Figure 5.9 for PVPA (4) prepared by the hydrolysis of PDMVP. The consistency of the calculated spectrum with the experimental one indicates that Bernouillian statistics are valid to describe the probabilities of the tetrad sequences of PVPA (4). The ^{1}H NMR spectrum of PVPA (4) is consistent with a chain structure composed of head-to-tail linked monomers of a nearly atactic configuration. Various tetrad sequences are drawn both in two and three dimensional projection, and in ball-and stick models in Figure 5.10 and Figure 5.8, respectively.

The ^{13}C-NMR spectrum of this polymer consists of two signals, a singlet at 35 ppm, and a doublet also centered at 35 ppm. The singlet was assigned to the methylene carbon, and the doublet to the methine carbon. The doublet arises from hyperfine splitting of the methine carbon with the phosphorous atom to which it was attached.

Table 5.4: Possible combination of the tetrad sequences with their probabilities

	Assignment
1	2.03 ppm → rrr+rmr, 1.18 ppm → mmm, 1.75 ppm → mrm + rrm/mrr, 1.46 ppm → mmr/rmm
2	2.03 ppm → rrr/mrr, 1.18 ppm → mmm, 1.75 ppm → rmr + mrm + rrr, 1.46 ppm → mmr/rmm
3	2.03 ppm → rrr/mrr, 1.18 ppm → mmm, 1.75 ppm → mmr/rmm + rrr, 1.46 ppm → rmr + mrm

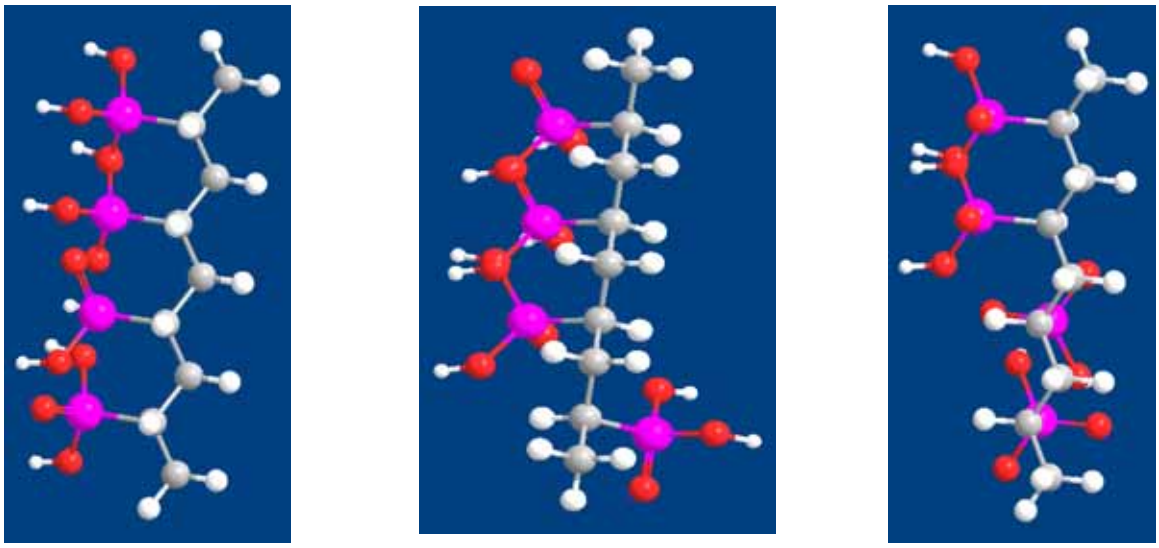

mmm mmr mrm

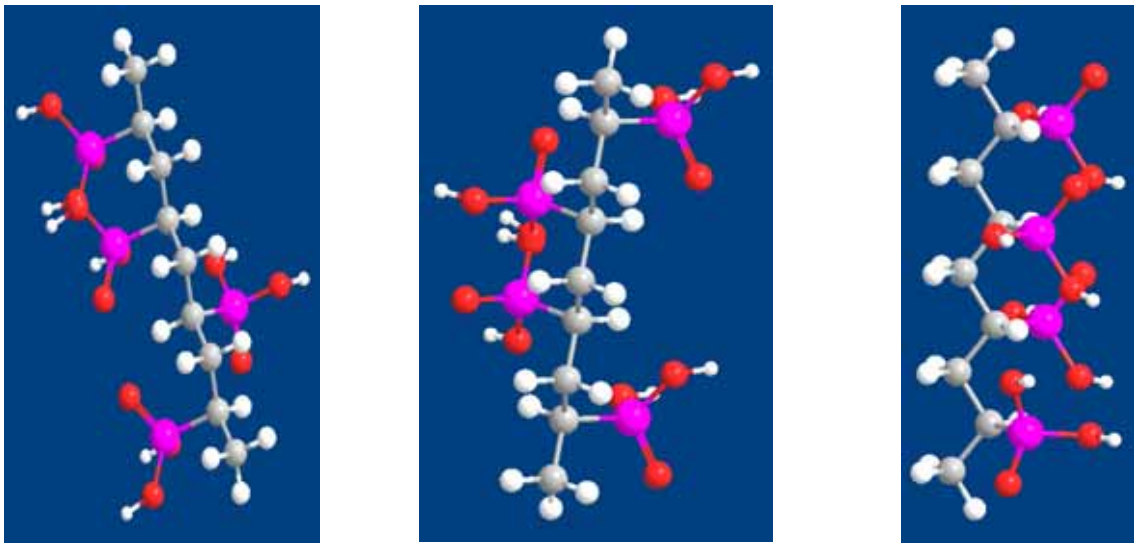

mrr rmr rrr

Figure 5.8: Ball-and-stick models of tetrad sequences of PVPA, rrr and mmm are equivalent to "isotactic" and "syndiotactic" (four repeat units are considered, and methyl groups are placed at the end and at the beginning of the chains).

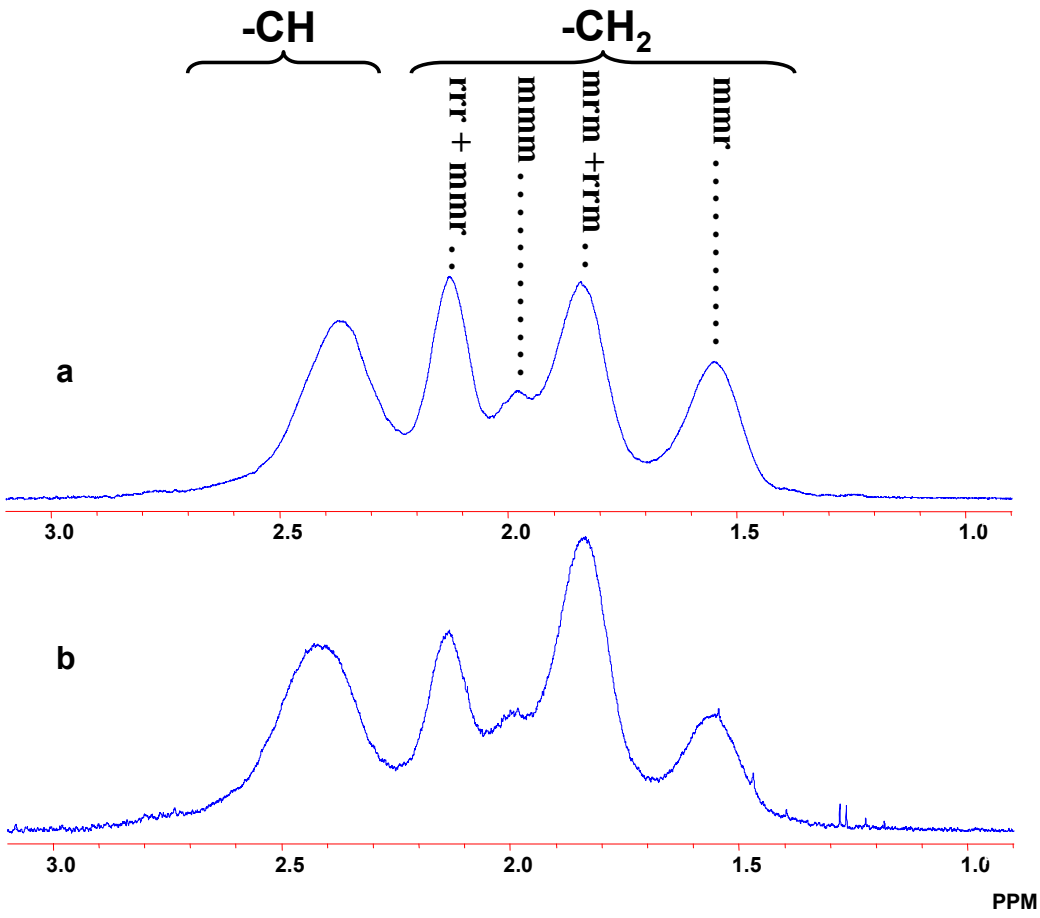

Figure 5.9: Solution ^{1}H-NMR (500 MHz) spectra in D_2O a) PVPA (4) after hydrolysis of PDMVP b) PVPA by direct polymerization of VPA.

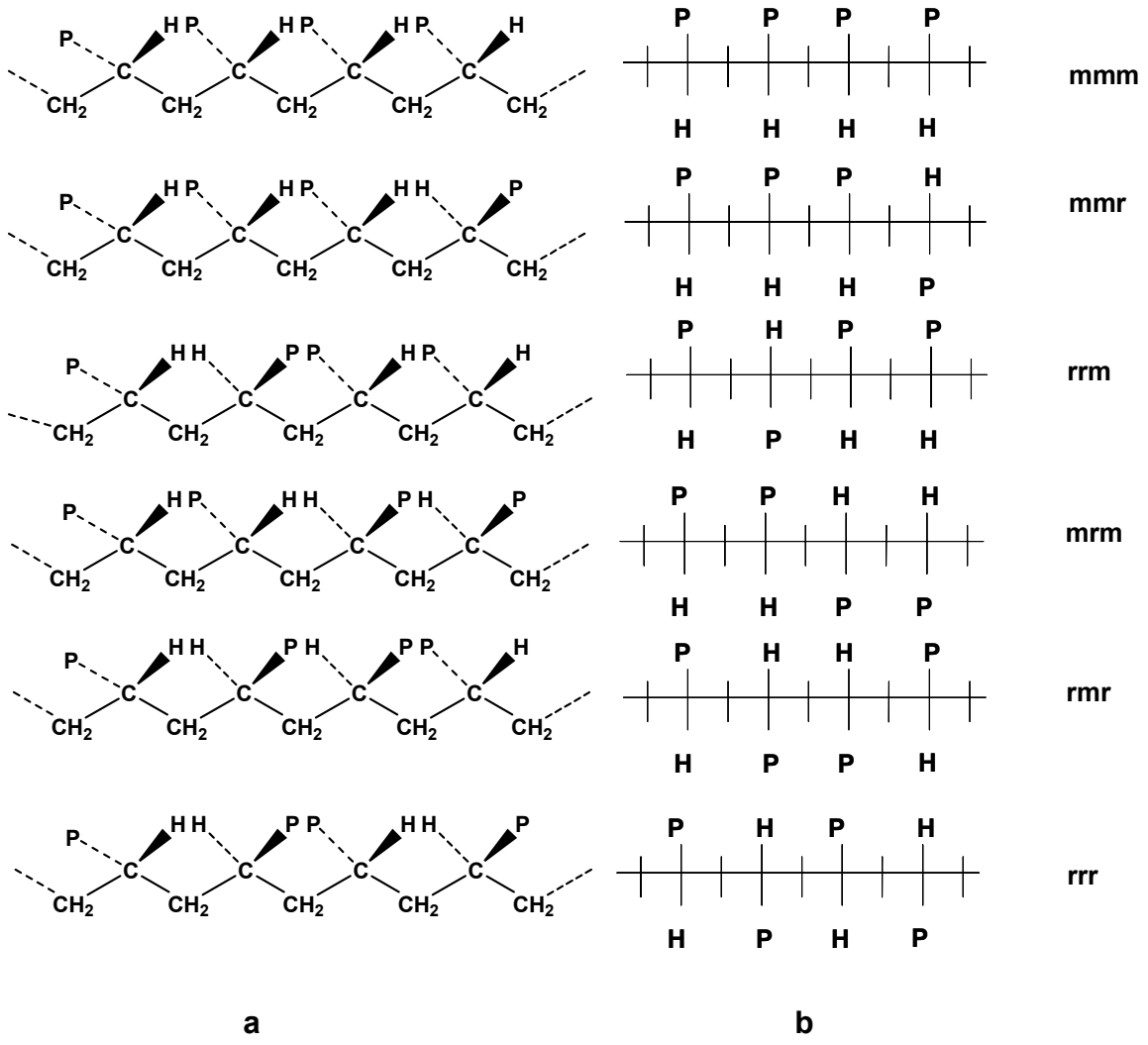

Figure 5.10: Tetrad sequences of PVPA in a) three dimensional b) in two dimensional representation (P represents the phosphonic acid group).

The ^{31}P-NMR spectrum exhibits 2 signals, a main resonance at 31.26 ppm, and another weak signal at 23 ppm. The position of the resonances is slightly different from those of PVPA (1) and they shift to higher field about 1.5 ppm, which can be regarded as a small change since ^{31}P has a large chemical shift range. The spectra were obtained at different times; this shift may be due to the temperature dependence of the spectra.

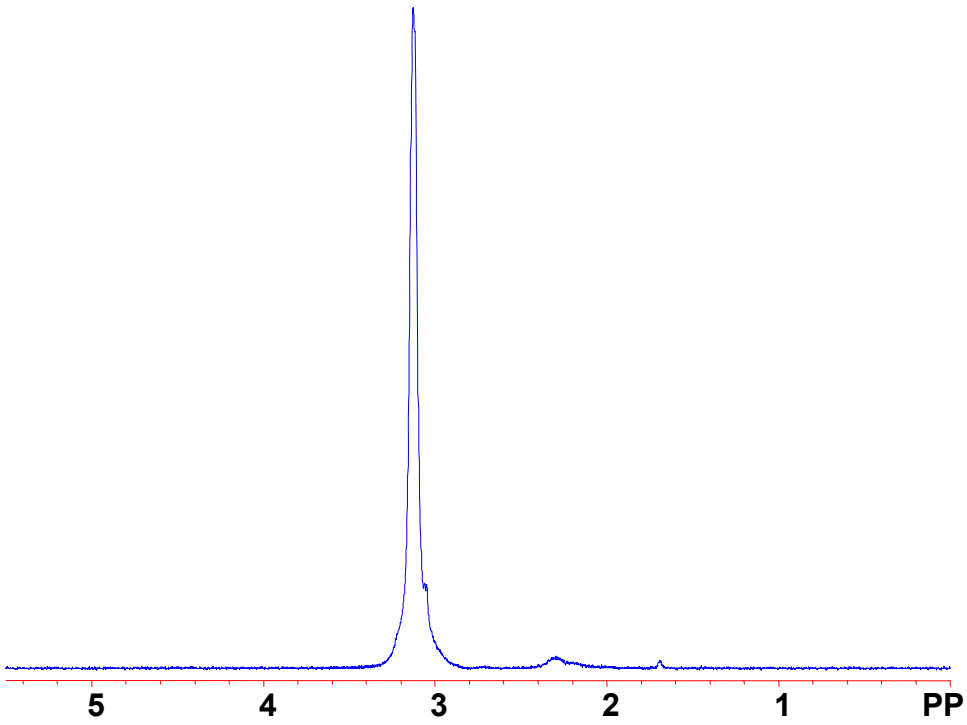

Figure 5.11: ^{31}P-NMR (176.3 MHz) spectra of PVPA (4)(50 mg/0.8 mL D20) at pH 1.1 at 303 K

5.2.4 Assignment of the ^{1}H-NMR Spectrum of PVPA (1) and Existence of the Defect Species

The pattern of the resonances in the ^{1}H-NMR spectrum of PVPA obtained by radical polymerization of VPA (Figure 5.9b) looked similar to that of PVPA (4) obtained by the hydrolysis of PDMVP, at first glance. However, the ratio of the signal intensities was substantially different beyond experimental error. This becomes obvious comparing the third row Table 5.3a with the equivalent row in Table 5.3b.

In order to explain the observed intensity pattern we needed to assume a more complicated structure of the polymer, PVPA (1). The nature of this complication becomes obvious looking to the ^{13}C-NMR spectra of PVPA (1) (Figure 5.7), which is already explained in 5.1.2, and comparing it with the ^{13}C NMR spectra of PVPA (4) (see 5.1.3). In short, comparing the ^{13}C-NMR spectra of PVPA (1) and PVPA (4) showed that PVPA synthesized by the polymerization of VPA has some other linkages additional to those present in the PVPA that was prepared by the hydrolysis of PDMVP. PVPA (4) only contains head-to-tail linkages. However, PVPA (1) also contains head-to-head and tail-to-tail links additional to the head-to-tail links. Head-to-head and tail-to-tail links form only during the polymerization of VPA since its polymerization proceeds over cyclopolymerization. These additional linkages cause the differences in the relative intensities of the resonances calculated and experimentally observed. To find out the fraction of the head-to-head and tail-to-tail links present in PVPA (1), it was tried to adjust the experimentally observed intensities of the resonances so that they become equal to the relative intensities of the resonances of the methylene protons in PVPA (4). Therefore, we need to subtract x and y from the relative intensity of the resonances located at 1.8 ppm, and 1.95 ppm, respectively. Then the new total intensity of the resonances due to the methylene sequences in PVPA (1) will be equal to (1-x-y). Knowing these, we can set the relative intensities of the resonances of PVPA (1) in its ^{1}H-NMR equal to those in the ^{1}H-NMR spectrum of PVPA (4) to calculate the quantity (x+y) by the following equations:

The new fraction of the resonance at 1.95 ppm among the methylene protons,

(0.125-y)/(1-x-y)= 0.103	(5.8)

The new fraction of the resonance at 1.8 ppm among the methylene protons,

(0.478-x)/(1-x-y)= 0.378	(5.9)

Solving these equations gave x+y as 0.235. In other words, a fraction of 0.235 among the initial total linkages belongs to the head-to-head and tail-to-tail linkages. The percent of the defects were calculated by

[(0.235)/(1)]x100 = 23.5%	(5.10)

Calculating the new weight of each resonance after subtracting the contributions to integrals due to the head-to-head and tail-to-tail species leads to the relative intensities in Table 5.3. A shift in the absolute values of positions of the signals was observed in the ^{1}H-NMR of PVPA (1) and PVPA (4) in Figure 5.9. The shift originated in a rather strong dependence of the values of the chemical shifts on temperature and may indicate that the spectra were obtained at slightly different temperatures although it was tried to set all the experimental conditions equal while acquiring ^{1}H-NMR spectra of these two samples.

As already discussed in 5.2.1, some anhydride species are present in the solutions of PVPA (1) and PVPA (4). ^{31}P-NMR data suggested that the fraction of these species is slightly different in PVPA (1) and PVPA (4). Also, the type of possible ring formation in PVPA (1) and PVPA (4) can be expected to be different. PVPA (4) can only form six membered rings, whereas the formation of five-and six- membered rings is possible in the case of PVPA (1). In other words, PVPA prepared by the polymerization of VPA can

either have five membered or six-membered or a combination of these two types of rings (Figure 5.13). Different types of rings can affect the position of the chemical shifts as shown for the low molecular derivatives of pyrolidine and piperidine that are five- and six-membered rings, respectively (Figure 5.12). The chemical shift of N-methyl carbon of the N-methylpyrrolidine is found as 42.6 ppm, whereas N-methylcarbon of the N-methyl piperidine resonates at 46.8 ppm in the ^{13}C-NMR.[105]

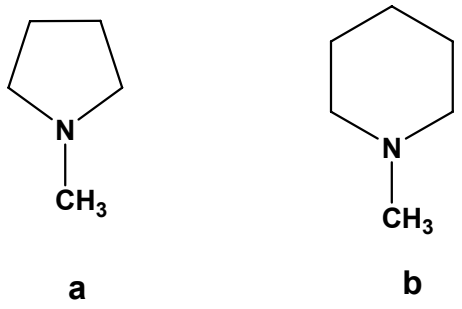

Figure 5.12: Chemical structures of a) N-methyl pyrrolidine b) N- methyl piperidine.

Shortly, the shift in the ^{1}H-NMR spectra of PVPA produced by two different ways is believed to be due to the type of cyclic structures. Although PVPA (4) has less condensated phopshonic acids anhydride groups in the solid state than PVPA (1), after dissolving both polymers in D_2O at the same concentration, PVPA (4) has a higher fraction of the cyclic structures than the PVPA (1) based on the ^{31}P-NMR studies. The efficiency with which the cyclic structures will be hydrolyzed will greatly depend on their stability. Additionally, the proportion of five- and six membered rings in the PVPA prepared by the polymerization of VPA will depend on the relative stability of the free radicals formed during the propagation step. At this stage of the study, we are not able to determine the type and proportion of the cyclic structures in the PVPA samples.

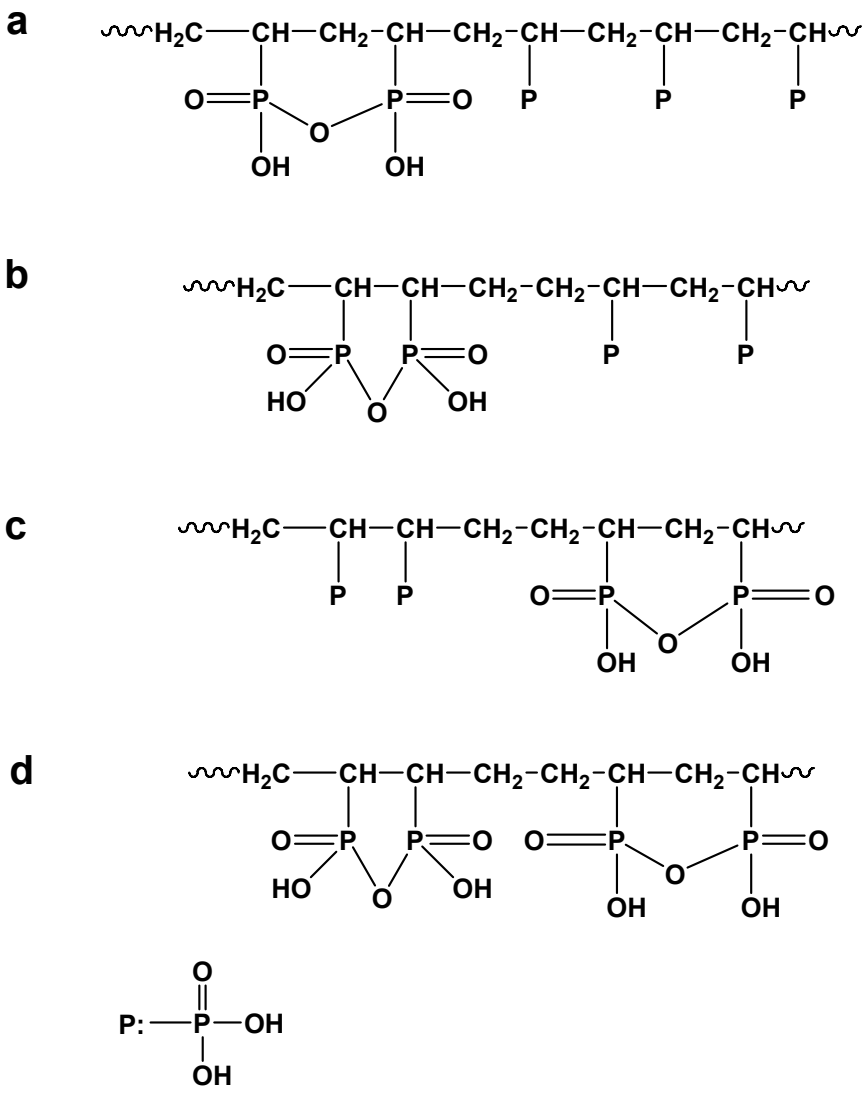

Figure 5.13: Possible types of rings in a) PVPA synthesized by the hydrolysis of PDMVP b,c,d) PVPA synthesized by the polymerization of VPA.

5.2.5 NMR Spectra of Different Molecular Weight PVPA

Having various molecular weight samples of PVPA synthesized by the polymerization of VPA in hand, ^{1}H-and ^{31}P-NMR spectra of these polymers were studied

in solution to understand whether the molecular weight has an influence on the appearance of the NMR spectra.

Figure 5.14 presents the ^{1}H-NMR spectra of PVPA (2) and PVPA (3). PVPA (2) and PVPA (3) have the main resonances observed in the ^{1}H-NMR spectrum of PVPA (1)[*]. Additionally, some sharp signals were observed between 1-1.5 ppm, which may belong to impurities. These impurities may be formed by the termination reactions occurring at the very early stage of polymerization. For example, radicals formed by the decomposition of initiator may attack the monomer, and the chain may be terminated.

The relative intensities of the signals in the ^{1}H-NMR spectrum of PVPA (2) are very similar to those in the ^{1}H-NMR of PVPA (1). PVPA (3) differs from higher molecular weight PVPA samples in terms of their relative intensities of the signals. The width of the resonance due to the methine proton is increasing with decreasing molecular weight. The presence of several signals under the broad resonance of the methine proton can be inferred from the ^{1}H-NMR spectrum of PVPA (3). However, these signals could still not be resolved separately.

[*] There is a slight shift also in the position of these resonances, this shift has its origins in the temperature dependence of the spectra. These spectra were not aquired at the same day, although the temperature was set to the same value in all experiments, it can slightly change during the experiments that are carried at different times

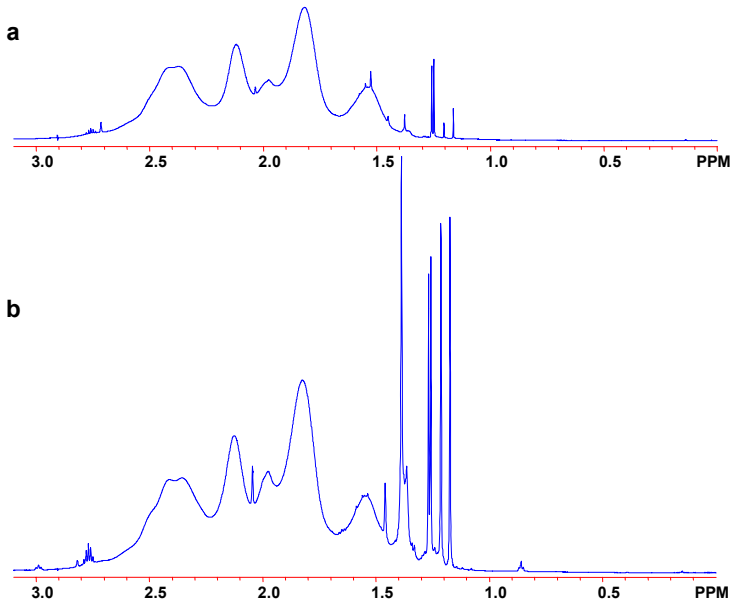

Figure 5.14: Solution ^{1}H-NMR (500 MHz) spectra in D_2O a) PVPA (2) b) PVPA (3) (50 mg/0.8 mL).

The ^{31}P-NMR spectra of all PVPA samples exhibited two signals, one of them was assigned to P=O and the other to P-O-P as already mentioned. The chemical shift of the resonances varies slightly which has its origins in the temperature dependence of the spectra. The relative intensity of resonances due to the condensated phopshonic acid species differs for different molecular weight samples both in solution and solid state.

5.3 Summary

We have used a combination of high resolution ^{13}C- and ^{1}H-NMR measurements to determine the tacticity of PVPA. ^{13}C-NMR revealed the presence of head-to-head and tail-to-tail structures, and ^{1}H-NMR data were used for the quantification of these

structures. PVPA synthesized by free radical polymerization of VPA was found to be nearly atactic. The assignment of the spectra and identification of the tacticity was challenging having only one polymer with unknown tacticity and NMR spectra with broad resonances. For the purpose of studying microstructure and tacticity of the macromolecules, various polymer samples are needed that are obtained by different techniques with different tacticities such as isotactic, syndiotactic and atactic. Having the NMR spectra of the polymers that are purely isotactic and syndiotactic, the spectrum of a polymer with unknown tacticity can be assigned. For example, to determine the tacticity of PAA, isotactic and syndiotactic PAA were synthesized by different polymerization techniques. The NMR spectra of PAA with unknown tacticity was assigned and the tacticity was identified by comparing the NMR spectra of the PAA with unknown tacticity with NMR spectra of isotactic and syndioactic PAA. This approach is used in the identification of many other macromolecules such as poly(tert-butyl acrylate),[106] poly(methylmethacrylate)[107] etc.. However, there are not many alternatives for the synthesis route of VPA. As already mentioned in Chapter 3, the anionic polymerization of its diethyl ester failed. The only possible synthesis route is the free radical polymerization of VPA an uncontrolled manner. The RAFT polymerization (which is a controlled radical polymerization) was not successful yet in polymerizing the VPA monomer.

The resolution of our ^{13}C-and ^{1}H-NMR spectra enables us to analyze the tacticity of PVPA on a tetrad level. The NMR analysis of poly(methyl acrylate) has already been achieved on a hexad level, and analysis of PAA has been reported at the pentad level.[98] It is important to be able to carry out the analysis of the polymers using as large

stereosequence as possible because more details about the microstructure of the polymers can be discerned from the longer stereosequences. The fact that the resonances of PAA both in its ^{1}H- and ^{13}C-NMR are better resolved than in the case of PVPA makes the acquisition of only CH and CH_2 spectra possible by irradiation with a suitable resonance frequency. This gives important clue to the assignment of the peaks belonging to the methylene and methine protons. However, acquisition of only CH or CH_2 spectra was impossible for PVPA due to the very close location of the signals belonging to methine and methylene groups.

As a conclusion, the microstructure of PVPA was described for the first time by high resolution NMR spectroscopy. Identification of the tacticity was possible by comparing the NMR spectra of PVPA with different synthetic routes, which gave insight to the polymerization mechanism of VPA. Investigation of the tacticity in vinyl polymers is important since the tacticity determines many of their physical properties such as their crystallizability, their softening or melting temperatures, and their mechanical behavior.[101] In the case of PVPA, stereochemistry may affect the condensation of phosphonic acid groups which is an important parameter determining its conductivity.

CHAPTER 6

CONDUCTIVITY

6.1 Introduction

The interaction of electromagnetic radiation with matter gives rise to transitions between the electronic, vibrational and rotational molecular energy states, which may be observed by UV/visible and infra-red absorption frequencies above about 10^{12} Hz. Absorptions due to the electric polarization and conduction processes are observed over the entire range between 10^{-6} and 10^{12} Hz. The response of a material to the electromagnetic waves in the frequency range between 10^{-6} and 10^{12} Hz may be observed by Broadband Dielectric Spectroscopy. In this range, dipolar relaxations arising from the reorientation motions of molecular dipoles and electrical conduction arising from the translational motions of electric charge carriers take place. Dielectric Spectroscopy provides important information about the dielectric properties of the material and dynamics of bound and mobile charge carriers. The magnitude of the effects and the frequency location of the energy absorption depends greatly on the physical and chemical nature of a material, temperature and pressure at which the material is studied.[108]

Electrical conductivity is a measure of how well a material accommodates the transport of electrical charge when potential is applied. The quantity of electrical charge that passes in a conductor per unit time is the current. The current passing through unit area perpendicular to the direction of flow is the current density *j*. The current density in the x direction is proportional to the potential gradient.

$$j = -\sigma \frac{\partial \phi}{\partial x} \quad (6.1)$$

The proportionality constant is σ, which is the conductivity of the substance. The unit of the conductivity is Sm^{-1}. The conductance, G, is defined as reciprocal resistance, R, and can be related to the conductivity as follows:[109]

$$G = \frac{1}{R} = \frac{\sigma A}{l} \quad (6.2)$$

Resistance is expressed in ohms, Ω, and conductance of a sample is expressed in Siemens. l and A is the length and the cross-sectional area of the sample, respectively.

6.2 Conductivity of Polymer Electrolyte Systems

A considerable amount of polymeric materials are known which conduct electricity by the migration of ions. These include both organic- and inorganic-based polymers. The majority of these materials consist of a salt dissolved in a polymer matrix. For example, $LiClO_4$ in poly(ethyleneoxide), where both the cations and anions contribute to the conductivity. There exists also electrolytes in which one charge, either anion or cation, is anchored to the polymer backbone or pendant group on the polymer so that electrical properties are clearly attributable to a known conducting species. This class of materials are called polyelectrolytes.[110]

The characterization of the basic electrical properties of a polymer electrolyte demands the determination of the total conductivity of the electrolyte as a function of temperature, identification of the different charged species contributing to conduction,

and transport numbers* as a function of temperature. Direct current, alternating current, and transport number measurements are the main techniques discussed in the literature for electrical characterization of ionically conducting polymers.[111]

6.3 Conductivity Measurements

6.3.1 Alternating Current Measurements

Alternating current (a.c.) methods represent the most popular approach to the determination of the electrical properties of polymer electrolytes. Simple cells with blocking electrodes may be used to determine the bulk electrolyte properties. Data obtained by the alternating current methods carry information not only about the long-range migration of ions but also about the polarization phenomena occurring within the cell, such as relaxation of the trapped ions. [111]

In an alternating current experiment, a sinusoidal voltage is applied to a cell and the resulting sinusoidal current passing through the cell is determined. Two parameters are required to relate the current flowing in consequence of the applied voltage. One of

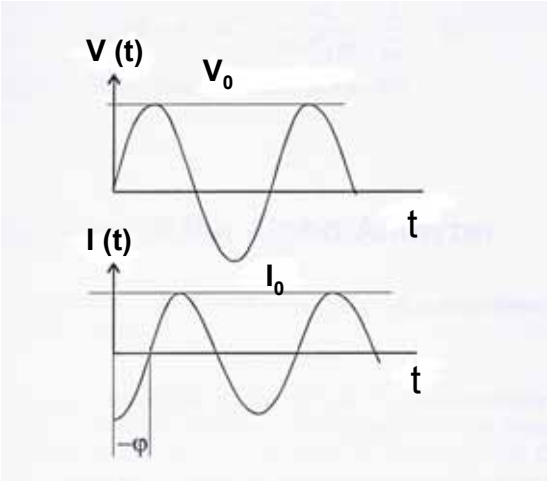

* Transference number indicates the fraction of the current carried by each charged species

Figure 6.1: Representation of the sinusoidal voltage and current at a given frequency, V= voltage, I = current, φ = phase difference between the potential and current.

these parameters represents the resistance and is equal to the ratio of the voltage and current maxima, V_{max} / I_{max}. The other parameter, φ, is the phase shift between the voltage and current. The combination of these two parameters represents the impedance, Z, of the cell. Generally, both the magnitude of the impedance $|Z| = V_{max} / I_{max}$ and its phase angle φ are functions of the applied frequency. The impedance is measured as a function of the frequency of the applied signal over a wide frequency range, typically from 1mHz to 1 MHz. Impedance is a vectorial quantity, possessing both magnitude and phase.

$V(t) = V_0 \sin(\omega t)$	(6.3)
$I(t) = I_0 \sin(\omega t + \phi)$	(6.4)

where ω is the frequency.

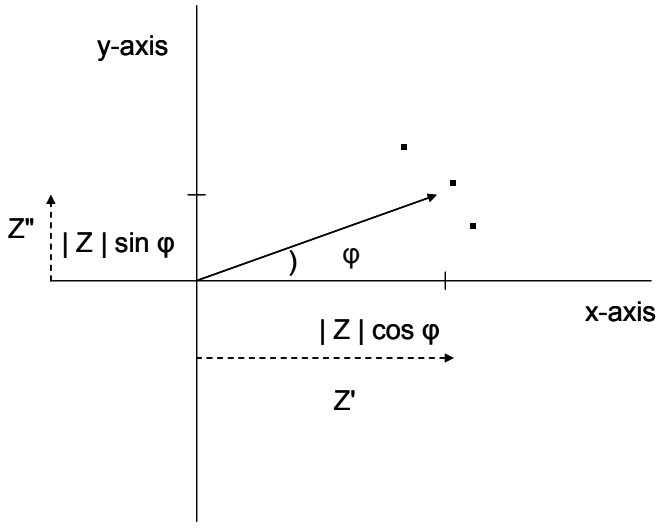

Figure 6.2: Representation of the impedance, Z, of a cell. Z' and Z" are respectively the real and imaginary components of the complex impedance $Z^* = Z' - i\,Z''$.

The impedance for each frequency measured is represented by a separate point on the vector diagram. The distance of the point from the origin corresponds to the magnitude if the impedance and the angle formed with the x-axis correspond to the phase difference between the voltage and current. The impedance vector may be written by its x and y components, which are $|Z| \cos \varphi$ and $|Z| \sin \varphi$, respectively. Impedance may be represented by a complex number $Z^* = Z' - i\,Z''$.

A typical a.c. experiment consists of determination of the complex impedance of a cell as a function of the signal frequency. The response of any cell to an a.c. signal can be represented by an equivalent circuit consisting of components such as resistors and capacitors, which individually represent charge migration and polarization occurring in the cell. Interpreting the results of an a.c. experiment relies on finding the equivalent circuit (Figure 6.3) which models the impedance data. The values for individual components may later be related to the electrical properties of the cell.

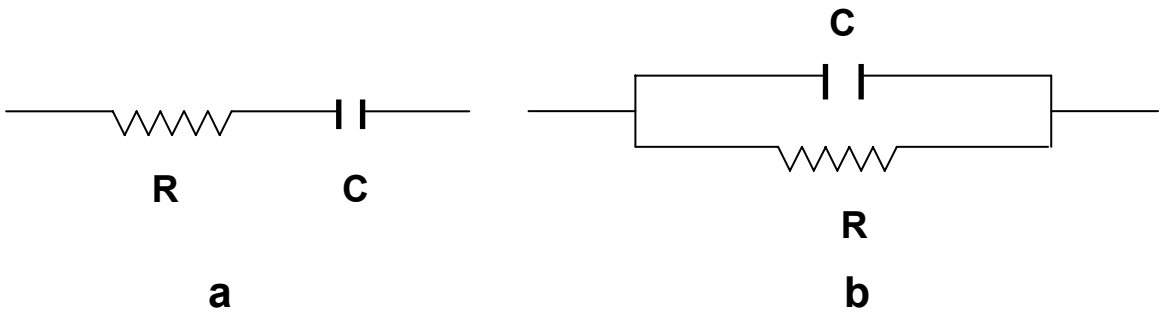

Figure 6.3: A cell with a capacitor and resistance connected in a) series b) parallel

A sinusoidal voltage applied to a resistor is always in the phase with the current passing through it. In other words, φ = 0 and the magnitude of the impedance is simply given by the resistance | Z | = R. The impedance is independent of the frequency. When a sinusoidal voltage is applied to a capacitor, voltage lags behind the current by 90˚, i.e. φ= - π/2. In this case, the magnitude of the impedance is frequency-dependent.:

$\lvert Z\rvert = \frac{1}{\omega C}$	(6.5)

where C represents the capacitance.

The impedance of an equivalent circuit is calculated by summation of impedances of the individual circuit elements as shown in Figure 6.3. When the components are connected together in series, the individual impedances are directly additive.

$Z = Z_C + Z_R$	(6.6)
$Z_R = R$ and $Z_c = \frac{1}{i\omega C}$	(6.7)
$Z_c = \frac{1}{i\omega C}$	(6.8)

Inserting (6.7) and (6.8) into the Equation (6.6), total impedance of a cell consisting of a resistor and capacitor in series (Figure 6.3a) can be found as

$Z^* = R - \frac{i}{\omega C}$	(6.9)

The impedance of a cell consisting of a resistor and capacitor connected in parallel (Figure 6.3b) can be written as in Equation (6.10)

$$\frac{1}{Z} = \frac{1}{Z_R} + \frac{1}{Z_c} \qquad (6.10)$$

The total impedance of this system can be given with the following equation:

$$Z^* = \frac{1}{\left(\frac{1}{R} + i\omega C\right)} = \frac{R - i\omega CR^2}{1 + (\omega CR)^2} = R\left[\frac{1}{1 + (\omega CR)^2}\right] - iR\left[\frac{\omega RC}{1 + (\omega RC)^2}\right] \qquad (6.11)$$

Equation (6.11) defines a semicircle in the complex impedance plane with a diameter R extending along the real axis from the origin. (Figure 6.4).

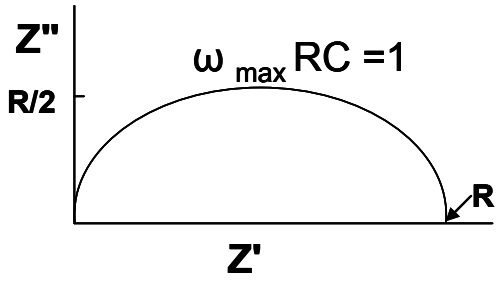

Figure 6.4: Complex impedance plot for a combination of resistor and capacitor in parallel .

At the frequency corresponding to the maximum of the semicircle, ω_{max}, the magnitude of the impedance of the resistor and capacitor are equal:

$R = \frac{1}{\omega_{max} C}$	(6.12)

Applying an a.c. voltage to a cell where a polymer electrolyte with only one type of mobile species is sandwiched between two blocking electrodes* and varying the frequency at the same time will result in a response as in Figure 6.5.

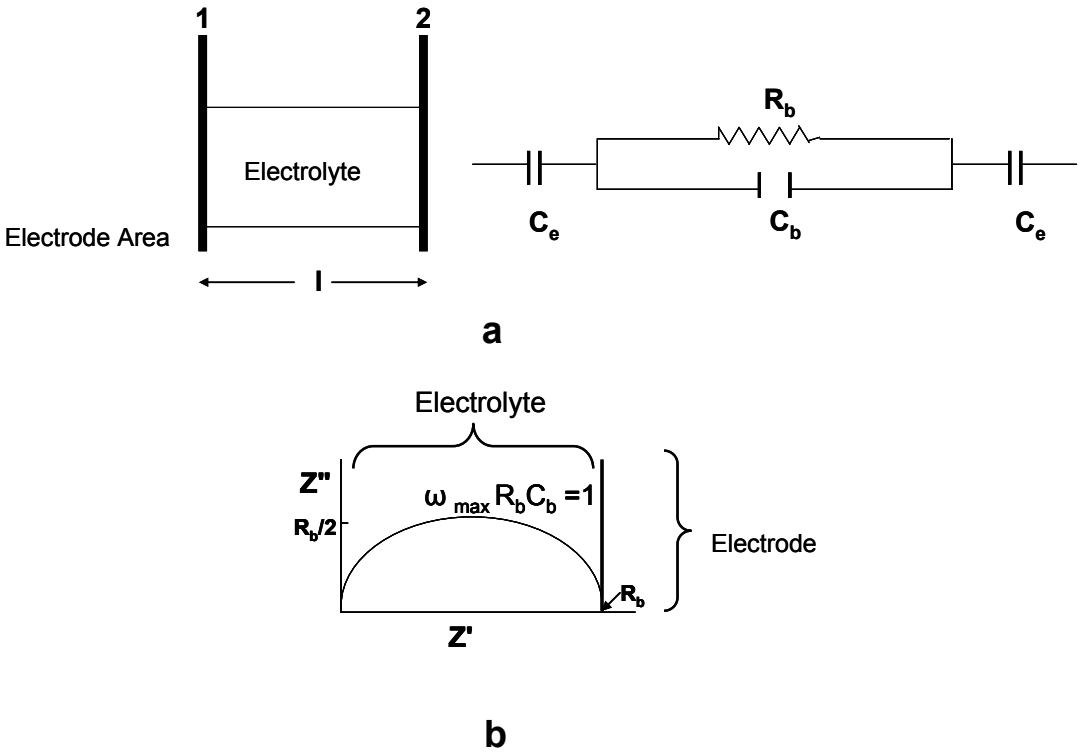

Figure 6.5: a) Schematic representation of a polymer electrolyte/ blocking electrode cell. R_b, electrolyte resistance; C_b electrolyte capacitance; C_e, electrode capacitance.

b) Simulated complex impedance plot for the circuit in (a)

C_b is simply related to the dielectric constant of the polymer,

* The mobile species in the electrolyte does not participate in any electrode reactions when blocking electrodes are considered.

$$C = \frac{\varepsilon\varepsilon_0 A}{l} \quad (6.13)$$

in which ε is the dielectric constant of the polymer, and ε_0 is the vacuum permittivity ($8.85 \times 10^{-14} Fcm^{-1}$). Since C_e is in series with the parallel combination of R_b and C_b, the total impedance can be obtained by adding the impedance of the capacitor C_e to that of the parallel RC combination

$$Z^* = R_b\left[\frac{1}{1+(\omega R_b C_b)^2}\right] - i\left(R_b\left[\frac{\omega R_b C_b}{1+(\omega R_b C_b)^2}\right] + \frac{1}{\omega C_e}\right) \quad (6.14)$$

Figure 6.5b represents the complex impedance plot predicted by the Equation (6.14). At high frequencies, when the impedance of the bulk resistance and capacitance are of the same magnetite $1/\omega C_b \approx R_b$, both bulk resistance and capacitance contribute to the overall impedance whereas the impedance of the electrode capacitance C_e is insignificant. Therefore, the circuit reduces to a parallel R_b C_b combination which gives rise to the semicircle in the complex impedance plane. At lower frequencies $1/\omega C_b >> R_b$ and therefore, C_b makes a negligible contribution to the impedance; the equivalent circuit reduces to a series of combination of R_b and C_e appearing as a vertical spike displaced at distance R_b along the real axis. At very low frequencies the equivalent circuit can be simplified to the electrode capacitance C_e only.

The high-frequency response yields information about the properties of the electrolyte generally. For example, the high frequency semicircle the bulk resistance R_b and ω_{max} can be extracted. Then bulk capacitance can be calculated by Equation (6.15).

$\omega_{max} R_b C_b = 1$	(6.15)
$C_b = \frac{1}{R_b \omega_{\max}}$	(6.16)

The dielectric constant, ε of the material can be calculated at the ω_{max}

$C_b = \frac{\varepsilon \varepsilon_0 A}{d} \Rightarrow \varepsilon = \frac{C_b d}{\varepsilon_0 A}$	(6.17)

On the other hand, the low frequency response provides information on the electrode/electrolyte surface. The complex impedance Z(ω) and its reciprocal Y(ω) depend on the geometry of a sample. Therefore, the dielectric properties of a material should be expressed in terms of intensive quantities, which are dielectric permitivity relative to vacuum ε (ω), electrical modulus M(ω) and electrical conductivity σ(ω). These quantities are related as follows:

$Z(\omega) = \frac{1}{Y(\omega)} = \frac{1}{i\omega C_0 \varepsilon(\omega)}$	(6.18)
$Y(\omega) = \frac{1}{Z(\omega)} = i\omega C_0 \varepsilon(\omega)$	(6.19)
$\varepsilon(\omega) = \frac{1}{M(\omega)} = \frac{1}{i\omega C_0 Z(\omega)} = \frac{Y(\omega)}{i\omega C_0}$	(6.20)
$M(\omega) = \frac{1}{\varepsilon(\omega)} = i\omega C_0 Z(\omega) = \frac{i\omega C_0}{Y(\omega)}$	(6.21)
$\sigma(\omega) = i\omega \varepsilon_v \varepsilon(\omega)$	(6.22)

6.3.2 Direct Current Measurements

Direct current (d.c.) techniques represent the most straightforward method which may be employed to measure ionic conductivity of the polymers. They can be performed both by two-terminal and four terminal cells. In both cases, the polymer electrolyte in question is sandwiched between two electrodes, and by the application of a direct current voltage, a constant current flows around the circuit. Figure 6.6 represents an equivalent circuit for a two-terminal cell, in which the current passing around the circuit must cross both electrode and electrolyte interfaces. This causes resistance. In other words, the applied voltage causes a current to flow through the electrode resistances and the electrolyte resistance in series as shown in Figure 6.6. The resistance of the circuit can be given by Equation (6.23). The resistance can be related to the electrical properties of the cell.

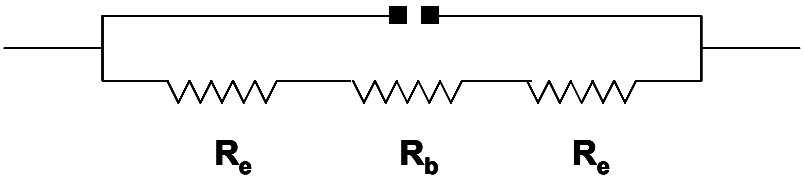

Figure 6.6: Equivalent circuit for a two-terminal cell, R_e and R_b represent the resistance of the electrode and electrolyte, respectively.

$\frac{V}{I} = (2R_e + R_b)$	(6.23)

Two-terminal measurements are subject to the problem of unknown and significant electrode resistance. The influence of electrode and electrolyte interface on the

measurements can be eliminated by adding another two electrodes. This makes the direct determination of the electrolyte conductivity possible. In a four-terminal cell, two electrodes serve only to pass a constant current through the cell whereas the other two electrodes act purely as voltage probes measuring the potential drop across a region of the electrolyte. The key to the elimination of the electrode resistances lies in the separation of the electrodes passing the current from those measuring the voltage.[111]

6.4 Transport Processess

Ionic transport in solids are described in terms of number of charges per carrier q_i, number of charge carriers per unit volume n_i, and the average mobility μ_i in an electric field.[112] The expression conductivity is the sum of all i carriers contribution (Equation(6.24)):

$$\sigma(T) = \Sigma q_i n_i(T) \mu_i(T) \quad (6.24)$$

The ion conductivity is related to the self diffusion coefficient, D, of the charged specied by the Nernst-Einstein Equation.

$$\frac{\sigma T}{D} = \frac{nq^2}{k} \quad (6.25)$$

where k is the Boltzmann constant.

Mobility is related to the diffusion coefficient by the following relation:

$\mu = \frac{qD}{kT}$	(6.26)

Temperature dependence of the ion hopping based conductivity in solids is described by Arrhenius equation (Equation (6.27)).

$\sigma = \sigma_0 \exp\left(\frac{-E_a}{RT}\right)$	(6.27)

where E_a, R, T, σ_0 present the activation energy, gas constant, and temperature, and preexponential factor, respectively.

In Arrhenius type of behavior, activation energy (energy barrier height) is the rate determining factor in the conduction process. Motion of ions in the polymer matrix is a thermally activated process based on hopping over energy barrier of ions posessing enough energy. With increasing temperature, more charged species posses enough energy to overcome the barrier. Therefore, the conductivity increases with increasing temperature. The preexponential factor is the limiting conductivity of the material at infinite temperature.

The temperature dependence of the conductivity in polymer electrolytes has often been taken as being indicative of a particular type of conduction mechanism.[111, 113] In particular, a distinction is generally made between systems that show an Arrhenius type behavior and those that present a curvature in plots of log σ versus inverse temperature.

Empirical equations based on the free-volume theory such as the Vogel-Tamman-Fulcher (VTF) equation (6.28) and Williams-Landel-Ferry (WLF) equation (6.29) have been used to describe the curvature of the log σ versus inverse temperature plots.

$$\sigma = \sigma_0 \exp\left(\frac{-B}{(T - T_0)}\right) \quad (6.28)$$

where T_0 is a reference temperature and σ_0 contains a $T^{-1/2}$ term in addition to other constants. A time-temperature superposition holds which allows to correlate data obtained at different frequencies and temperature by a shift factor*, a_T. A and B are experimental constants frequently found as A= -17.44 and B=51.6. T_g is the glass transition temperature.[111]

$$\log a_T = \frac{A(T - T_g)}{B + T - T_g} \quad (6.29)$$

6.5 A Mechanism for Iontransport by Funke

In solid electrolytes mass and charge are generally transported by the hopping motion of charged defects. The mobile defects may be vacancies or disordered ions. The hopping motion of the charged defects is strongly influenced by their repulsive interaction. Understanding of the macroscopic properties like conductivity requires consideration of the interactions between the mobile defects.[114] In case of strong dilute strong liquid electrolytes, models considering the Coulomb interaction among ions were introduced by Debye, Hückel, Onsager, and Falkenhagen.[115-117] A model for the

* Shift factor is the ratio of any mechanical relaxation process at temperature T to its value at some refence temperature.

interpretation of ion transport mechanism in solid ionic conductors was proposed by Funke, which is based on the models of Debye and Hückel. The ideas of Funkes model will be very briefly mentioned here. [114, 118, 119]

A lattice consisting of mobile and immobile ions are shown in Figure 6.7a. Due to the Coulomb interaction, the mobile ions tend to stay at some distance from each other. The potential experienced by the central ions results from the presence of immobile ions and from the interactions with other mobile defects. The potential provided by the immobile ions is called periodic lattice potential $V_p(x)$, while the potential due to the interactions of the mobile ions with other defects is named as Coulomb potential, V_c (x). The total potential of the central ion can be given by Equation (6.30), where x is the distance.

$$V_{total}(x) = V_c(x) + V_P(x) \quad (6.31)$$

Figure 6.7b illustrates the total potential experienced by the central given under the condition that the central ion is in its relaxed position with respect to others so that V_c has its minimum at the site of the defect (x=0). If the central charged defect, originally residing at site A, is thermally activated, it can hope to a vacant neigbouring site, B (Figure 6.7c). The system of charged defects tends to recover a relaxed configuration. The system has two probabilities to recover a relaxed configuration. The first probability is that the central defects hops back from B to A, which is energetically favourable

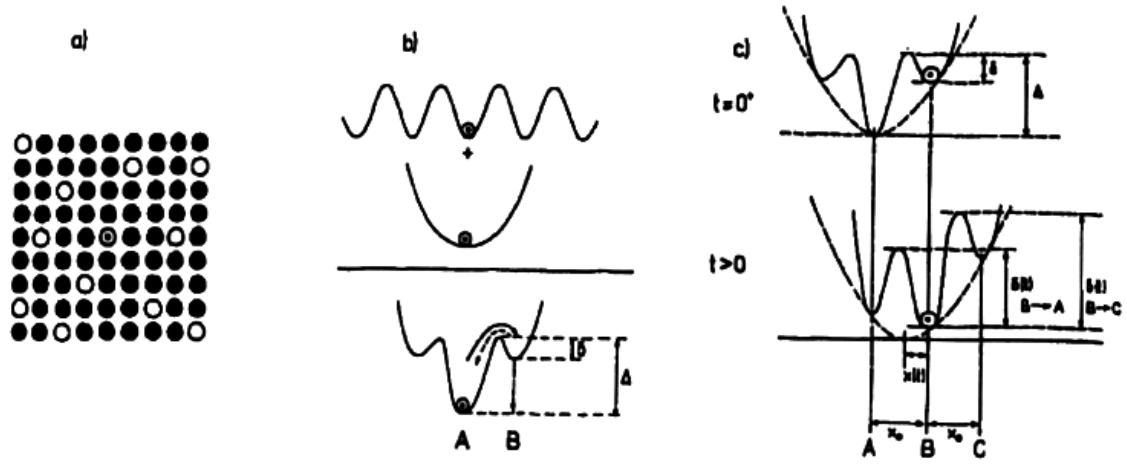

Figure 6.7: a) Ions in a sublattice: Central ion (⊙), mobile ion (○), immobile ion (●) b) potential of the central ion c) development of the potential around the cenral ion with time after a hop.[114]

since the potential energy experienced by the defect at site A is lower than that of at site B. The other possibility is that the neighboring defects rearrange and relax with respect to the newly occupied site. In this case, the Coulomb minimum moves towards site B. The energetical status of the central defect becomes favourable. Thus, the probability of its backhop tends to zero as the Coulomb minimum approaches to site B. Eventually, the hop becomes successful, and V_{total} (x) is shifted by the distance between neighbouring sites, x_0, as shown in Figure 6.7c. The development of the system with time after the hoping of the central charged defect from site A to site B at time t = 0 is desribed in terms of two mathematical functions called W(t) and g(t). W(t) describes the probability of the backward hop of the defect from B to A at t>0. When the defect hops from site A to site B at t = 0, the Coulomb potential starts to shift from A towards B as its neighborhood

starts to relax. The shift of the Coulomb potential is described the function g(t). The mathematical equations for these two functions are not given in this work.

6.6 Solid State Nuclear Magnetic Resonance

Knowledge concerning the chemical environment and proton motion is crucial for understanding the conduction mechanism of proton conducting materials. Impedance spectroscopy has been the most standard method to study the proton conducting materials. It yields bulk conductivity data through the measurement of charge transport but it does not directly provide information about the local mobility. Solid State NMR spectroscopy is a powerful probe of ion motion on the molecular level since it allows us to selectively observe the nuclei of interest.[120, 121] Such information is helpful to give a fundamental understanding of the observed differences in the proton conductivity. ^{1}H chemical shift values provide information about the chemical environments of the protons and the line widths at various temperatures give an insight into the mobility. ^{1}H-NMR spectrum of solid polymers often exhibits severely broad signals due to the strong ^{1}H-^{1}H homonuclear dipolar coupling* and the random orientation of the molecule. In recent years, fast magic angle spinning (MAS) has been used to average the ^{1}H-^{1}H dipolar couplings* and thereby achieve high resolution spectra for organic solids. For MAS NMR experiments, the sample is inclined by a specific angle (the magnitude of the magic angle is 54.74°[122]) with regards to the magnetic field and spun fast during the

* The dominant interaction is the dipole-dipole coupling in solids. It is based on the interaction of the small local fields of the nuclear magnetic moments. Therefore, dipole-dipole coupling is independent of the applied magnetic field and depends on the spatial arrangement of the nuclei. The strength of the coupling decreases as the internuclear distance increases. In liquids, ions and molecules reorient rapidly on the NMR time scale. As a conseqeunce the direct dipole-dipole interactions are cancelled by motional averaging.

signal acquisition. This can effectively reduce or removes the aniosotropic interactions. are averaged out. However, since the strength of dipolar interactions can be used to determine the relative mobility of protons, methods which can selectively retrieve information about the dipolar interaction removed by MAS are useful. Double quantum filtering pulse sequences such as back-to-back allows us to recouple the dipolar couplings between the protons which are rigid on the time scale of the pulse sequence and which are close to each other in space.

The results of some Solid State NMR experiments that are important for the discussion of conductivity behavior of PVPA are briefly mentioned in this chapter. The details of the NMR techniques are not given here.

6.7 Conductivity of PVPA

PVPA is an interesting macromolecule with the highest density of phopshonic acid functions tethered to the polymer backbone. As already mentioned in Chapter 1, the details of the polymerization of VPA and the properties of the polymer were studied since PVPA is a potential candidate to be a component of PEMs in a low humidity environment at operating temperatures higher than 100 °C. There is no detailed report about the proton conducting properties of homopolymer to the best of our knowledge other than commercially available PVPA, which was only briefly mentioned in a comparison with its composites.[30] This chapter presents the conducting properties of "pure" PVPA as the key constituent of polymer electrolyte membranes. The formation of phosphonic acid anhydrides influences the conductivity of PVPA to a large extent.

Dielectric Spectroscopy was used to investigate the conductivity and Solid State NMR was suggested as a tool to detect and quantify the anhydride formation in phopshonic acid species for the first time. PVPA with different molecular weight and microstructure were investigated in terms of their proton conductivity as well as self-condensation of the phosphonic acid groups to have a better understanding of relationships between structure and property.

6.7.1 Temperature Dependence of Conductivity of PVPA

The proton conductivity behavior of PVPA of known molecular weight, and microstructure was investigated by Dielectric Spectroscopy in an open system under dry conditions. PVPA samples were exposed to different drying procedures, followed by conductivity measurements to determine the influence of the different drying procedure on the conductivity as well as on the formation of phosphonic acid anhydride species. All samples displayed frequency-independent plateau regions in their alternating current versus frequency plots. The direct current conductivity of the samples was estimated from the alternating current plateaus.

The proton conductivity of the high molecular weight (M_w=62 000 g/mol), and nearly atactic PVPA (1) synthesized by free radical polymerization of VPA was recorded after drying the sample at 50 °C under reduced pressure to a constant weight. The conductivity of PVPA (1) was measured in four steps by using the temperature program 1, which is already described in the second chapter. This temperature program allowed us to follow the changes in the conductivity between 20 and 210 °C. The frequency dependent conductivity data of vacuum dried and annealed PVPA (1) are given in Figure 6.8 and Figure 6.9, from which direct current conductivity of PVPA (1) estimated.

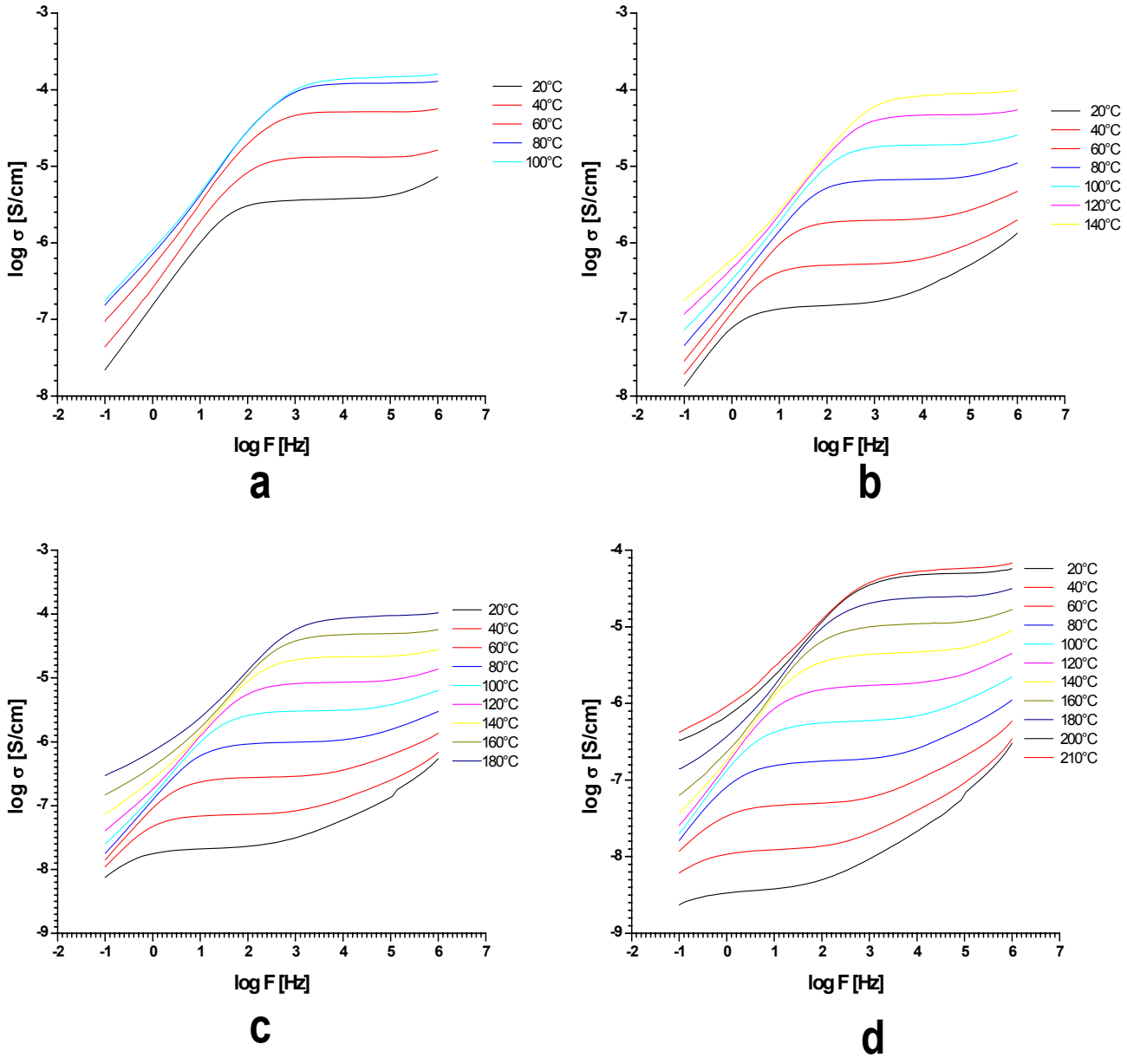

Figure 6.8: Frequency dependent proton conductivity plots of PVPA (1) in the temperature regime of a) 20-100 °C b) 20-140 °C c) 20-180 °C d) 20-210 °C.

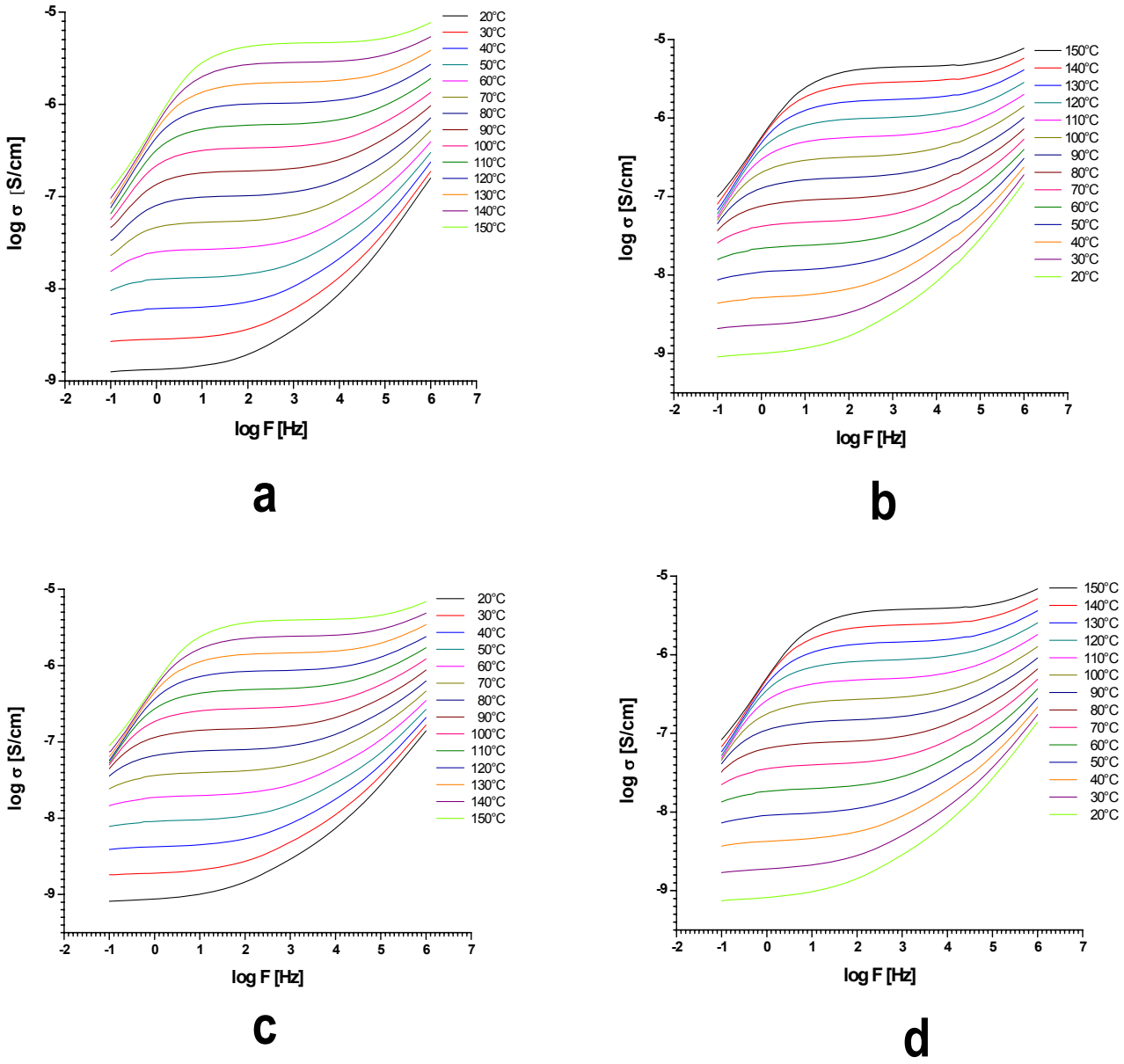

Figure 6.9: Frequency dependent proton conductivity plots of 2 days annealed PVPA (1) in the temperature range of a) 20-150 °C (1st heating cycle) b) 150-20 °C (1 st cooling cycle c) 20-150 °C(2nd heating cycle) d) 20-210 °C(2nd cooling cycle).

The direct current conductivity of a vacuum dried- and annealed- PVPA (1) was plotted as a function of temperature between 20 °C and 210 °C (Figure 6.10). The data were tried to be fitted to VTF, WLF, and Arrhenius equations. The best fit was obtained when the

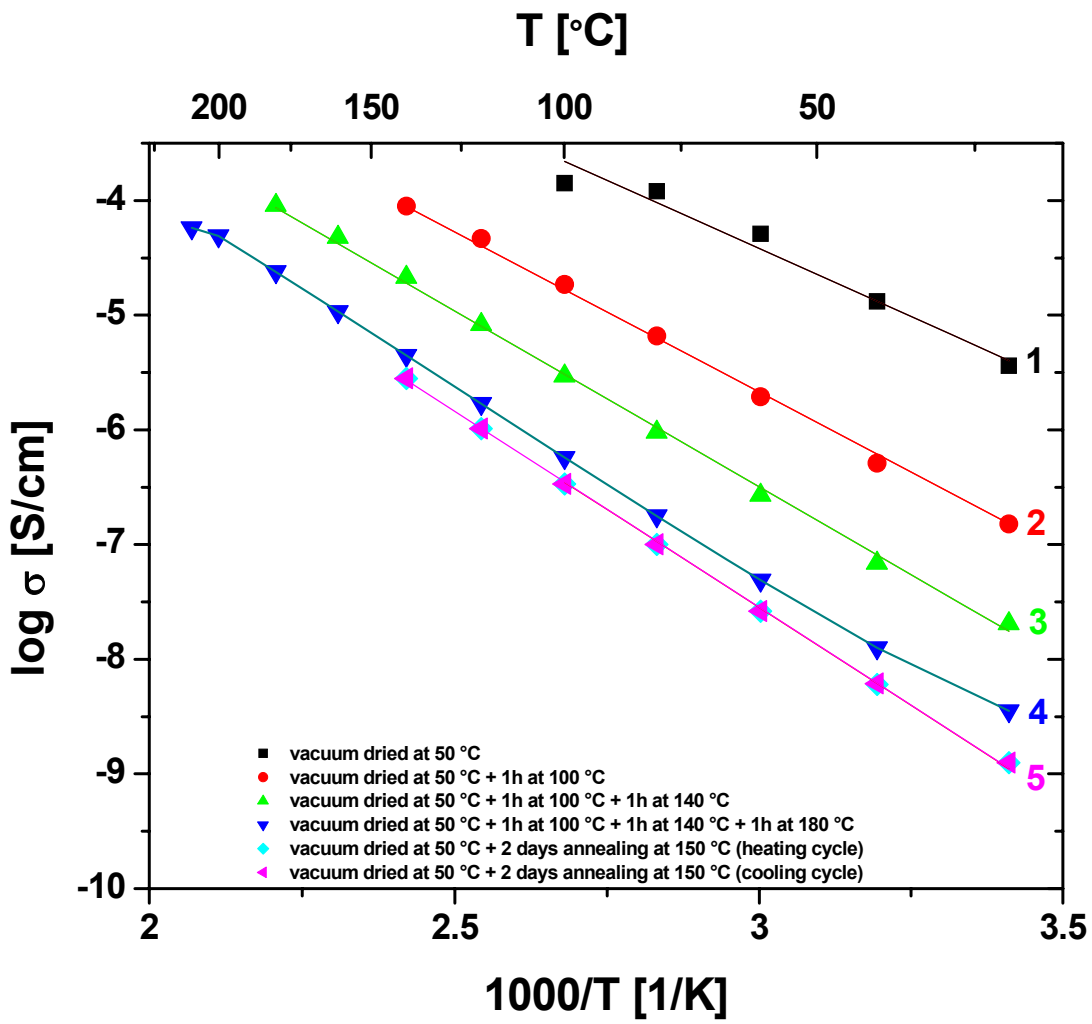

Figure 6.10: Conductivity of high molecular weight PVPA (1) (M_w = 62 000 g/mol) as a function of temperature after several heat treatments (solid lines represent the fit of the data to Arrhenius equation).

data was fitted to the Arrhenius law. Solid lines in represent the fitting of the data to Arrhenius equation. Actually, there is a slight leveling off in the conductivity at 100 °C at the end of the first data set in Figure 6.10. Thus, the data points seem to be curved slightly. However, the reason for this leveling off in the conductivity at 100 °C is due to the water loss. Thereby, we obtain similar values for the conductivity at 80 °C and 100 °C at the first heating cycle. In other words, the data did not reveal the signature of VTF or WLF behavior in the temperature range studied.

The preexponential factor and activation energy for conductivity were extracted from the slope and intercept of the log σ versus T^{-1} plot. The preexponential factor and activation energy obtained from the conductivity data of PVPA (1) are given in Table 6.1. All five data sets (labeled from 1 to 5 in Figure 6.10) reach the same limiting conductivity at infinite temperature. In other words, they share a common of preexponential factor, which is around 500 S/cm. However, the data sets have different the activation energy. The activation energy was found to increase as the sample was exposed to higher temperatures and longer times.

Table 6.1: Activation energy and preexponential factor for PVPA (1) extracted from the conductivity data

Sample	**Temperature regime**	**log σ_0**	**E_a (kJ)**
vacuum dried PVPA (1) at 50 °C	20-100 °C	2.7	45
vacuum dried PVPA (1) at 50 °C	20-140°C	2.7	53
vacuum dried PVPA (1) at 50 °C	20-180 °C	2.7	58
vacuum dried PVPA (1) at 50 °C	20-210 °C	2.7	63
2 days annealed PVPA (1) at 150 °C	20-150°	2.7	65

The fit of the temperature dependent conductivity data to Arrhenius equation suggests that the conductivity in PVPA is based on the ion (proton) hopping in the temperature range between 20 °C and 210 °C. In other words, ion hopping resulting in the observed conductivity is a thermally activated process. As already mentioned in 6.5, hopping takes place when protons have enough energy to overcome energy barrier. They first hope to intermediate energy levels before relaxation occurs and they reach to their final position. These intermeadite energy levels are shown in Figure 6.11 ΔE_1 represents the energy barrier to be overcome for a hop to the lowest intermediate energy level. As shown in

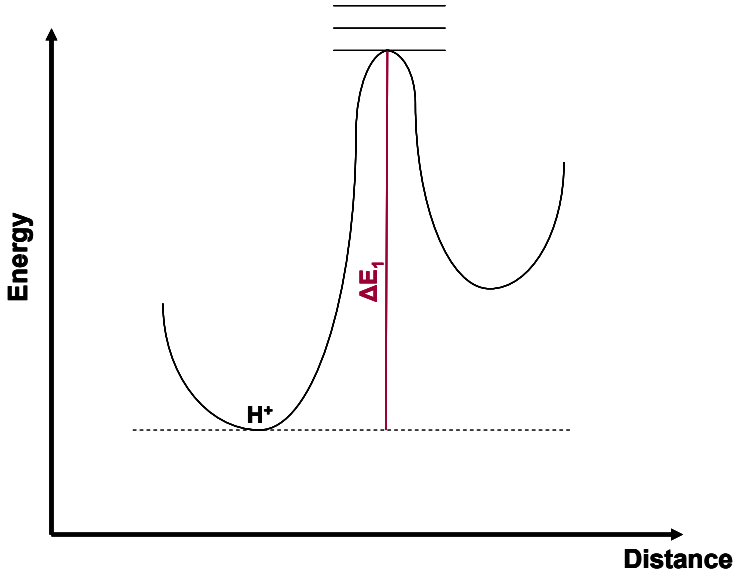

Figure 6.11: Energy diagram before hopping

Table 6.4, the activation energy increases as PVPA (1) was exposed to higher temperatures and longer times indicating that the ions have to hopp to a higher intermediate energy level. This can happen when the lower intermeadiate energy levels are not available any more. The hypothetic distribution of the intermediate energy levels

is shown in Figure 6.12. The unavalibility of some low energy intermediate levels implies that some of the intermediate steps are lost. In other words, some slices are removed from the distribution curve. As a result of this, protons now have to hopp to a higher inter mediate energy level, which is in accordance with the increasing value of the activation energy for PVPA (1).

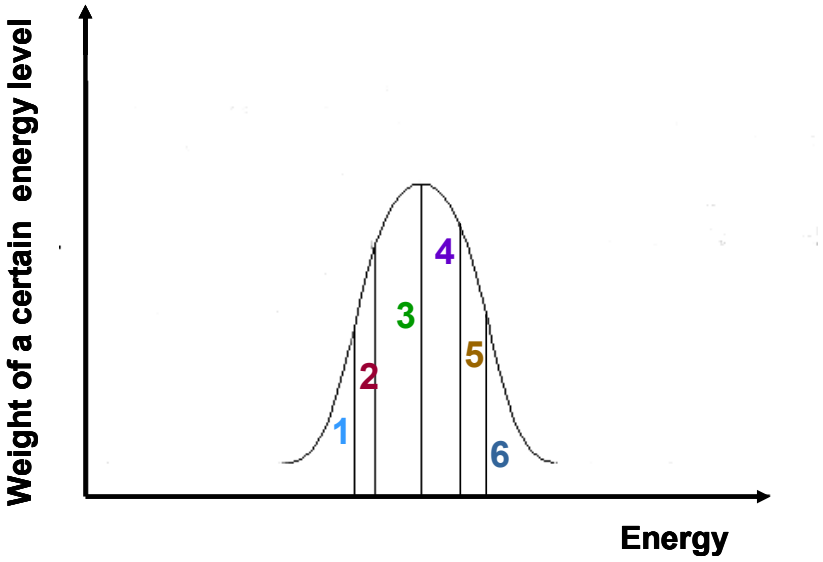

Figure 6.12: Hypothetic distribution of intermediate energy levels (numbers denote different slices of the distribution curve)

The presented conductivity data suggests that the temperature dependence of the conductivity behavior of PVPA (1) can be desribed by Arrhenius equation. Whether the conduction in PVPA follows an Arrhenius type law is not clear yet, but the available conductivity data suggest that the temperature dependence of conductivity does follow Arrhenius behavior in the range of 20 to 210 °C. However, it is worth to mention that our conductivity measurements cover only a very small window in temperature. It has been

already reported that temperature dependence of some polymer electrolytes display Arrhenius behavior at low temperatures and VTF behavior at high temperatures. This probability still exists for PVPA case.

Conductivity of PVPA (1) increases as temperature increases among each data set. However, the conductivity decreases relatively upon exposing the sample to higher temperatures and longer times, which becomes clear when the conductivity values of each data set (Figure 6.10) at a certain temperature were compared. The conductivities at 20 °C and 80 °C for each step of measurement are given in for the sake of simplicity in Table 6.2.

Table 6.2: The log conductivity of PVPA (1) at 20 °C, at 80 °C

Data set	**log $\sigma_{20\,°C}$ (S/cm)**	**log $\sigma_{80\,°C}$ (S/cm)**
1	-5.5	-3.9
2	-6.9	-5.2
3	-7.7	-6.1
4	-8.4	-6.7
5	-8.91	-7.0

6.7.2 The Correlation between Conductivity and Formation of Anhydride Species

As already mentioned, the conductivity of PVPA (1) is decreasing when the polymer was exposed to higher temperatures and longer times. The presence of water improves the proton conductivity of PVPA at low temperatures. The decrease in the

conductivity at a given temperature in the successive measurements indicates that the water content of the samples is reduced, which leads to the undesired formation of phosphonic acid anhydride species, which will be discussed in more details in 6.6.1. Once these species are formed, conductivity is lowered since a fraction of mobile protons are lost during this process. The fraction of phopshonic acid anhydride species at two data points in Figure 6.10 and the revelant conductivity values are given in Table 6.3. After vacuum drying of PVPA (1) at 50 °C to the constant weight, the fraction of cyclic anhydride species was found 14%, and conductivity of this sample was $3.2x10^{-6}$ (S/cm) at 20 °C. It is assumed that the number of cyclic phopshonic acid anhydride species stays constant during each heating cycle.

Evolution of water is a time taking process and occurs at different rates at various temperatures. The rate of the reduction of water content of the sample is expected to be more pronounced at higher temperatures (above the boiling point of water). To allow more time for the evolution of water, PVPA (1) was annealed at 150 °C for 2 days, and its conductivity was measured between 20 °C and 150 °C by using the second temperature program. Upon annealing of PVPA (1) at 150 °C for 2 days, the fraction of the cyclic anhydrides were enhanced to 43%.This leads to a decrease in the proton conductivity when compared to the conductivity of the sample at 20°C which was dried at 50 °C to constant weight. Conductivity data of the annealed PVPA (1) were acquired during both heating and cooling cycles in the range of 20 and 150 °C. The conductivity values remained unchanged in successive measurements as shown in Figure 6.13.

Table 6.3: The log conductivity of PVPA (1) at 20 °C and fraction of phosphonic acid anhydride*

Data set	log $\sigma_{20\,°C}$ (S/cm)	Fraction of P-O-P (%)
1	-5.5	14
5	-8.9	43

This may indicate that the water evolution that can take place under these conditions is complete in the annealed sample, and therefore, the conductivity does not change any more. The fraction of the phosphonic acid anhydride species after 2days annealing at 150 °C was 43%, and the conductivity of the sample was 1.3×10^{-9} (S/cm).

Formation of the cyclic anhydride species decreases the number of protons available for conduction. The fraction of the remaining P-OH does not provide information about the number of charge carriers since not all available protons may take part in the conduction process. The number of the charge carriers in the sample will greatly depend on other factors such as self-dissociation of PVPA. However, the fraction of anhydride species and the corresponding conductivity values indicate that there should be other factors changing with temperature in addition to the number of charge carriers. To be able to explain the decrease observed in the conductivity, one has to assume that mobility is also changing with temperature in addition to the number of charge carriers. The conductivity of PVPA should be expressed in terms of the following equation:

$$\sigma(T) = n(T)\mu(T)e \qquad (6.32)$$

* The detection and quantification of the phopshonic acid anhydride species will be discussed in details in later sections of this chapter.

However, determination of the diffusion coefficients is necessary to confirm this idea. Combining the knowledge in diffusion coefficients with conductivity data in the Nernst-Einstein equation is expected to lead to a better understanding of proton conduction mechanism in PVPA. On the basis of the conductivity data and diffusion coefficients of the low molecular weight compounds, namely 1-heptylphosphonic acid,[22] the proton conduction is expected to take place by a vehicle mechanism at low temperatures in the presence of water, and after the evolution of water at high temperatures, the structure diffusion will be the dominant conduction mechanism as expected from the pronounced amphoteric character of the phosphonic acid group.

6.7.3 Conductivity of PVPA (1) at Constant Temperature

The conductivity of PVPA was also investigated at constant temperature (100 °C) between 10^{-1} and 10^{6} Hz. The change of conductivity of PVPA (1) was monitored by using the third temperature program described earlier in the experimental section. The sample was heated to 100 °C very quickly, the moment when the temperature of the sample reached to 100 °C is defined as time zero. The conductivity decreases by more than two orders of magnitude when the sample is kept at 100 °C for 24 h. The data obtained was fitted by two different functions, which are given in Equations (6.33) and (6.34). In both case, an offset for the conductivity was added (A and B in Equations (6.33) and (6.34), respectively) to these functions since the value of the conductivity cannot reach zero. t is time, σ_i is the conductivity at t=0, k is the rate with which the conductivity is decreasing.

$\sigma(t) = A + \sigma_i e^{-kt}$	(6.33)

$\sigma(t) = B + \frac{\sigma_i}{1 + \sigma_i kt}$	(6.34)

The conductivity data of PVPA (1) at constant temperature can be better described by Equation (6.34) rather than by Equation (6.33). This becomes more clear by comparing the two different fits of the data when y axis of the conductivity plot is in a logarithmic scale (Figure 6.13). The reason why the decay of conductivity fits better to the mathematical function in Equation (6.34) is not clear yet. Most probably, the conductivity of PVPA is a complicated result of many different processes as in most polymer electrolytes.[111]

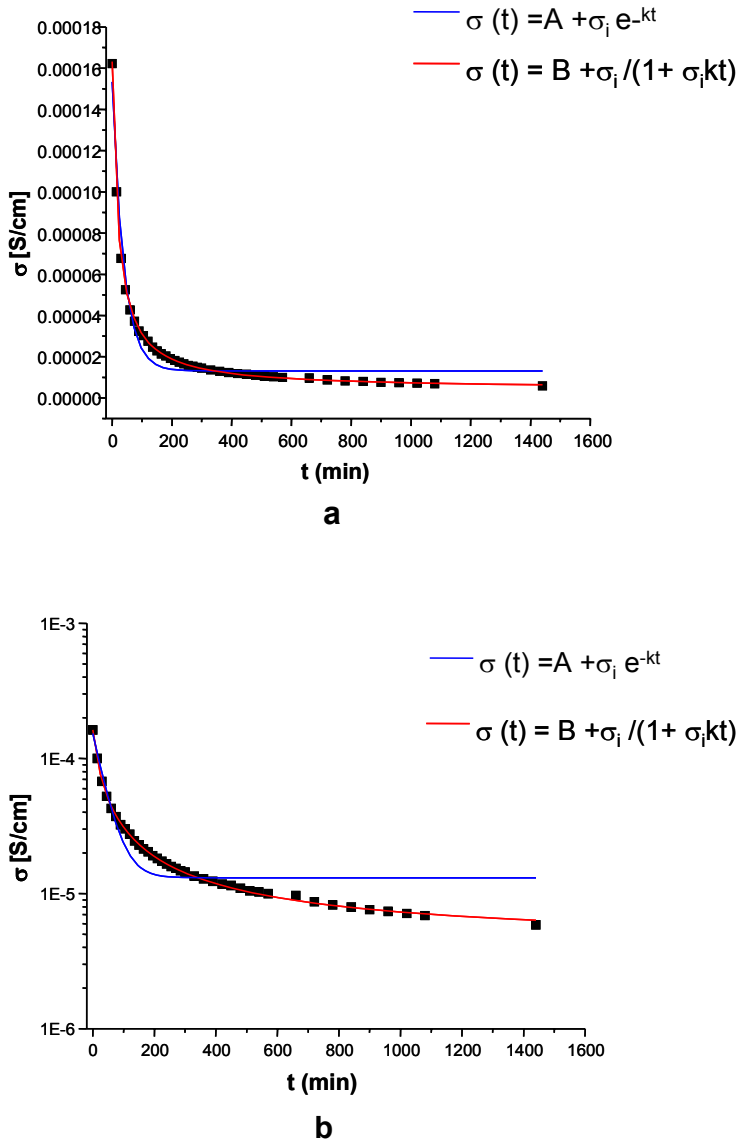

Figure 6.13: Conductivity of PVPA (1) as a function of time at constant temperature (100°C), y axis in a) linear b) logarithmic scale.

6.7.4 Effect of Molecular Weight on Conductivity

The conductivity behavior of PVPA different in chain length samples was studied between 20 and 210 °C in the range of 10^{-1} and 10^{6} Hz. The frequency dependent

conductivity data of different molecular weight PVPA samples are presented in Figure 6.14, Figure 6.15, and Figure 6.16. The direct current conductivity of the samples was estimated from the alternating current plateaus and they were plotted as a function of temperature between 20 and 210 °C (Figure 6.17, Figure 6.18, Figure 6.19).

All PVPA samples displayed conductivity between 20 and 210 °C. The conductivity behavior of PVPA (2), PVPA (3), and PVPA (4) resemble the conductivity behavior of the high molecular weight PVPA (1), which is already discussed in details in 6.7.1. The conductivity of all PVPA samples increase as temperature is increased. However, a drop in conductivity was observed when the samples were exposed to higher temperatures and longer times due to the water loss and formation of cyclic anhydride species. The fraction of phosphonic acid anhydride species PVPA (2), PVPA (3), and PVPA (4) were not studied by Solid State NMR.

The conductivity data of different PVPA samples seem to fit to the Arrhenius equation as in the case of the high molecular weight PVPA (1). The fit of the data to the Arrhenius equation is shown with the solid lines in the temperature dependent conductivity plots. The preexponential factor and activation energy for each sample was extracted from the intercept and the slope of log σ versus T^{-1} plots, respectively (Table 6.4). The data sets obtained after different heat treatments of the same polymer sample reach the same limiting conductivity at infinite temperature. However, they differ in their activation energy. These observations are valid for all PVPA samples.

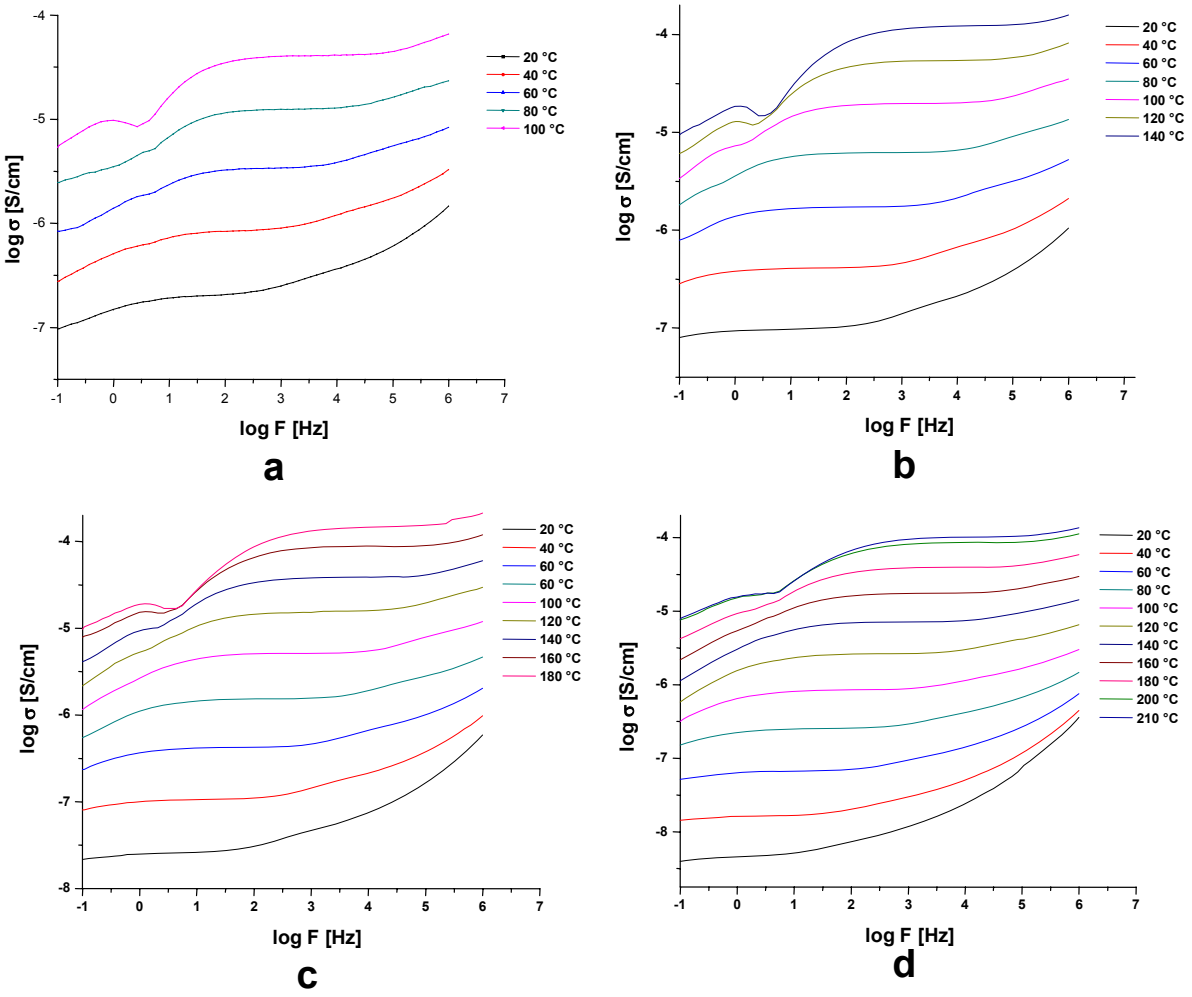

Figure 6.14: Frequency dependent conductivity plots of PVPA (2) in the temperature regime a) 20-100 °C b) 20-140 °C b)-20-180 °C d) 20-210 °C.

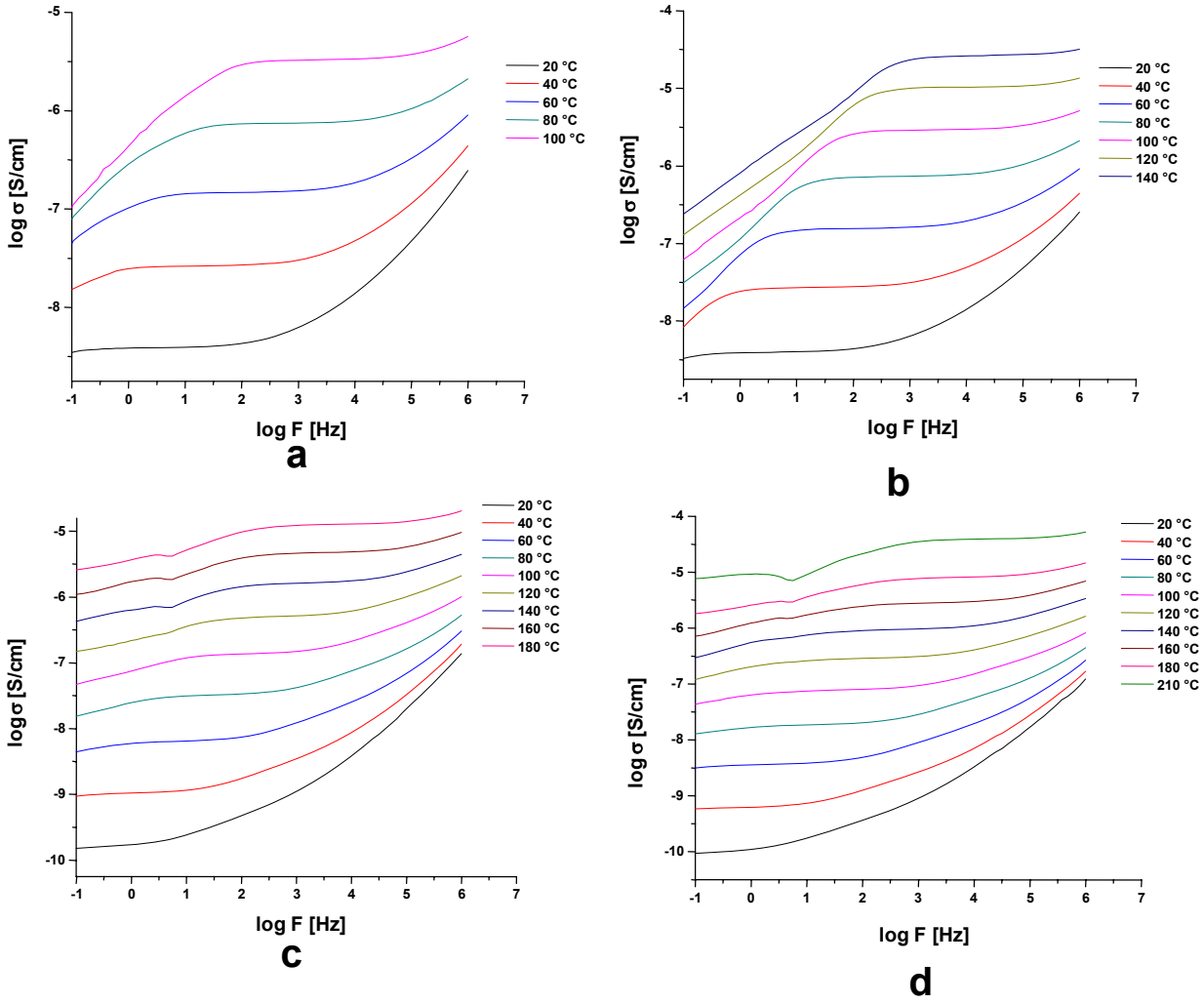

Figure 6.15: Frequency dependent conductivity plots of PVPA (3) in the temperature regime a) 20-100 °C b) 20-140 °C b)-20-180 °C d) 20-210 °C.

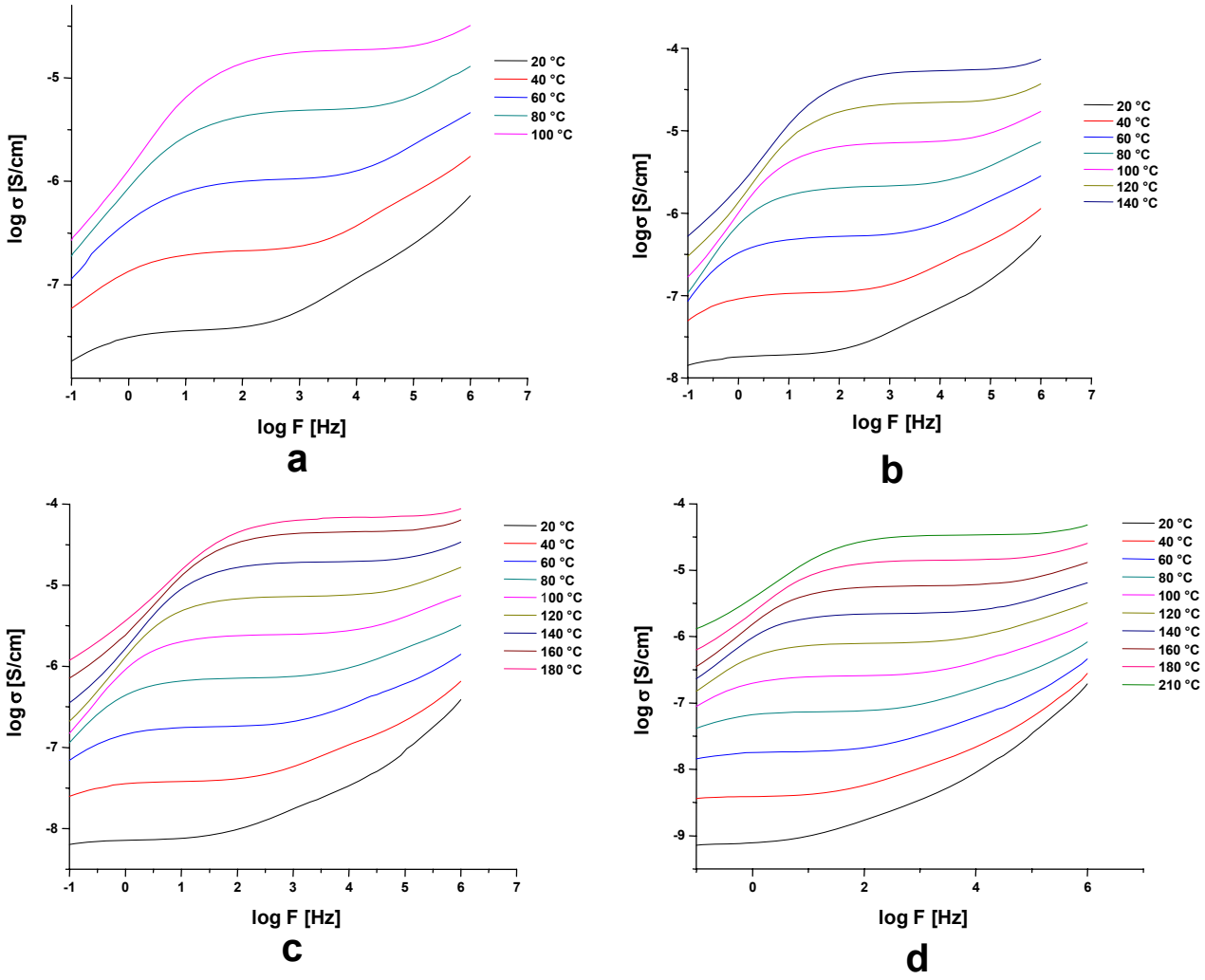

Figure 6.16: Frequency dependent conductivity plots of PVPA (4) in the temperature regime a) 20-100 °C b) 20-140 °C b)-20-180 °C d) 20-210 °C.

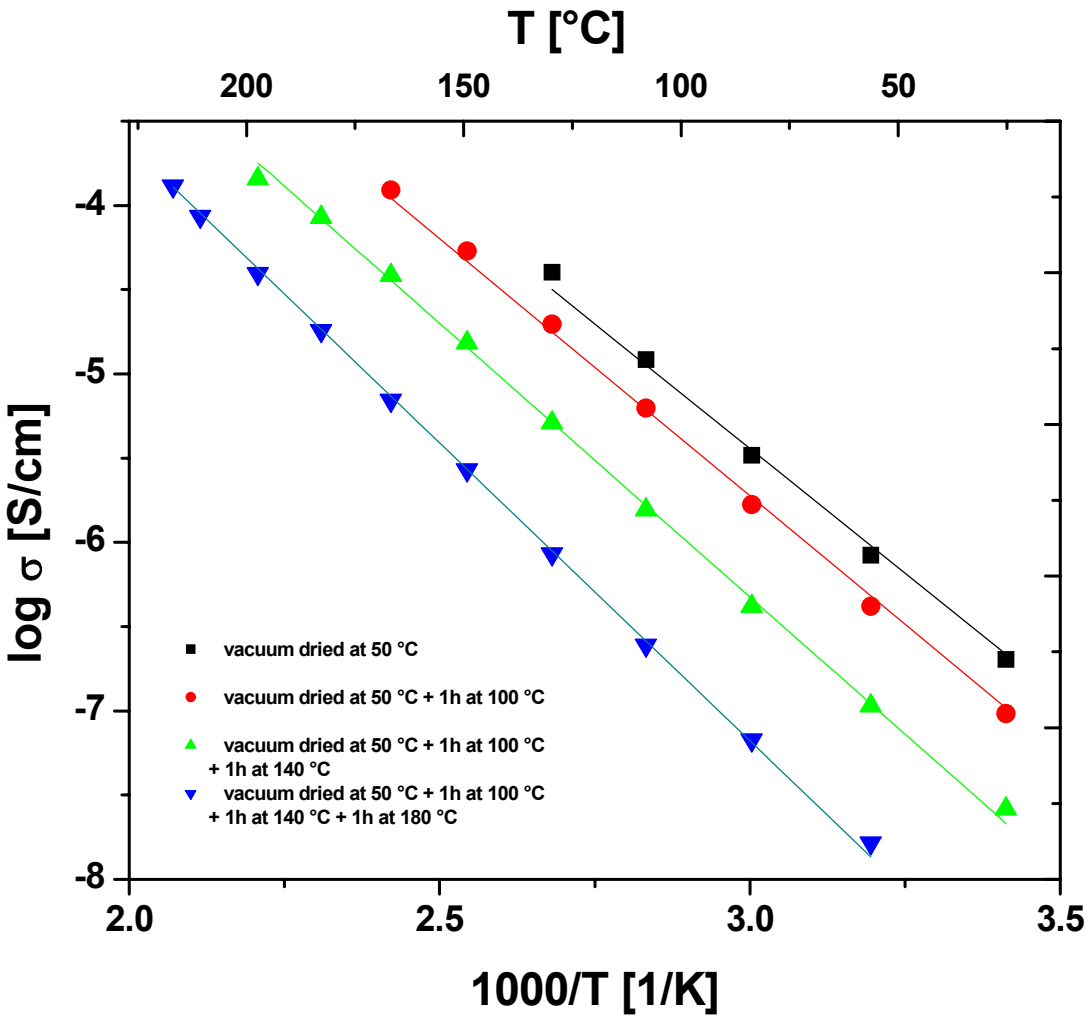

Figure 6.17: Conductivity of PVPA (2) (M_w = 44 700 g/mol) as a function of temperature (solid lines represent the fit of the data to Arrhenius equation).

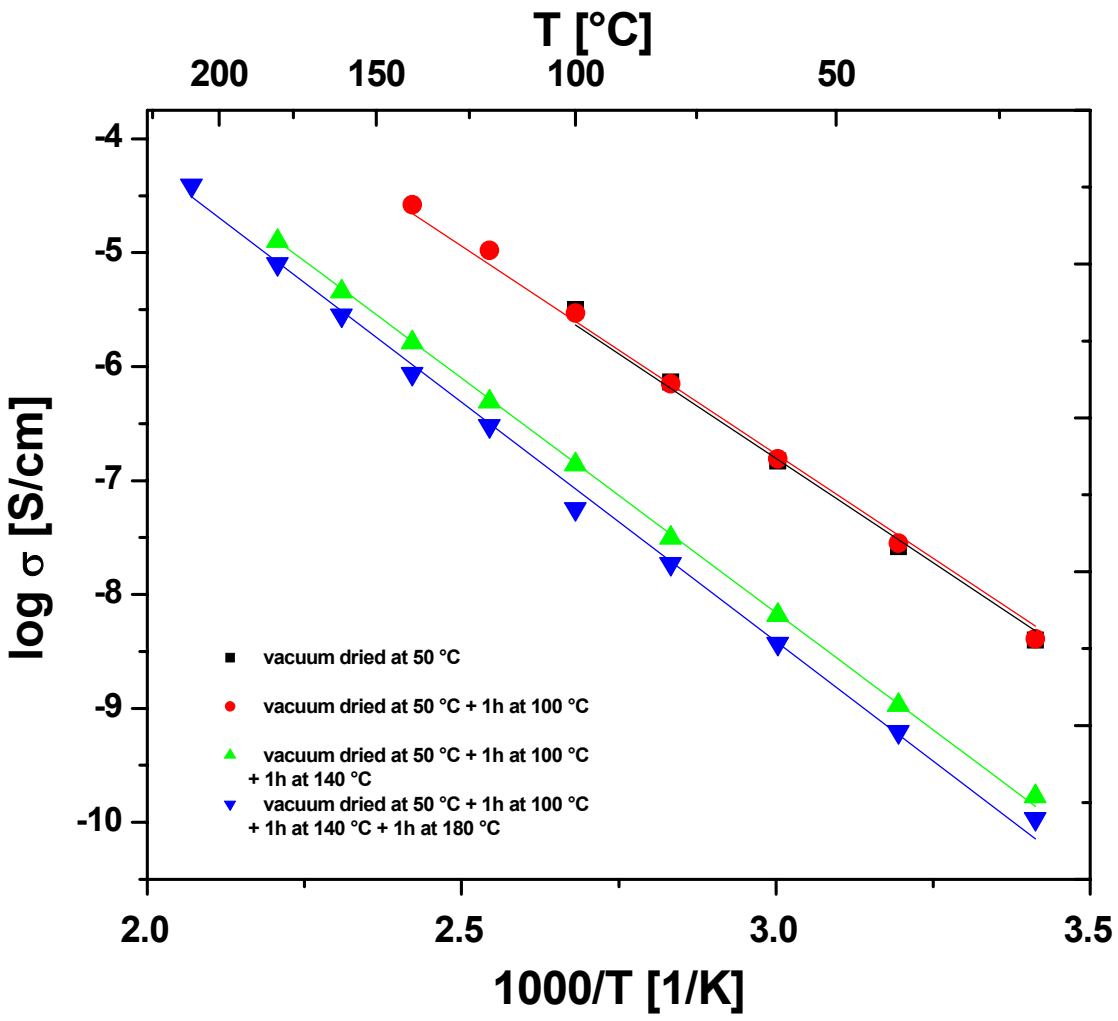

Figure 6.18: Conductivity of PVPA (3) as a function of temperature (solid lines represent the fit of the data to Arrhenius equation).

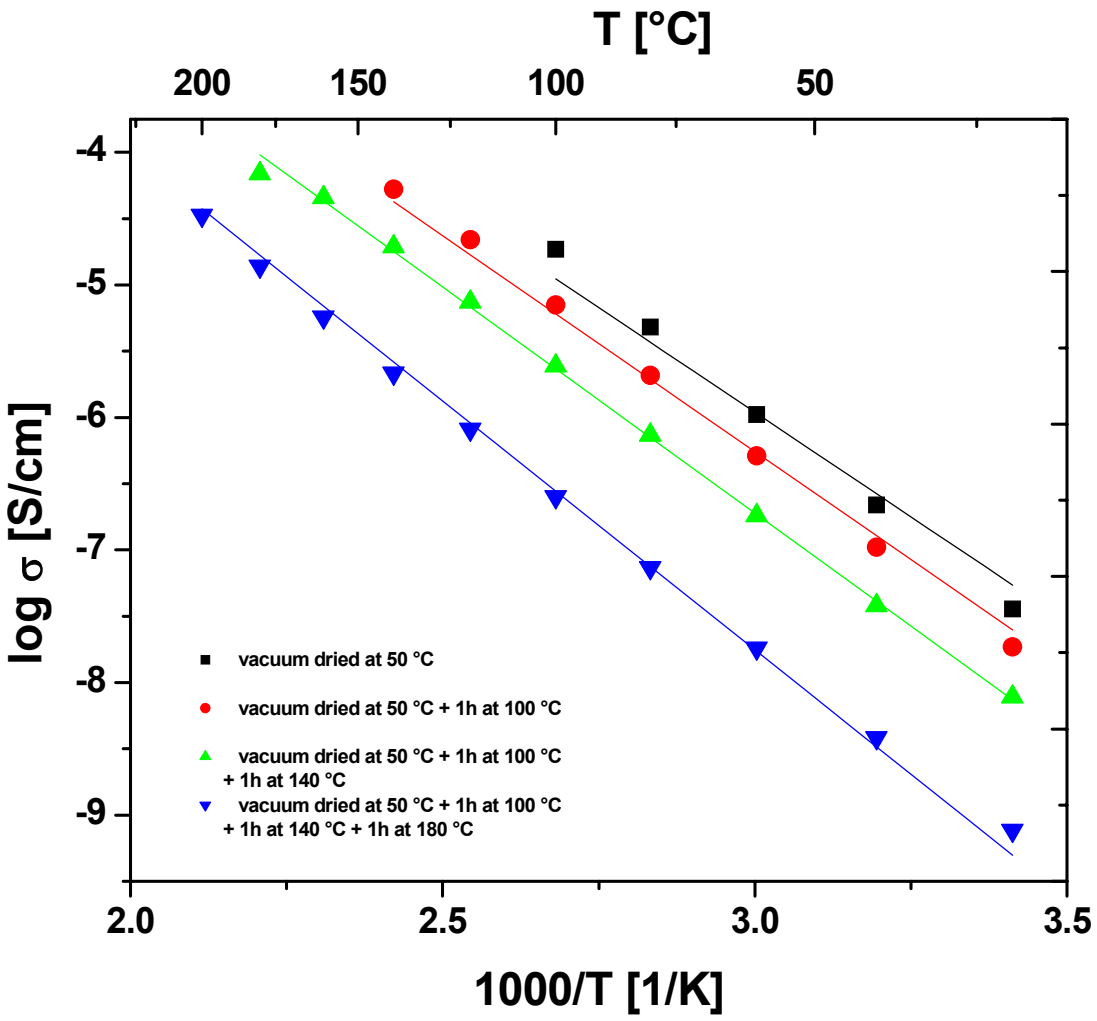

Figure 6.19: Conductivity of PVPA (4) as a function of temperature (solid lines represent the fit of the data to Arrhenius equation).

Table 6.4: Activation energy and preexponential factor extracted from conductivity data of a) PVPA (2) b) PVPA (3) c) PVPA (4).

a)

Temperature regime	log σ_0	E_a (kJ)
20-100 °C	3.4	55
20-140°C	3.4	59
20-180 °C	3.4	62
20-210 °C	3.4	68

b)

Temperature regime	log σ_0	E_a (kJ)
20-100 °C	4.3	70
20-140°C	4.3	70
20-180 °C	4.3	79
20-210 °C	4.3	81

c)

Temperature regime	log σ_0	E_a (kJ)
20-100 °C	3.5	60
20-140°C	3.5	62
20-180 °C	3.5	65
20-210 °C	3.5	72

The increase in activation energy for different PVPA samples can be interpreted in the same way as for PVPA (1). Due to the removal of low intermediate energy levels from the energy distribution curve, protons have to overcome a higher energy barrier for hopping, which results in an increase of activation energy.

The conductivitiy data of different PVPA samples were overlayed for a comparison in the temperature regime between 20 and 210 °C. The data of each heating cycle for four different PVPA samples are shown in the same plot in Figure 6.20.

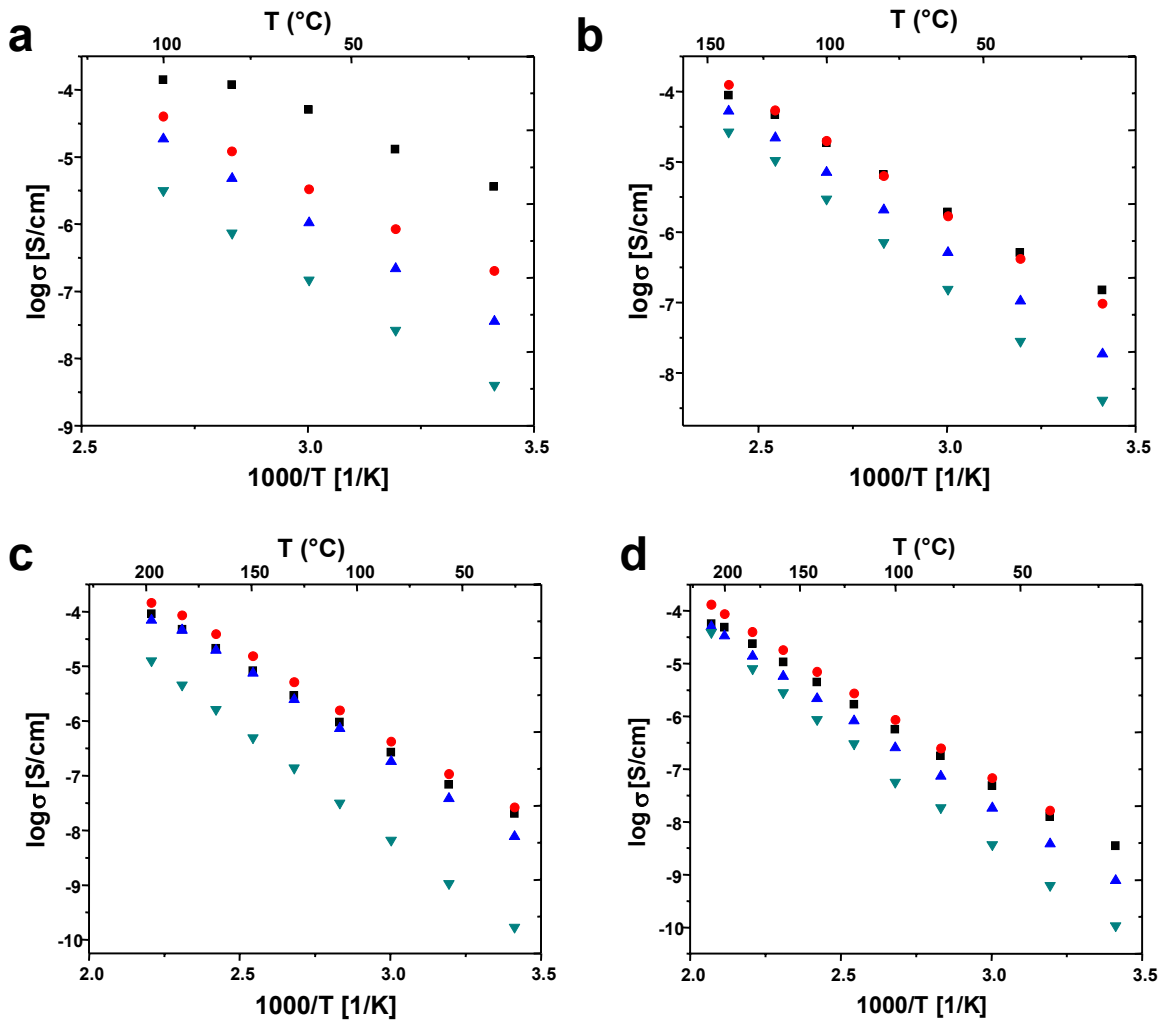

Figure 6.20: Temperature dependence of proton conductivity of PVPA of various molecular weights between a) 20-100 ˚C b) 20-140 ˚C c) 20-180 ˚C d) 20-210 ˚C (■ PVPA (1)(M_w = 62 000 g/mol)(● PVPA (2))(M_w = 44 700 g/mol) ▲ PVPA (3) (M_w X), ▼ PVPA(4) (M_w X) (X: not known)).

The various samples have different conductivities at the beginning of the measurement. The highest molecular weight PVPA displays the highest conductivity initially, and the conductivity is lowest for the shortest polymer obtained by the polymerization of VPA. The initial difference in the proton conductivity of the various

PVPA samples may be explained by their different water content. However, after the heat treatment at 100 °C for 1 hour, the conductivity of PVPA (1) and PVPA (2) become very similar, and at the end of the first temperature program, all PVPA exhibit almost the same conductivity.

At temperatures below the boiling point of water, water contributes to the proton conductivity to a large extent. The water molecules can act as additional proton solvents and contribute to the proton transport either by self-diffusion while carrying a proton (vehicle mechanism) or by rapid exchange of protons via hydrogen bridges (hopping mechanism). Both cases will improve the conductivity and reduce the activation energy for proton hopping.[123] Therefore, difference in the water content of the samples leads to different conductivity values. After evolution of water from the polymer samples, they exhibit similar conductivity values independent of the molecular weight.

As mentioned in the experimental part, pellets were prepared to perform the conductivity studies of PVPA. However, it was also tried to cast membranes from the aqueous solutions of these polymer samples. Good quality films were obtained only with the highest molecular weight sample. It was not possible to prepare films of the materials with shorter chains good enough for conductivity measurements. The films were very fragile, and holes were formed during the drying procedure. Although current results imply that the molecular weight does not play role in the conductivity at higher temperatures, the mechanical properties of the various chain length polymers are different, which is important for preparation of the proton exchange membranes.

6.8 Solid State NMR Studies of PVPA

6.8.1 Formation and Quantification of Phosphonic Acid Anhydride Species

The formation of phosphonic acid anhydride species may result from either condensation of two P-OH groups next to each other along the same chain, or the condensation of P-OH groups on different chains. In other words, P-O-P linkages can form either intra- or intermolecularly (Scheme 6.1). The formation of P-O-P linkages has already been proposed in the case of commercial PVPA from Polyscience, which was soluble in water at room temperature. Heating the sample increased the time required for dissolution. After being heated to 500 °C or higher, the polymer became insoluble.[124] The reason for the insolubility of the polymer was reported to arise from the formation P-O-P linkages. We think that the condenstation of phoshonic acid groups takes place intramolecularly since the polymer after the heat treatments described above is still completely soluble in water.

The presence of the condensated phopshonic acid species was detected by Solid State NMR Specstroscopy. ^{1}H magic angle spinning (MAS) NMR spectrum of PVPA (1) displays two major resonances at 2.3 and 10.6 ppm, which are assigned to the backbone protons (CH_2 and CH) and P-OH protons, respectively (Figure 6.21a). ^{1}H chemical shift

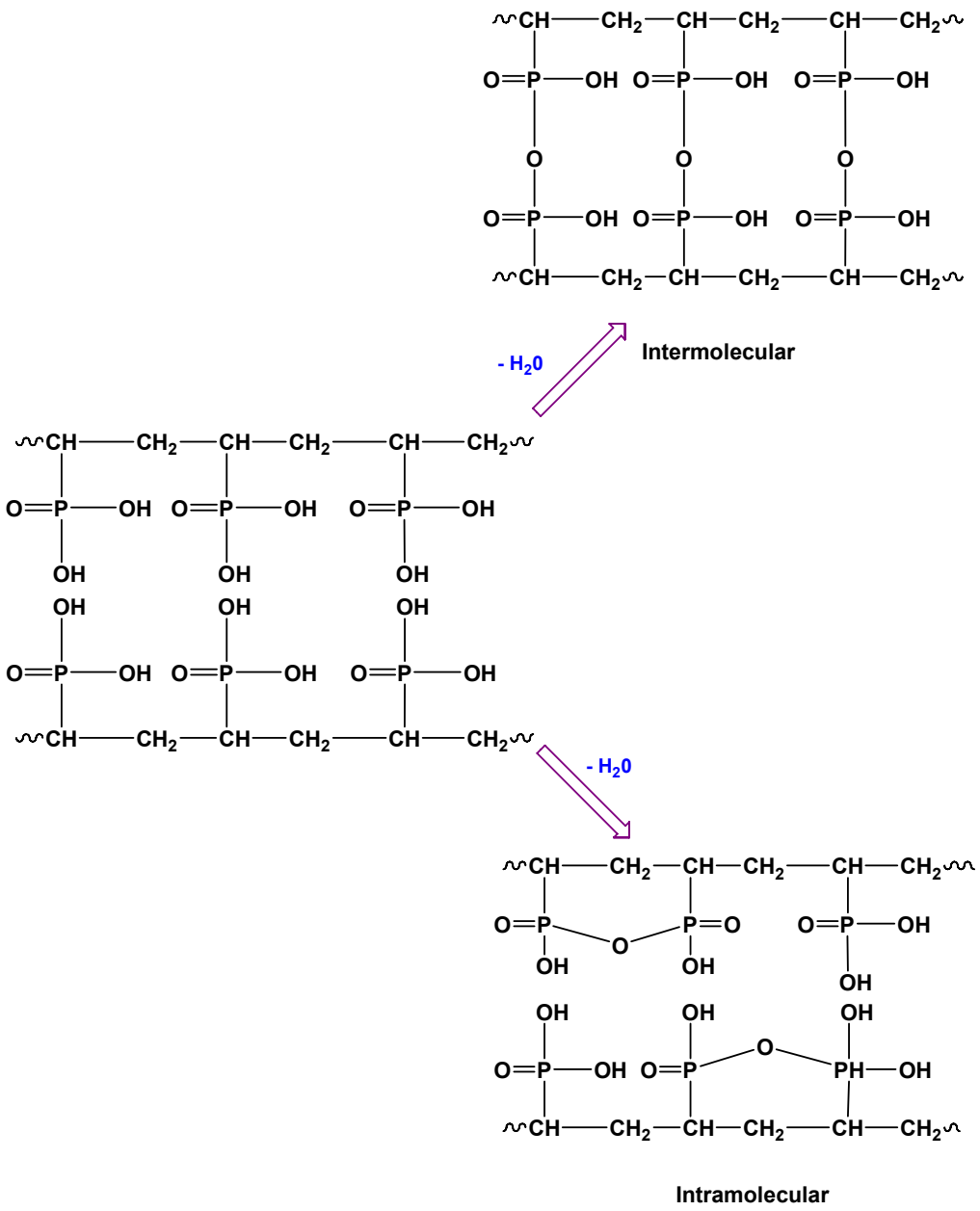

Scheme 6.1: Intramolecular and intermolecular anhydride formation in PVPA.

is very sensitive to the hydrogen bonding.[125] Therefore, ^{1}H-MAS NMR also provides information about the nature of the hydrogen bonding.[125] The correlations between the ^{1}H chemical shift and the nature of the hydrogen bonding have been studied for carboxylic acids and phosphoric acid. A larger shift was observed for systems with shorter O---O

distances. In other words, strong hydrogen bonding causes a downfield shift. Similarly, the downfield shift to 10.6 ppm of P-OH signal indicates the presence of a strong hydrogen bonding between phopshonic acid groups of PVPA. The relative intensities of the resonances at 2.3 ppm to that of at 10.6 ppm should be 3 to 2 considering the repeating unit of the polymer. The excess intensity of P-OH resonance can be attributed to the water molecules undergoing fast exchange through hydrogen bonding. It is worth to note that the NMR signal intensity is affected by the relaxation and mobility. Therefore, it is problematic to use the intensity of P-OH signal for a precise quantitative analysis of water content. However, the minor resonance at 6.6 ppm indicates the presence of a small amount of water trapped in the system.

The ^{31}P-MAS NMR spectrum of PVPA was dominated by a resonance at 33 ppm due to the phosphonic acid groups. A weak shoulder was observed at 25 ppm (Figure 6.21b), which was assigned to the phosphonic acid anhydride. The spectrum was deconvoluted by WIN-NMR to obtain the intensity of each signal. The ratio of the intensity of the resonance at 25 ppm to the sum of the intensities of the signals at 25 ppm and 33 ppm gave the fraction of the phosphonic acid anhydride species. The fraction of the anhydride form was found as 14% for PVPA (1) dried at 50 °C to the constant weight. To see the effect of the temperature on the formation of anhydride species, ^{31}P-MAS NMR and ^{1}H-MAS NMR spectra of the annealed PVPA (1) was recorded. As a result of annealing, the fraction of phosphonic acid anhydride species was enhanced, which was indicated by an increase in the relative signal intensity of the resonance at 25 ppm in the ^{31}P-MAS NMR spectrum of PVPA (1). After annealing PVPA (1) at 150 °C for 2 days, the polymer possessed 43% condensated phopshonic acid groups. A

correlation between the fraction of phosphonic acid anhydride species and the conductivity of PVPA (1) is given in, and the effect of the phosphonic acid anhydride groups on the conductivity is discussed in 6.7.2.

^{1}H-MAS NMR spectrum of PVPA (1) confirmed the formation of condensated phosphonic acid species by a decrease in the P-OH signal intensity. The intensity of the P-OH resonance was expected to decrease since the number of OH protons decreases upon formation of phopshonic acid anhydride species. Both ^{1}H- and ^{31}P-NMR results are consistent with the assignment of the phosphonic acid anhydride resonance, and additionally, they confirm the enhancement of the phopshonic acid anhydride formation at higher temperatures, which leads to the observed decrease in the proton conductivity.

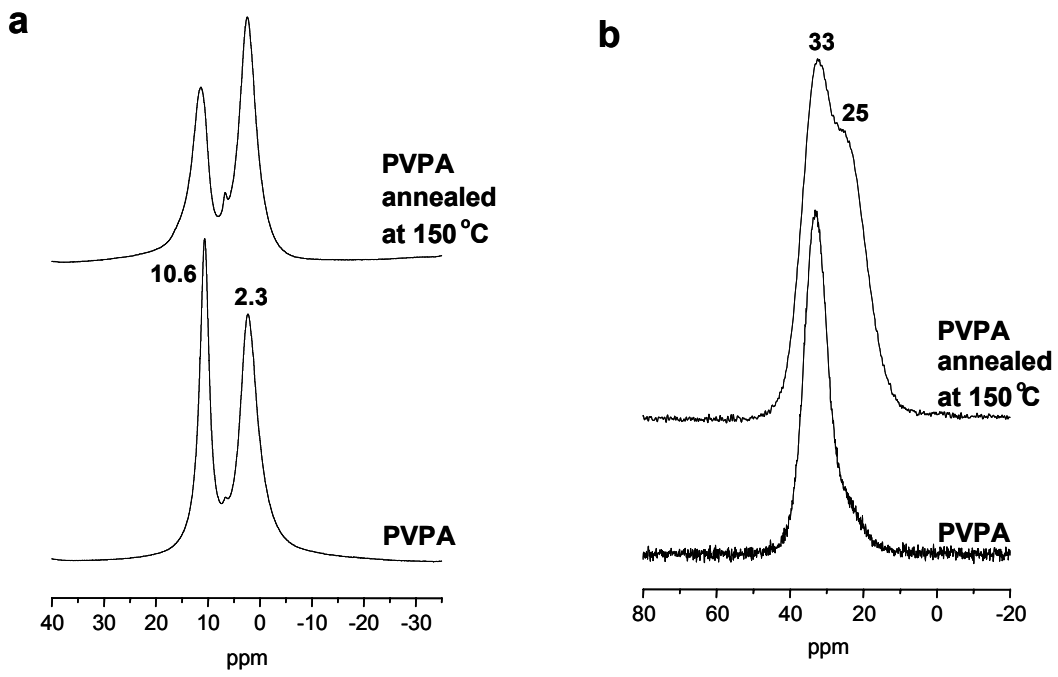

Figure 6.21: a) ^{1}H and (b) ^{31}P MAS NMR spectra of PVPA as synthesized and annealed at 150 °C. All spectra were acquired at room temperature without temperature control and with spinning speeds of 30 kHz. Under these conditions, the real temperature of the sample is between 50 and 60 °C due to the frictional heat. The same conditions were used to collect other spectra unless noted else wise.

6.8.2 Identification of Mobile Protons

Variable temperature studies were performed in the range of 303 K to 430 K to study the dependence of the mobility on the temperature. A continuous and significant line narrowing was observed for the P-OH protons as temperature increases, while variation in the line width with the temperature is seen for the backbone protons. However, negligible change in the peak position is seen. In other words, the absence of temperature dependence of the chemical shift of P-OH may imply that the nature of

hydrogen bonding is not changing with increasing temperature in the case of PVPA. Solid State NMR studies of a dried Nafion sample revealed the dependence of the proton chemical shift on temperature. The reason for that was given as the weakening in the effective hydrogen bond strength of the sulfuric acid protons.[126] As already mentioned, only line narrowing was observed as an effect of temperature on the ^{1}H MAS NMR spectra in PVPA. Normally, line narrowing with increasing temperature is explained as fast exchange kinetics of temperature-dependent structures, e.g.

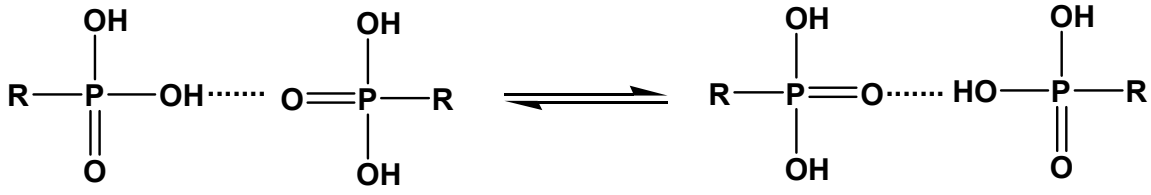

Scheme 6.2: Possible fast exchange process between phosphonic acid groups.

Temperature dependent NMR experiments provide information about exchange processes. If the exchange is fast, we will observe only a single line, which reflects the average chemical shifts of each species. This is the case that is encountered in the temperature dependent ^{1}H-MAS NMR experiments of PVPA (1) (Figure 6.22). The line narrowing of the P-OH proton with increasing temperature indicates that a fast exchange occurs in the temperature range investigated. On the contrary, the backbone protons appear to be immobile on the NMR scale, which suggest that the polymer backbone is rigid. The change in the line width as a function of temperature in the fast exchange limit can be correlated to the exchange rate, from which of the activation energy associated with this process can be calculated. The line width of P-OH resonance shows a linear

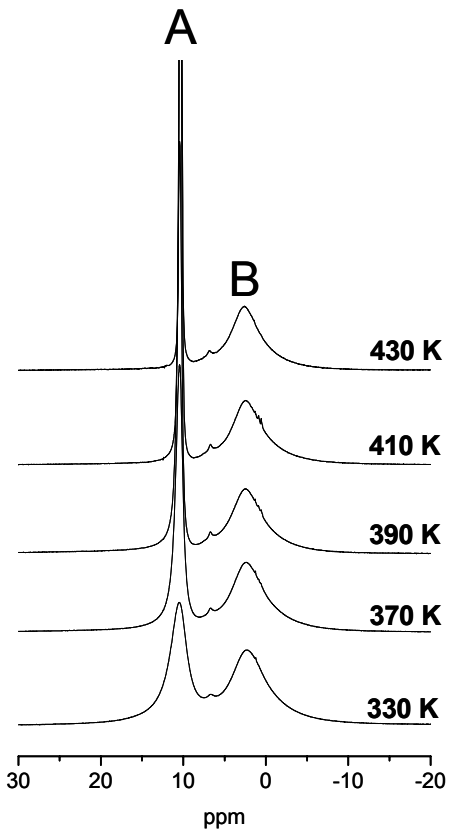

Figure 6.22: ^{1}H variable temperature MAS NMR spectra of PVPA (1). The temperature was calibrated taking into account the frictional heat induced by high speed MAS.

on the inverse temperature and activation energy for the proton motion is determined as 25 kJ/mol from the fitting to the Arrhenius equation.* To have a better understanding of relationship between conductivity and activation energy, it can be useful to compare the activation energies for PVPA (1) obtained by Solid State NMR to that of reported for Nafion, which is the benchmark in the proton conducting membranes.[123] The activation energy for Nafion was reported as around 9 kJ.

* The data relevant to the calculation of activation energy by solid state NMR is not shown here, this part of the work was performed in collaboration with Dr. Y.J. Lee.

6.8.3 Rigidity of the Polyvinyl Backbone (Detection of Immobile Protons)

Other than OH protons attached to the phosphonic acid functionality, PVPA possesses protons on the polymer backbone. In order to investigate the effect of temperature on the mobility of the backbone protons, ^{13}C CP MAS spectra were obtained at room and elevated temperatures as shown in Figure 6.23.

At room temperature, a single ^{13}C resonance at 32 ppm was observed, which was assigned to the polyvinyl backbone. The resolution was not good enough to make a more detailed assignment of the ^{13}C-NMR spectrum. The spectrum remains unchanged at elevated temperature. The temperature behavior of ^{13}C-NMR, in conjunction with the ^{1}H VT NMR data suggests that the backbone protons are immobile at least on NMR time scale. No glass transition was observed in the temperature range studied. When a substance undergoes a glass transition, a dramatic decrease in the line widths occurs, which is not the case for PVPA. Other than Solid State NMR, we also used Differential Scanning Calorimetry in the temperature regime between 20 °C and 300 °C to observe whether PVPA undergoes glass transition. However, we did not detect any glass transition.[127*]

[*] The thermal properties of PVPA have been investigated in collaboration with Dr. A. Kaltbeitzel. The thermograms are not shown in this work.

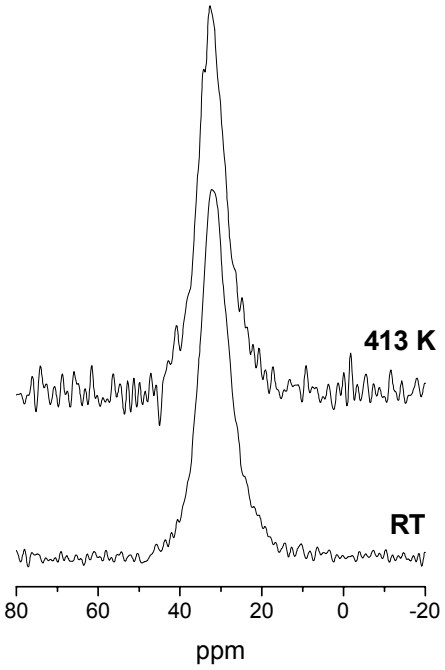

Figure 6.23: ^{13}C CP MAS NMR spectra acquired at various temperatures.

6.8.4 Effect of Drying on the Formation of Phosphonic Acid Anhydride Species

The effect of the drying procedure on the formation of phosphonic acid anhydrides and the conductivity of PVPA (1) was already discussed partially in the previous section by a comparing the conductivity behavior of two PVPA samples, which had been treated differently prior to the conductivity measurements. Other than these two samples, we investigated only freeze-dried PVPA (1) as well as one-day annealed PVPA (1) at 150 °C by ^{1}H- and ^{31}P-MAS NMR. Both ^{31}P- and ^{1}H-MAS NMR spectra of PVPA samples exposed to different drying conditions are given in Figure 6.24.

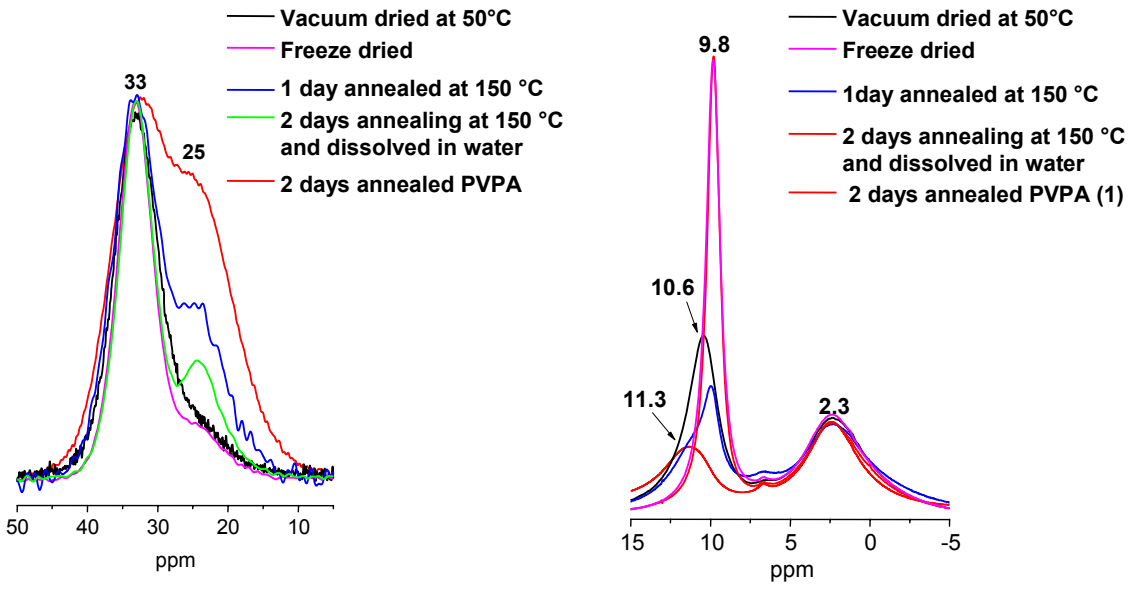

Figure 6.24: The effect of drying on the formation of phopshonic acid anhydride: a) ^{31}P-MAS NMR and b) ^{1}H-MAS NMR of PVPA exposed to different drying conditions.

It is expected that these PVPA samples differ in their water content since they are dried differently. Qualitative information about their relative water content can be obtained by the position of the P-OH resonance in their ^{1}H-MAS NMR spectra. Due to the fast exchange between water molecules and phosphonic acid group, position of the P-OH signal shifts depending on the water content. Taking into account the fact that the resonance of pure water appears at 4.8 ppm, a gradual shift to lower frequency is predicted as the water content increases. Bearing this information in mind we can order the samples in the increasing water content as follows:

2 days annealed PVPA < 1day annealed PVPA< vacuum dried PVPA< freeze-dried PVPA

^{1}H-MAS NMR spectra of PVPA exposed to different drying conditions differ in the position of their P-OH signal as well as the relative intensity and the line width of this signal. Comparing the intensity of the P-OH resonance with that of backbone protons

clearly reveals the decrease of the number of OH protons in the annealed samples. This is consisted with the suggestion that some of the OH protons are lost due to the formation f phosphonic acid anhydride at high temperature. The line width for P-OH resonance in ^{1}H-MAS NMR spectrum becomes narrower as the water content of the sample increases. The P-OH resonance of 2 days annealed PVPA(1) at 150 °C annealed displayed the broadest line width. The position of the resonance due to the polymer backbone protons remains unchanged no matter which sample is under investigation.

^{31}P-MAS NMR spectra of all PVPA samples exhibit 2 resonances at 33 and 25 ppm due to the phosphonic acid and phosphonic acid anhydride functionality. As expected, the relative intensities of these peaks vary depending on the drying procedure indicating that PVPA (1) samples exposed to different heat treatments contain different fraction of phosphonic acid anhydride species. We only calculated the fraction of cyclic anhydride species for two samples, namely, for the vacuum dried PVPA at 50 °C and 2 days annealed PVPA (1) at 150 °C. The fraction of cyclic anhydrides in vacuum dried PVPA (1) and 2 days annealed PVPA (1) was found as 14% and 43%, respectively. The effect of these cyclic anhydride species on the conductivity is already discussed in 6.6.1.

The reversibility of phosphonic acid anhydride formation was studied by dissolving the annealed PVPA in water for 4h at room temperature followed by freeze-drying. ^{31}P MAS NMR of this sample after freeze drying has more condensated groups than the dried PVPA (1) indicating that not all the phosphonic acid anhydride species formed during the annealing procedure were hydrolyzed to free acid. This reveals that the reaction leading to the formation of phosphonic acid anhydride species is not completely reversible. The reversibility of this process may depend on the experimental conditions.

We found out that phosphonic acid anhydride signal almost vanished in the ^{31}P-MAS NMR spectrum after annealing the sample at 250 °C for 5 h and storing the polymer at room temperature under 98% relative humidity for 2 days.[127]

6.8.5 Double Quantum Spectrum of PVPA

^{31}P two dimensional double quantum (DQ) spectroscopy reveals information about the spatial proximity between the different phosphonic acid groups. Since the intensity of a double quantum signal is a function of inverse internuclear distance, and recoupling times. DQ signal can provide information about the internuclear distances by carefully choosing recoupling times. For example, presence of ^{31}P-^{31}P spin pairs within a distance of 0.4 nm is expected to give rise to a DQ signal when back-to-back pulse sequence is applied with 260 μs recoupling times (8 rotor periods under 30 kHz MAS condition). Double quantum coherences are generated only from relatively strong dipole-dipole couplings, in other words from the spins in very close proximity to each other. Weak dipolar couplings, in other words the spin pairs separated further apart can be detected by extending the recoupling times. ^{31}P DQ experiments have been successfully applied to various phosphate glasses to determine the connectivities between phosphorous.[125, 128]

Figure 6.25 displays the two dimensional DQ NMR spectra of PVPA obtained at 430 K. Autocorrelation signals among phosphonic acid pairs (n) and among acid anhydride pairs (na), respectively, are observed along the diagonal at 8 τ recoupling, indicating each moiety is in close contact to each other. The diagonal represents the dipolar couplings between the like ^{31}P in PVPA. There is DQ cross peak indicating the

correlation between phosphonic acid and anhydride designated as na. At longer recoupling time, the autocorrelation signal among phosphonic acid (n) and cross peak between both acid moieties (na) increase in intensity, while the autocorrelation signal of acid anhydride pairs (a) remains unaffected. The stronger autocorrelation signal from the acid anhydride at short recoupling time suggest that these phosphorous are closer in space in comparison to the normal phosphonic acid groups. This is expected from the geometry of the anhydride. The P-P distances are 3.0 nm for the phosphonic acid anhydride and 4.9-5.3 nm for phosphonic acid. The existence of DQ cross peak between two acid moieties indicates spatial proximities between phosphonic acid and phosphonic acid anhydrides. This demonstrates that there is no domain separation between phosphonic acid and phosphonic acid anhydride. Thus, it is clear that the condensation of phosphonic acid occurs randomly throughout the system without forming any domain segregation.

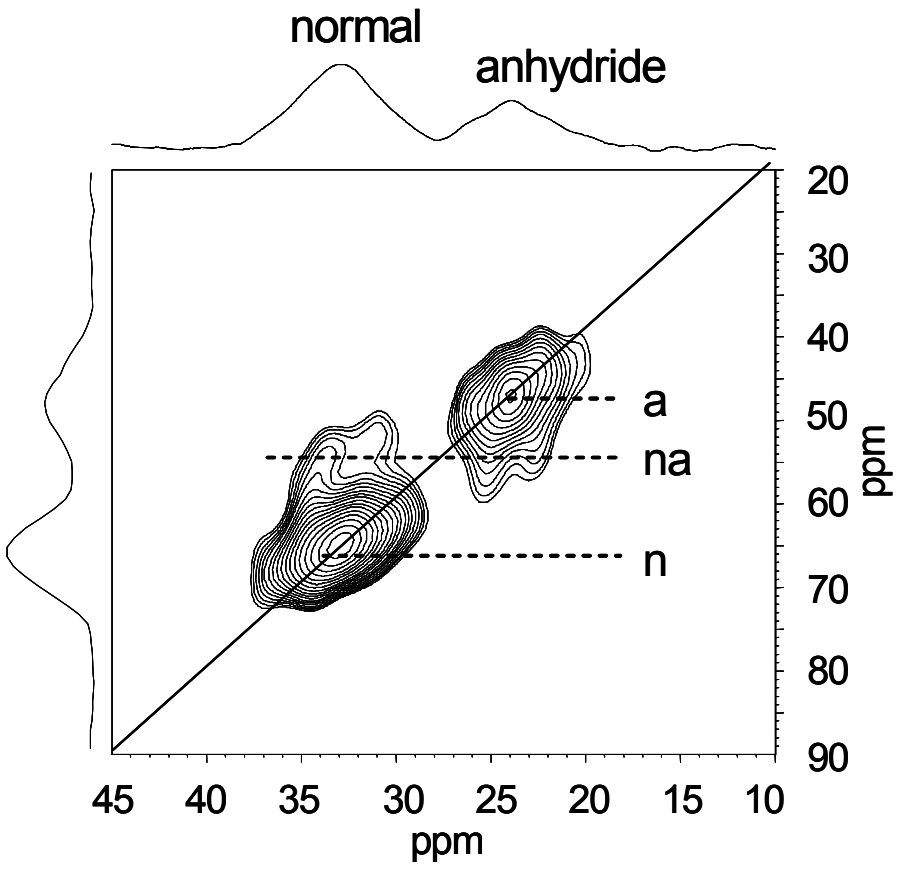

Figure 6.25: ^{31}P 2D DQF spectrum of PVPA acquired at 430 K with τrcpl = 8 τR.

6.9 Summary

Poly(vinylphosphonic acid) is the simplest representative of the class of the polymers having tethered phosphonic acid groups. The conductivity behavior of PVPA of known microstructure and molecular weight was investigated as a function of temperature between 20 °C and 210 °C, and as a function of time at constant temperature (100 °C).

PVPA conducts in the temperature regime between 20 °C and 210 °C. The presented conductivity data suggest that the temperature dependence of conductivity follows an Arrhenius behavior within the temperature range studied. The proton

conduction in PVPA seems to be facilated by the presence of water at low temperatures where it acts as a vehicle.

The differences in the microstructures of PVPA samples is a consequence of the different polymerization mechanisms of VPA and DMVP as already discussed in Chapter 3 in details. Polymerization of DMVP proceeds by head-to-tail addition. Therefore, the PVPA obtained by the hydrolysis of PDMVP has a more regular structure compared to the PVPA obtained by the direct polymerization of VPA since it only contains head-to-tail linkages, whereas the polymerization of VPA leads to the presence of head-to-head and tail-to-tail in addition to head-to-tail linkages. In other words, regioisomerism was observed in the case of PVPA obtained directly by polymerization of VPA. The possible types of the rings that can form are different for these two PVPA samples. PVPA samples having various types of the rings in the structure can lead to a difference in the conductivities depending on the relative stability of these rings. The presence and formation of cyclic phosphonic acid anhydride species was detected by Solid State NMR. Formation of these groups influences conductivity by a large extent. The formation of these cyclic anhydride species is unavaidable due to thermal treatment of the polymer after synthesis.

There are many open questions about mechanisms involved in the conductivity of PVPA. It is still unclear whether the conductivity can be described by only Arrhenius behavior at elevated temperatures.

CHAPTER 7

CONCLUSION AND OUTLOOK

Polymers with proton conducting units tethered to a polymer backbone was suggested as an alternative to polymer electrolytes, where the conductivity greatly depends on the presence of water and therefore, the operating temperature of the fuel cell must be maintained below the boiling point of water. PVPA contains a high concentration of phosphonic acid groups, and provides a good model system for the study of the correlation of the structure and proton conduction mechanisms. The details of the synthesis of PVPA and the properties of the resulting polymer were investigated for the first time with emphasis on its potential application in fuel cells that are supposed to operate at temperatures higher than 100 °C in a low humidity environment as the key constituent of polymer electrolyte membranes.

The possible synthetic routes leading to PVPA were explored. Free radical polymerization at 80 °C or higher temperatures is the only route available for direct polymerization of VPA. The reason for the failure of polymerizations of VPA at lower temperatures is due to the peculiar polymerization mechanism of VPA. A detailed analysis of the ^{1}H- and ^{13}C-NMR spectra of PVPA prepared by free radical polymerization of VPA revealed that it contained a substantial fraction of head-head and tail-tail linkages. This unexpected result suggested that the polymer was actually formed by cyclopolymerization starting from the vinylphosphonic acid anhydride which may be present in equilibrium with the free acid.

Free radical polymerization of VPA gave a high molecular weight* (M_w of 6.2 x 10^4g/mol) atactic PVPA. The microstructure, as revealed by NMR spectra, was described for the first time for this type of polymer. The solution properties which characterize PVPA as a polyelectrolyte were reported. Additionally, the properties relevant for the application of PVPA in fuel cells were investigated. All PVPA samples displayed conductivity in the temperature regime (20-210 °C) studied. Conductivity data of PVPA suggest that the temperature dependence of conductivity of PVPA follows an Arrhenius type of behavior between 20 and 210 °C. It was attempted to understand the nature of the proton conduction in PVPA. The phosphonic acid functionality in PVPA undergoes condensation leading to the formation of cyclic anhydrides, which was enhanced at elevated temperatures. Formation of cyclic anhydrides affects the proton conductivity to a large extent.

To have a clearer picture of the underlying complex conduction mechanism, the proton mobility of the polymer should be investigated at various temperatures. In order to use PVPA as a proton exchange membrane in fuel cells, the conductivity of the polymer should be improved since 10^{-2} S/cm is the minimum conductivity at room temperature that is required by the industry. PVPA alone is rigid because of the presence of a high concentration of phosphonic acid groups, which are bonded by hydrogen bridges to each other. The rigidity of the polymer may be decreased by the reduction of the concentration of phopshonic acid groups, which may be achieved by the copolymerization of VPA with other comonomers. If the comonomers are chosen appropriately, it may be possible to change the dissolution behavior of PVPA. Since PVPA is water-soluble and water is

* The high molecular weight polymer was obtained when the initiator concentration was 0.1 mol percent relative to the monomer.

produced during the operation of the fuel cell, the polymer may be washed out with time unless it is used in a protected way. Achieving copolymers of VPA that are insoluble in water may solve this problem. Knowledge about the polymerization mechanism of VPA will be very helpful to develop synthetic procedures to obtain copolymers of VPA.

References:

1. Carrette, L.; Friedrich, K. A.; Stimming, U. *ChemPhysChem* **2000,** 1, (4), 162.
2. Kordesch, K. V. *Electrochim. Acta* **1971,** 16, 597.
3. Larminie, J.; Dicks, A., *Fuel Cell Systems Explained*. 2 ed.; John Wiley & Sons Inc: England, 2003.
4. Savadogo, O. *Journal of New Materials for Electrocehmical Sytems* **1998,** 1, 47.
5. Cohen, R. In *Gemini Fuel Cell System*, Power Sources Conference, 24-26 th May, 1966; 1966; p 21.
6. Gierke, T. D. *J. Electrochem. Soc.* **1977**, (134), 319c.
7. Kreuer, K. D. *J. Membr. Sci.* **2001,** 185, 29.
8. Kreuer, K. D. *Solid State Ionics* **1997,** 97, (1), 1.
9. Ianniello, R.; Schmidt, V. M.; Stimming, U.; Strumper, J.; Wallan, A. *Electrochim. Acta* **1994,** 39, 1863.
10. Baschuk, J. J. *Int. J. Energy. Res.* **2001**.
11. Wainright, J. S.; Wang, J. T.; Savinelli, R. F.; Litt, M.; Moadell, H. *Proc. - Electrochem. Soc.* **1994,** 94, 255.
12. Defendini, F.; Armand, M.; Gorecki, W.; Berthier, C. *Extended Abstract, Electrochemical Society,San Diego Meeting 3* **1986**, 86.
13. Donoso, P.; Gorecki, W.; Berthier, C.; Defendini, F.; Poinsignon, C.; Armand, M. *Solid State Ionics* **1988,** 28, 969.
14. Petty-Weeks, S.; Zupanic, J. J.; Swedo, J. R. *Solid State Ionics* **1988,** 31, (2), 117.
15. Przyluski, J.; Wioczerek, W.; Potarzweski, Z.; Saiti, P.; Giadano, N., *Recent Advances in Fast Proton Conducting Materials and Devices*. WorldScientific: Singapore, 1990.
16. Wainright, J.; Wang, J. T.; Weng, D.; Savinelli, R. F.; Litt, M. *J. Electrochem. Soc.* **1995**, (142), L121.
17. Kreuer, K. D.; Fuchs, A.; Ise, M.; Spaeth, M.; Maier, J. *Electrochim. Acta* **1998,** 43, (10-11), 1281.
18. Kreuer, K. D., *Solid State Ionics: Science and Technology New Proton Conducting Polymers for Fuel Cell Applications*. World Science Publishing: Singapore, 1998; p 263.
19. Schuster, M.; Meyer, W. H.; Wegner, G.; Herz, H. G.; Ise, M.; Schuster, M.; Kreuer, K. D.; Maier, J. *Solid State Ionics* **2001,** 145, 82.
20. Lee, S. Y.; Scharfenberger, G.; Meyer, W. H.; Wegner, G. *Adv. Mater.* **2005,** 17, (5), 626.
21. Scharfenberger, G.; Meyer, W. H.; Wegner, G.; Schuster, M. F. H.; Kreuer, K. D.; Maier, J. *Fuel Cells* **2006,** 6, (3-4), 237.
22. Schuster, M.; Rager, T.; Noda, A.; Kreuer, K. D.; Maier, J. *Fuel Cells* **2005,** 5, (3), 355.
23. Vanysek, P., *Handbook of Chemistry and Physics*. 76 ed.; CRC Press: NY, USA, 1995.
24. Meng, Y. Z.; Tjong, S. C.; Hay, A. S.; Wang, S. J. *Eur. Polym. J.* **2003,** 39, 627.
25. Stone, C.; Daynard, T. S.; Hu, L. Q.; Mah, C.; Steck, A. E. *Jounal of New Materials for Electrochemical Systems* **2000,** 3, 43.

26. Allcock, H. R.; Hofmann, M. A.; Ambler, C. M.; Morford, R. V. *Macromol.* **2002,** 35, 3484.
27. Florjanczyk, Z.; Wielgus-Barry, E.; Poltarzweski, Z. *Solid State Ionics* **2001,** 145, (1-4), 119.
28. Yamabe, M.; Akiyama, K.; Akatsuka, Y.; Kato, M. *Eur. Polym. J.* **2000,** 36, 1035.
29. Steininger, H.; Schuster, M. F. H.; Kreuer, K. D.; Maier, J. *Solid State Ionics* **2006,** 177, (26-32), 2457.
30. Yamada, M.; Honma, I. *Polym.* **2005,** 45, 2986.
31. Pike, R. M.; Cohen, R. A. *J. Polym. Sci.* **1960,** 44, 531.
32. McIvor, R. A.; Grant, G. A.; Hubley, C. E. *Can. J. Chem.* **1956,** 34, 1611.
33. Berghauser, G.; Uhlig, F. U.S. Patent 4,153,461. 1979.
34. Anbar, M.; John, G. A. S.; Scott, A. C. *J. Dent. Res.* **1974,** 53, (4), 867.
35. Ellis, J.; Wilson, A. D. *J. Mater. Sci. Lett.* **1990,** 9, 1058.
36. Braybook, J. H.; Nicholson, J. W. *J. Mater. Chem.* **1993,** 3, (4), 361.
37. Park, C. H.; Nam, S. Y.; Lee, Y. M. *J. App. Poly. Sci.* **1999,** 74, 83.
38. Eom, G. T.; Oh, S. Y.; Park, T. G. *J. App. Poly. Sci.* **1998,** 70, 1947.
39. Arcus, C. L.; Matthews, R. J. S. *Chemistry and Industry* **1958,** 28, 890.
40. Erdemi, H.; Bozkurt, A. *Eur. Polym. J.* **2004,** 40, 1925.
41. Levin, Y. A.; Romanov, V. G.; Ivanov, B. Y. *Vysokomol. Soyed.* **1975,** A17, (4), 766.
42. Jin, S.; Gonsalves, K. E. *Macromol.* **1998,** 31, 1010.
43. Kosolapoff, G. M. *J. Am. Chem. Soc.* **1952,** 74, 3427.
44. Kosolapoff, G. M. *J. Am. Chem. Soc.* **1948,** 70, 1971.
45. Billmeyer, J. F. W., *Textbook of Polymer Science*. 3 ed.; John Wiley and Sons: 1970.
46. *Polymer Handbook*. 4 ed.; John Wiley and Sons Inc.: NY, USA, 1999.
47. Moedritzer, K. *J. Am. Chem. Soc.* **1961,** 83, 4381.
48. Feng, X.; Pan, C.; Wang, J. T.; Liu, Y.; Pan, C. Y. *Macromol. Chem. Phys.* **2001,** 202, (3403).
49. Liu, Y.; Pan, C. Y. *J. Polym. Sci. Part A: Polym. Chem.* **1997,** 35, 3403.
50. Coote, M. L.; Krenske, E. H.; Izgorodina, E. I. *Macromol. Rapid. Commun.* **2006,** 27, 473.
51. Goto, A.; Fukuda, T. *Prog. Polym. Sci.* **2004,** 29, 329.
52. Li, C.; Han, J.; Ryu, C. Y.; Benicewicz, B. C. *Macromol.* **2006,** 39, 3175.
53. Perrier, S.; Takolpuckdee, P. *J. Polym. Sci. Part A: Polym. Chem.* 43, 5347.
54. Moad, G.; Solomon, D. H., *The Chemistry of Free Radical Polymerization*. 1 ed.; Elsevier Science Inc.: 1995.
55. McCormick, C. L.; Lowe, A. B. *Acc. Chem. Res.* **2004,** 37, 312.
56. Bamford, C. H.; Eastmond, G. C.; Ward, J. C. *Proceedings of Royal Society* **1963,** A 271, 357.
57. Anseth, K. S.; Scott, A. R.; Peppas, N. A. *Macromol.* **1996,** 29, 8308.
58. Bokias, G.; Durand, A.; Hourdet, D. *Macromol. Chem. Phys.* **1998,** 199, 1387.
59. Schildknecht, C., *Vinyl and Related Polymers*. John Wiley and Sons Inc.: NY, USA, 1962.
60. Oiu, J.; Charleux, B.; Matyjaszweski, K. *Prog. Polym. Sci.* **2002,** 26, (10), 2083.

61. Patten, T. E.; Matyjaszewski, K. *Adv. Mater.* **1998,** 10, 901.
62. Kuchta, F. D.; Herk, A. L. V.; German, A. N. *Macromol.* **2000,** 33, 3641.
63. Chiefari, J.; Chong, Y. K.; Ercole, F.; Krstina, J.; Jeffery, J.; Lee, T. P. T.; Madunne, R. T. A.; Meijs, G. G.; Moad, C. L.; Moad, G.; Rizzardo, E.; Thang, S. H. *Macromol.* **1998**, (31), 5559.
64. Ladaviere, C.; Dorr, N.; Claverie, J. P. *Macromol.* **2001,** 34, 5370.
65. Eisenberg, H.; Mohan, G. R. *J. Phys. Chem.* **1959,** 63, 671.
66. Aldermann, V. V.; Hanford, W. E. U.S. Patent 2,348,705. 1944.
67. Jones, G. D.; Barnes, C. E. U.S. Patent 2,515,714. 1950.
68. Breslow, D. S.; Hulse, G. E. *J. Am. Chem. Soc.* **1954,** 76, 6399.
69. Overberger, C. G.; Baldwin, D. E.; Gregor, H. P. *J. Phys. Chem.* **1950,** 72, 4864.
70. Kern, W.; Schulz, R. C. *Angew. Chem.* **1957,** 69, (5), 153.
71. Breslow, D. S.; Kutner, A. *J. Polym. Sci.* **1958,** 27, 295.
72. Bingöl, B.; Meyer, W. H.; Wagner, M.; Wegner, G. *Macromol. Rapid. Commun.* **2006,** 27, 1719.
73. Liu, Z.; Brooks, B. W. *Polym. Int.* **1998,** 45, 217.
74. Miller, M. L.; Donnell, K. O.; Sokgman, J. *J. Colloid. Sci.* **1962,** 17, 649.
75. Skoog, D. A.; Holler, F. H.; Nieman, T. A., *Principles of Instrumental Analysis*. 5 ed.; Saunders College Publishing: San Fransisco, USA, 1998.
76. Wang, D.; Elisseeff, J. H., Photopolymerization. In *Encyclopedia of Biomaterials and Biomedical Engineering*, Marcel Dekker: 2004; p 1212.
77. Sarac, A. S. *Progress in Polymer Science* **1999,** 24, 1149.
78. Quhadi, T.; Forte, R.; Jerome, R.; Fayt, R.; Theyssie, P. 1984.
79. Quhadi, T.; Forte, R.; Jerome, R.; Fayt, R.; Theyssie, P. 1988.
80. Fayt, R.; Forte, R.; Jacobs, C.; Jerome, R.; Quhadi, T.; Teyssie, P.; Varshney, S. K. *Macromol.* **1987**, (20), 1442.
81. Varshney, S. K.; Hauteeker, J. P.; Fayt, R.; Jerome, R.; Teyssie, P. *Macromol.* **1990**, (23), 2618.
82. Mandel, M., *Ecylopedia of Polymer Science and Engineering*. Wiley: NY, USA, 1987; Vol. 11.
83. Burke, S. E.; Barett, C. J. *Langmuir* **2003,** 19, 3297.
84. Molyneaux, P., *Water Soluble Synthetic Polymers*. CRC Press: Florida, USA, 1983.
85. Katchalsky, A.; Spinik, P. *J. Polym. Sci.* **1947,** 2, 432.
86. Woodbury, C. P. *J. Phys. Chem.* **1993,** 97, 3623.
87. Nagasawa, M.; Murase, T.; Kondo, K. *J. Phys. Chem.* **1965,** 69, 4005.
88. Plamper, F. A.; Becker, H.; Lanzendörfer, M.; Patel, M.; Wittemann, A.; Ballauff, M.; Müller, A. H. E. *Macromol. Chem. Phys.* **2005,** 206, 1813.
89. Onouchi, H.; Hasegawa, T.; Kashiwagi, D.; Ishiguro, H.; Maeda, K.; Yashima, E. *Macromol.* **2005,** 38, 8625.
90. Crofts, P. C.; Kosolapoff, G. M. *J. Am. Chem. Soc.* **1953,** 75, 3379.
91. Kodama, H.; Miyajima, T.; Mori, M.; Takahshi, M.; Nishimura, H.; Ishiguro, S. *Colloid Polym. Sci.* **1997,** 275, 938.
92. Kawaguchi, Y.; Nagasawa, M. *J. Phys. Chem.* **1969,** 73, (12), 4382.
93. Mandel, M. *Polym. J.* **1970,** 6, 807.

94. Lagueci, A.; Ulrich, S.; Labille, J.; Rouge, N. F.; Stoll, S.; Buffle, J. *Eur. Polym. J.* **2006,** 42, 1135.
95. Speiser, R.; Hills, C. H.; Eddy, C. R. *J. Phys. Colloid Chem.* **1945,** 49, 334.
96. Arnold, A.; Overbeek, J. T. G. *J. Phys. Chem.* **1950,** 69, 192.
97. Kern, W.; Herold, W.; Scherhag, B. *Makromol. Chem.* **1955/1956,** 17, 231.
98. Tonelli, A. E., *NMR Spectroscopy and Polymer Microstructure: The Conformational Connection*. VCH: NY, USA, 1989.
99. Koenig, J. L., *Chemical Microstructure of Polymer Chains*. Wiley Interscience Publ: NY, USA, 1980.
100. Frisch, H. L.; Mallows, C. L.; Bovey, F. A. *J. Chem. Phys.* **1966,** 45, 1565.
101. Bovey, F. A. *Acc. Chem. Res.* **1968,** 1, 175.
102. Gottlieb, H. E.; Kotlyar, V.; Nudelmann, A. *J. Org. Chem.* **1997,** 62, 7512.
103. Gunther, H., *NMR Spectroscopy*. John Wiley and Sons Inc.: NY, USA, 1996.
104. Chang, C.; Muccio, D. D.; Pierre, T. S. *Macromol.* **1985,** 18, 2154.
105. Kodaira, T.; Liu, Q. Q.; Satoyamka, M.; Urushisaki, M.; Utsumi, H. *Polym.* **1999,** 40, 6947.
106. Suchoparek, M.; Spevacek, J. *Macromol.* **1993,** 26, 102.
107. Nishioka, A.; Yamaguchi, I.; Shimizu, H. *J. Polym. Sci.* **1960,** 45, (145), 232.
108. Kremer, F.; Schönhals, A., *Broadband Dielectric Spectroscopy*. Springer: Heidelberg, Germany, 2004.
109. Atkins, P. W., *Physical Chemistry*. 2 ed.; Oxford University Press: Oxford, England, 1999.
110. Hardy, L. C.; Schriver, D. F. *J. Am. Chem. Soc.* **1085,** 107, 3823.
111. MacCallum, J. R.; Vincent, C. A., *Polymer Electrolye Reviews*. Elsevier Applied Science: NY, USA, 1987; Vol. 1.
112. Owen, J., Ionic Conductivity. In *Comprehensive Polymer Science*, Geoffrey, A., Ed. Pergamon Press: Oxford, England, 1989.
113. Armand, M. *Solid State Ionics* **1983,** 9, (10), 945.
114. Funke, K. *Solid State Ionics* **1986,** 18-19, 183.
115. Debye, P.; Hückel, E. *Phys. Z.* **1923,** 24, 185.
116. Debye, P.; Falkenhagen, H. *Phys. Z.* **1928,** 29, 401.
117. Onsager, L. *Phys. Z.* **1926,** 27, 388.
118. Funke, K.; Hoppe, R. *Solid State Ionics* **1990,** 40, 200.
119. Funke, K. *Mat. Res. Soc. Symp. Proc.* **1991,** 210, 97.
120. Goward, G. R.; Schuster, M. F. H.; Sebastiani, D.; Schnell, I.; Spiess, H. W. *J. Phys. Chem. B* **2003,** 106, 9322.
121. Hickmann, B. S.; Mascal, M.; Titman, J. J.; Wood, I. G. *J. Am. Chem. Soc.* **1999,** 121, 11486.
122. Grimmer, A. R.; Blümich, B., *Solid State NMR I: Methods*. Springer Verlag: Heidelberg, Germany, 1994.
123. Mauritz, K. A.; Moore, R. B. *Chem. Rev.* **2004,** 104, 4535.
124. Jiang, D. D.; Yao, Q.; McKinney, M. A.; Wilkie, C. A. *Polym. Degrad. Stab.* **1999,** 63, 423.
125. Harris, R. K.; Jackson, P.; Mervin, L. H.; Say, B. J. *J. Chem. Soc., Faraday. Trans. 1* **1988,** 84, (11), 3649.
126. Ye, G.; Janzen, N.; Goward, G. R. *Macromol.* **2006,** 39, 3283.

127. Kaltbeitzel, A.; Schauff, S.; Steininger, H.; Bingöl, B.; Brunklaus, G.; Meyer, W. H.; Spiess, H. W. *Solid State Ionics Conference Papers* submitted.
128. Feike, M.; Graf, R.; Schnell, I.; Jager, C.; Spiess, H. W. *J. Am. Chem. Soc.* **1996,** 118, 9631.

Appendix I: NMR Spectra

A: ^{1}H-NMR spectra of poly(vinylphosphonic acid)s and polyphopshonates before purification to determine the conversion

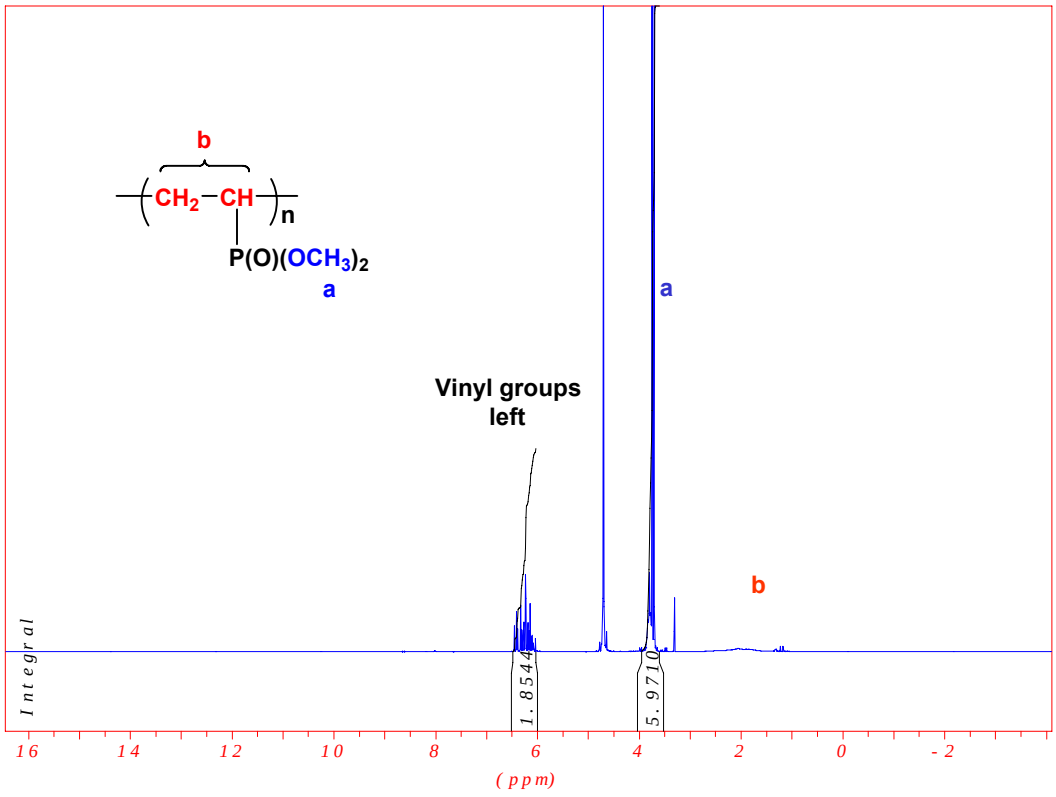

Figure 1: ^{1}H-NMR (300 MHz) spectrum of PDMVP in D_2O

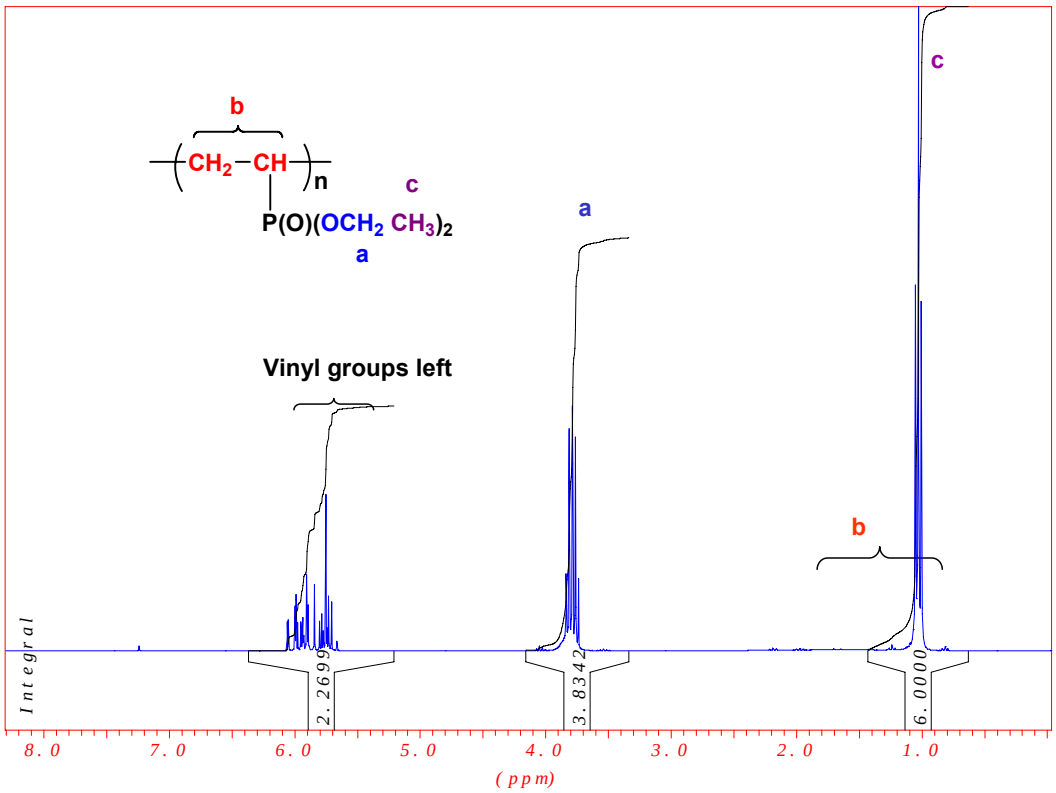

Figure 2: ^{1}H-NMR (300 MHz) spectrum of PDEVP in $CDCl_3$

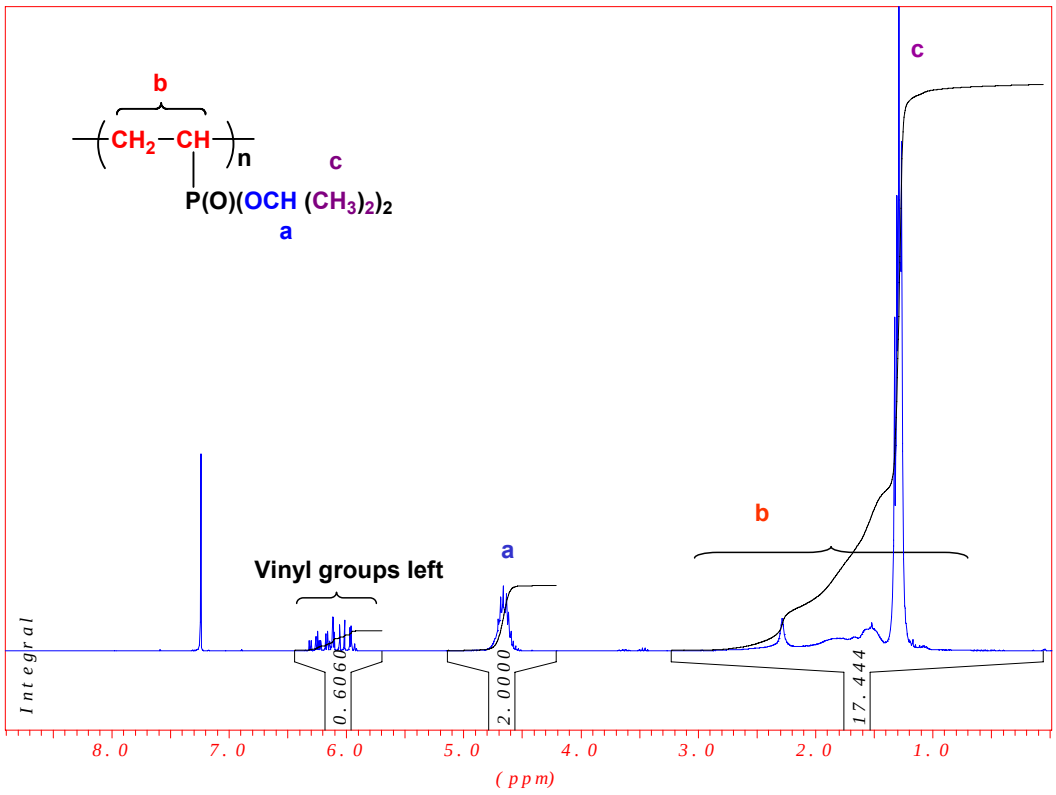

Figure 3: ^{1}H-NMR (300 MHz) spectrum of PDISP in $CDCl_3$

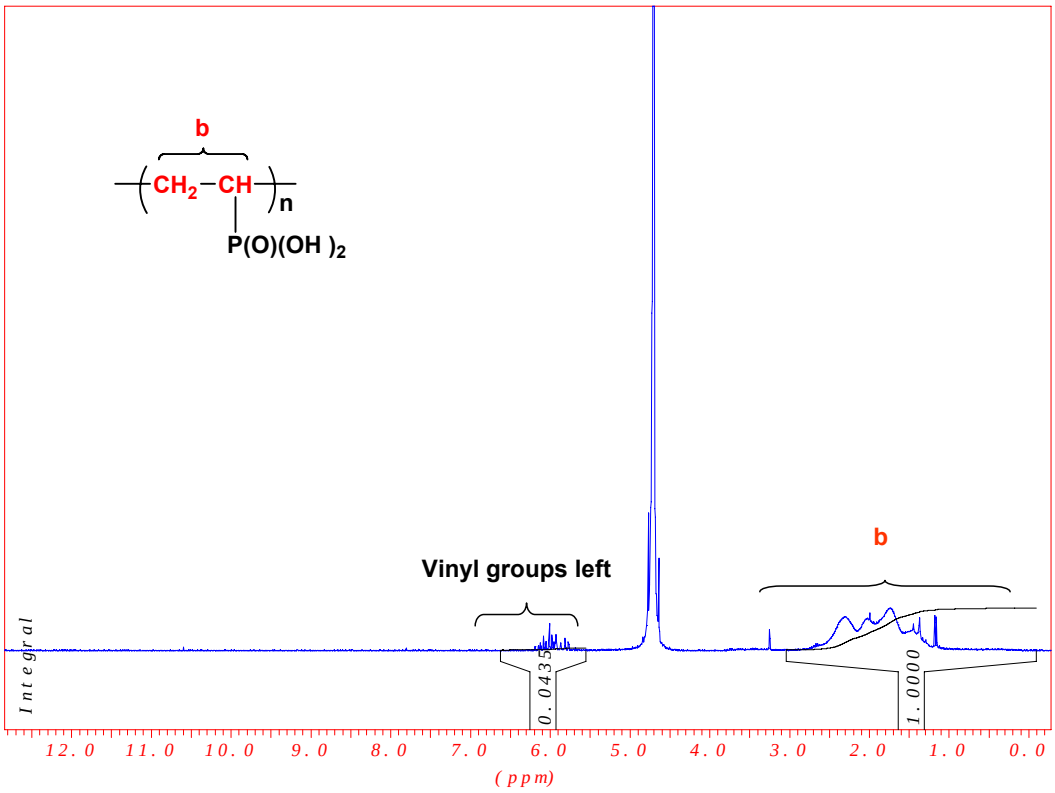

Figure 4: ^{1}H-NMR (300 MHz) spectrum of PVPA (2) in D_2O

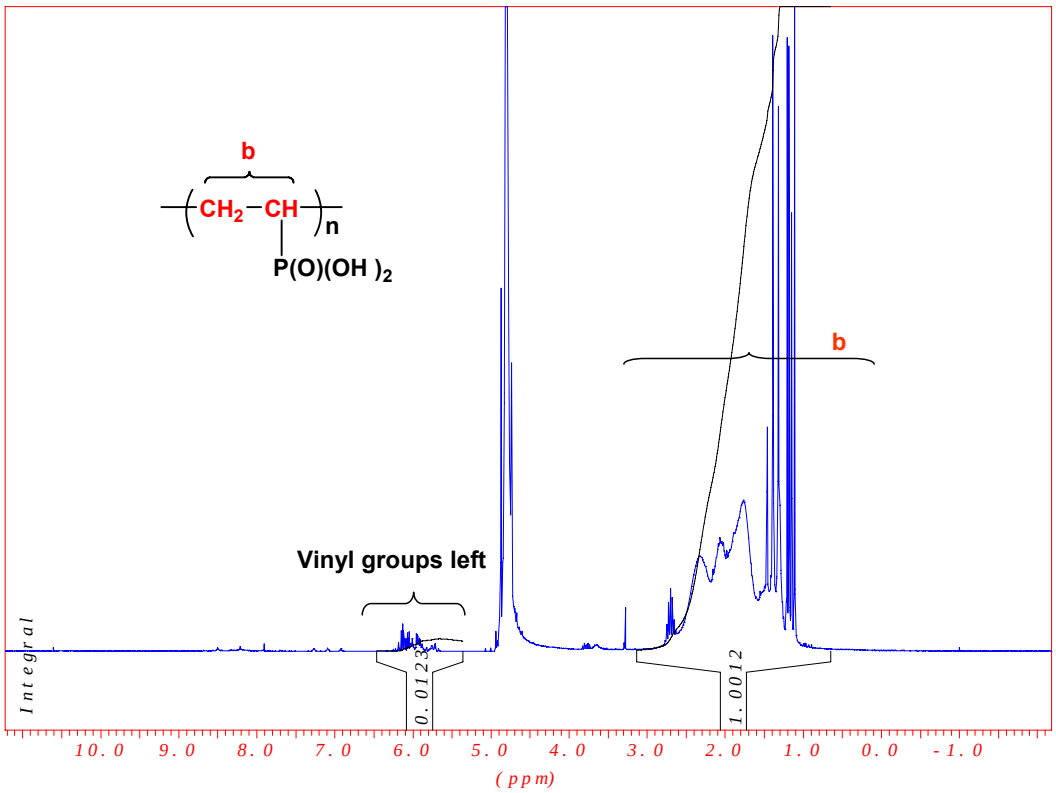

Figure 5: ^{1}H-NMR (300 MHz) spectrum of PVPA (3) in D_2O

B: ^{1}H- NMR spectra of Poly(vinylphosphonates) after purification

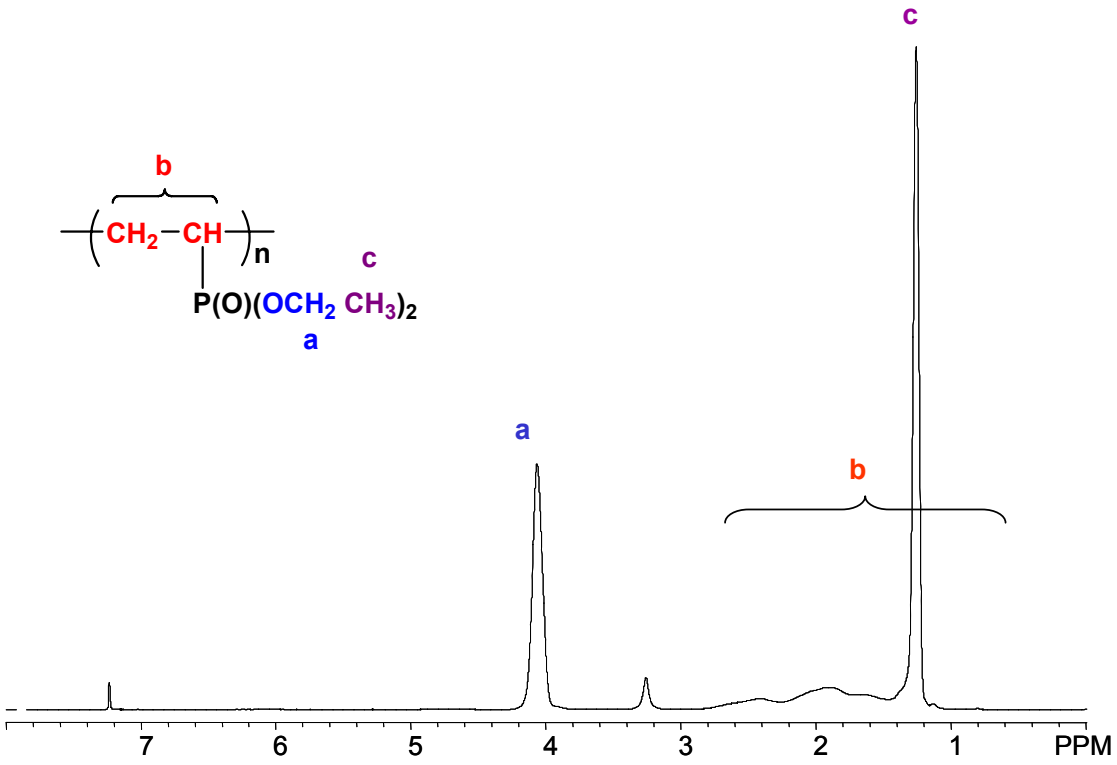

Figure 6: ^{1}H-NMR (500 MHz) spectrum of PDEVP (50 mg/0.8 mL $CDCl_3$)

\

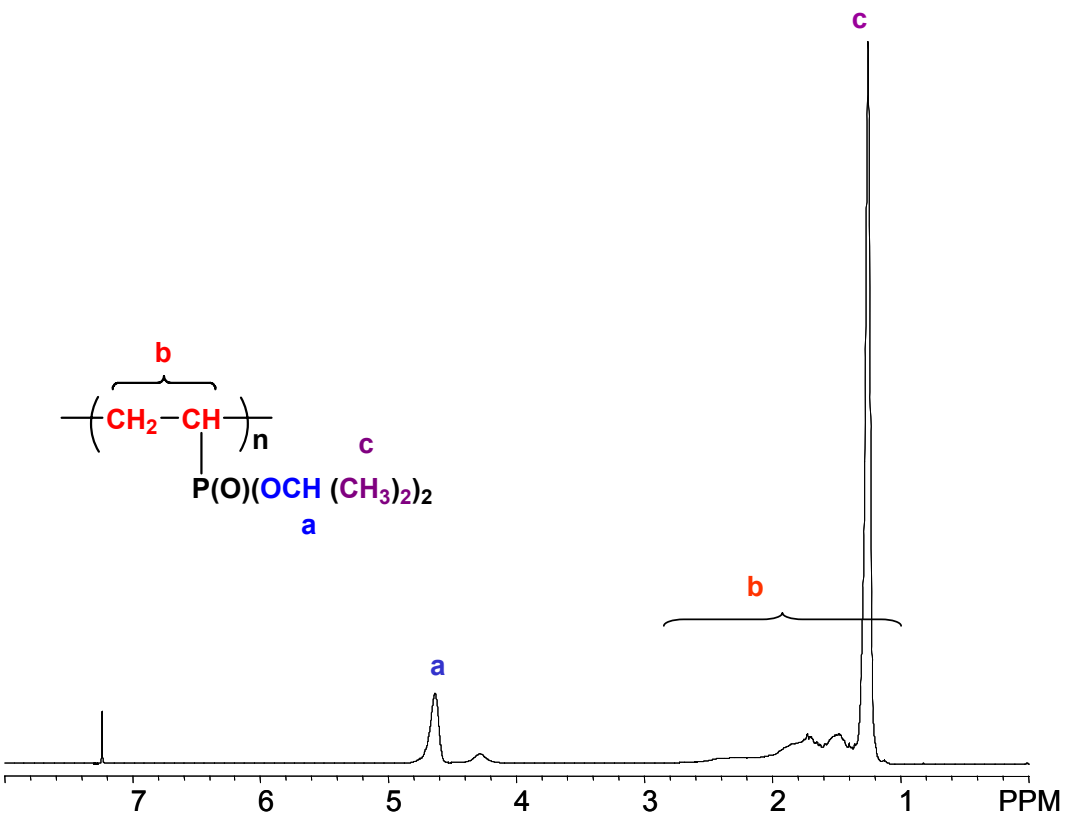

Figure 7: ^{1}H-NMR (500 MHz) spectrum of PDISP (50 mg/0.8 mL $CDCl_3$)

Appendix II: IR Spectra

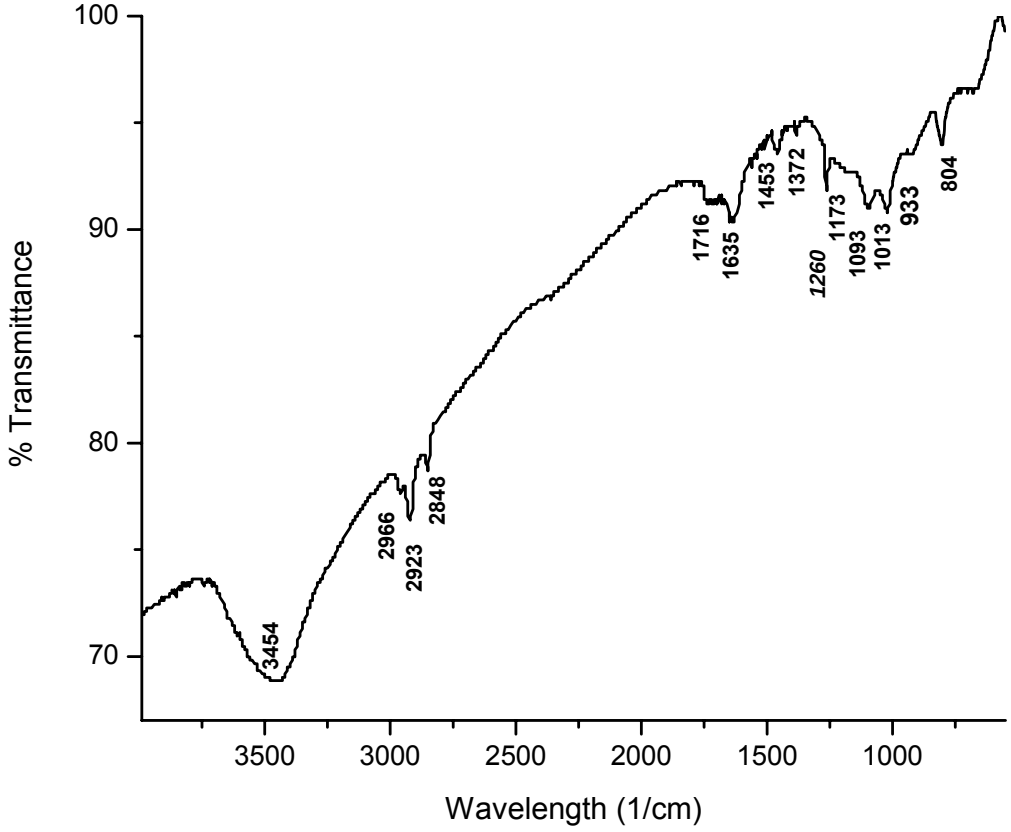

Figure 1: IR spectrum of PVPA (1)

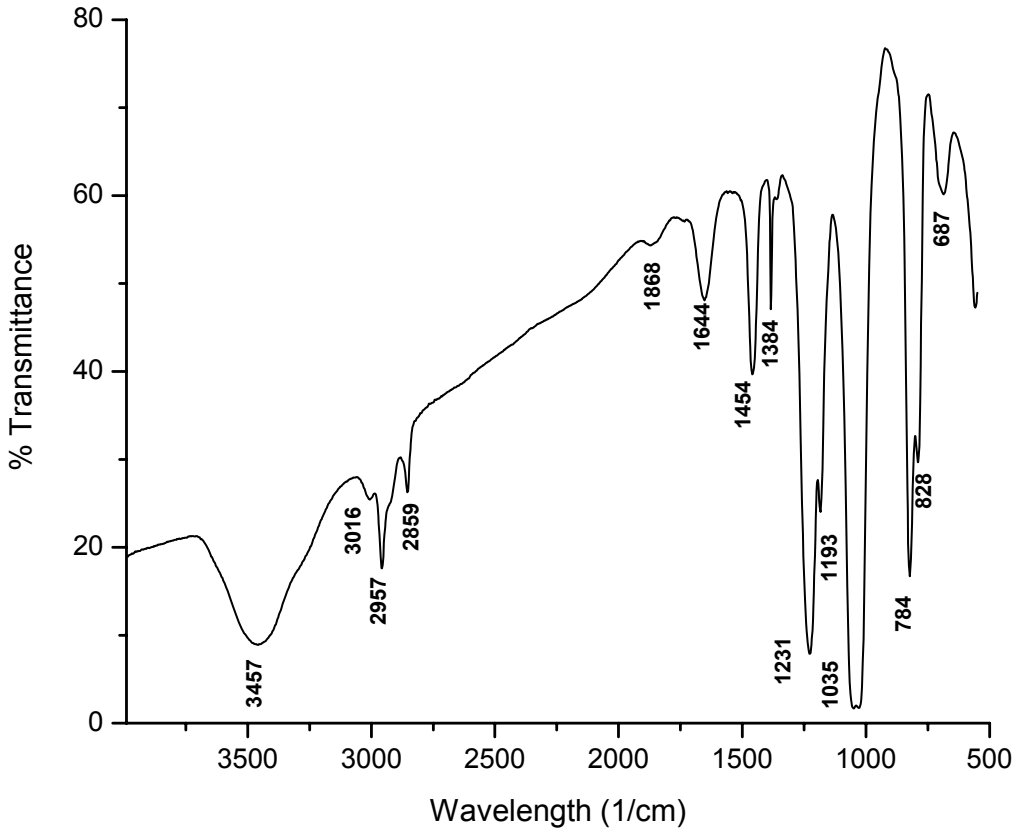

Figure 2: IR spectrum of PDMVP

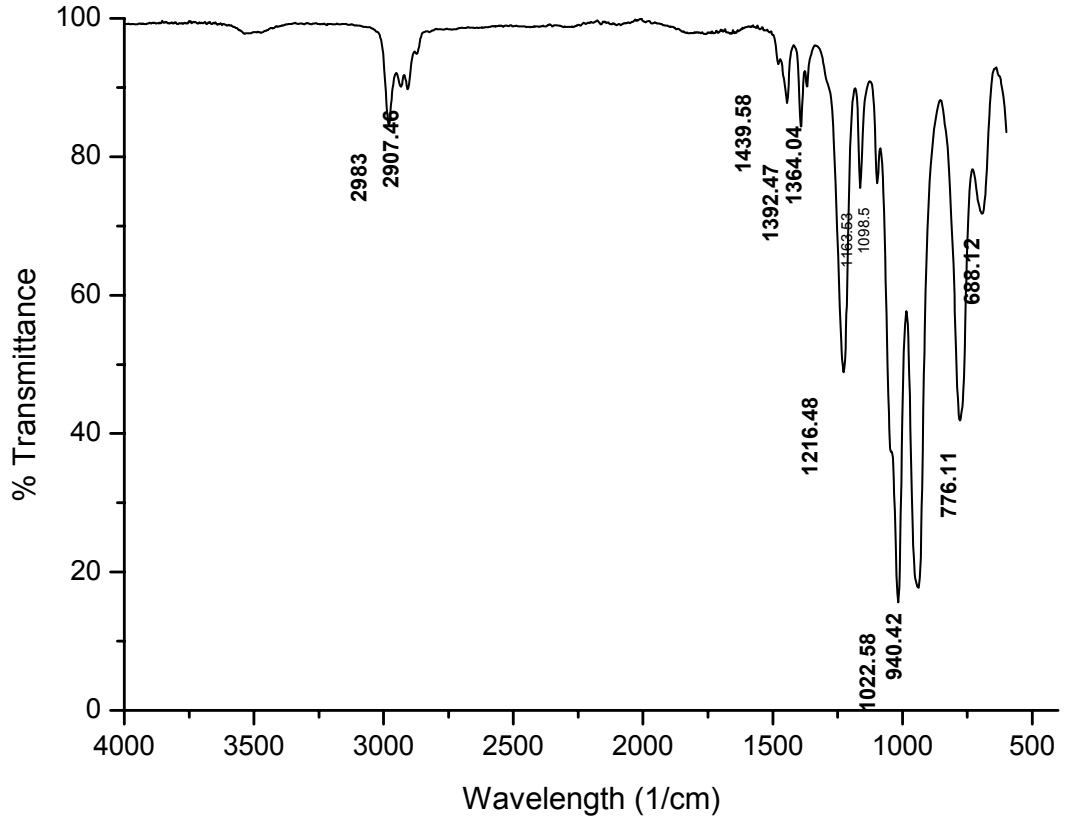

Figure 3: IR spectrum of PDEVP

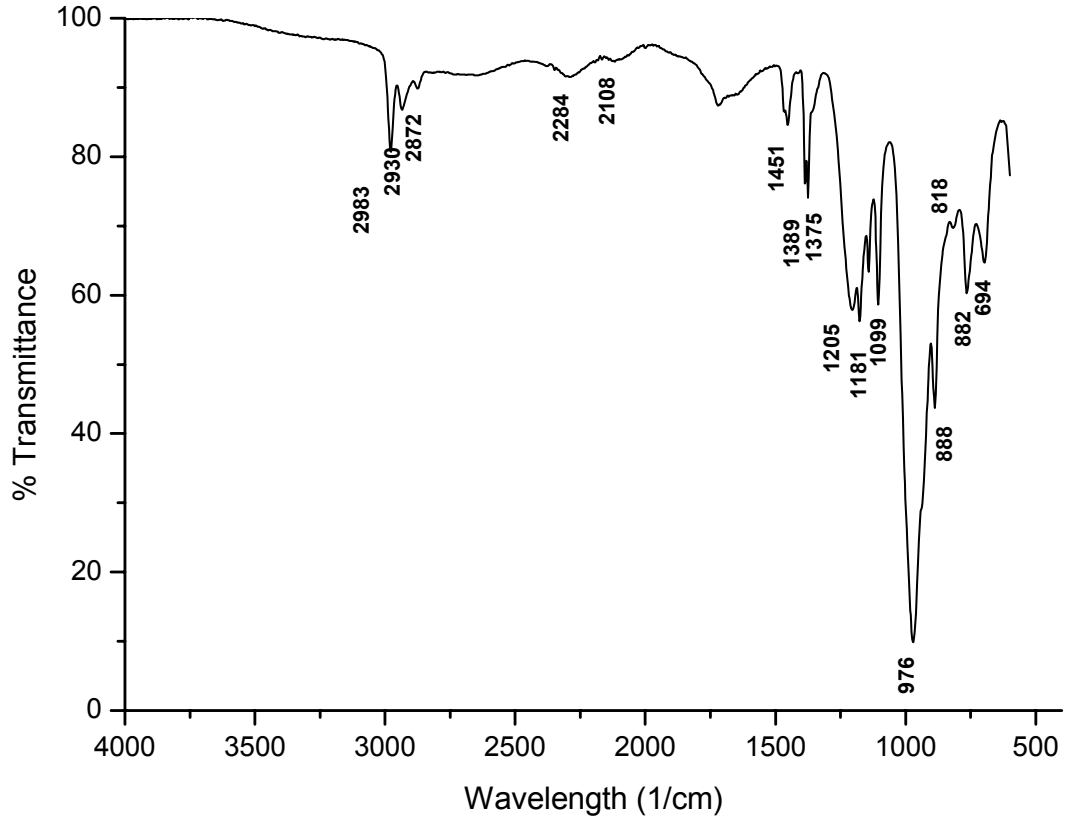

Figure 4: IR spectrum of PDISP

APPENDIX III: Synthetic Procedure for Photopolymerization of VPA, DEVP, and DISP, Redox Polymerization of VPA, Polymerization of Salts of VPA, and Anionic Polymerization of DEVP

3.1 Materials

Only the chemicals which are not described in the experimental section (Chapter 2) are mentioned here. 2,2-dimethoxy-2-phenylacetophenone (Aldrich, 98%), ammonium persulfate (APS) (Aldrich, 98%), N,N,N'N'-tetramethylethylenediamine (TEMED) (Aldrich, 98%), 4,4-Azobis(4-cyanovaleric acid) (Aldrich, 98%), secondary butyllithium solution in cyclohexane (Aldrich) were used as received.

3.2 Photopolymerization of VPA, DISP, and DEVP

VPA (0.09 mol, 9.723 g) and 2,2-dimethoxy-2-phenylacetophenone (0.009 mol, 2.3 g) were dissolved in methanol (70 mL). DISP (0.0356 mol, 7 mL) and 2,2-dimethoxy-2-phenylacetophenone (0.00356 mol, 0.91 g) were dissolved in methanol (70 mL). DEVP (0.0455 mol, 7 mL), and 2,2-dimethoxy-2-phenylacetophenone (0.00455 mol, 1.166g) were dissolved in methanol (70 mL). All polymerization reactions were irradiated by a mercury lamp at room temperature.

3.3 Redox Polymerization of VPA

VPA (0.0025 mol), APS (0.00005 mol), TEMED (0.00000533 mol) were reacted in water. Both mol percent of APS to VPA and TEMED to APS were varied in different experiments. The mol percent of APS to VPA and TEMED to APS was varied between 2 and 0.1, and 10 to 1, respectively.

3.4 Polymerization of Salts of VPA

A solution of VPA (3 M) was prepared in water (5 mL), which was titrated against sodium hydoxide solution to adjust the pH of the reaction medium differently.AIBA was used as initiator. The mol percent of the initiator to monomer was 0.1. The reaction mixture was heated at 80 °C for several hours. The pH dependent polymerization was also investigated in the presence of an acid initiator, 4,4-Azobis(4-cyanovaleric acid) under the same reaction conditions as AIBA.

3.5 Attempted Anionic Polymerization of DEVP

The anionic polymerization of DEVP was carried out with secondary butyllithium as initiator in tetrahydrofuran. Both monomer, and solvent were distilled and all glasware were degased prior to the polynerization. First, DEVP (5g) was dissolved in tetrahydrofuran (50 mL), which was cooled to – 78 °C before the addition of the initiator. The mol ratio of secondary butyllithium to monomer was 0.004. Methanol (1 mL) was used to quench the polymerization. The same procedure was repeated in the presence of lithium chloride (2.6 mmoles). Morover, diphenylbutyllithium was also tried as a more sterically hindered initiator. The reactions with diphenylbutyllithium were carried out both in the absence and presence of LiCl. All experimets were carried out at two different temperatures, -78 °C, and at room temperature.